The Anomalous Magnetic Moment of the Nucleon in Cavity QCD

M. S. O'Connor

A thesis submitted in partial fulfillment
of the requirements for
the degree of
Doctor of Philosophy

Department of Physics
University of Cape Town
June 19, 1991

Abstract

Perturbative quantum chromodynamics is developed in a spherical cavity using a symmetric form of the Gell-Mann and Low theorem. This formalism allows one to generate any desired term in the perturbation series, in a manner which is similar to the familiar Feynman rules in free space. In this work, all corrections to order eg^2 in the electromagnetic and strong coupling constants which contribute to the magnetic moment of a baryon are generated using this formalism.

The $O(eg^2)$ radiative corrections to the magnetic moment of the nucleon are calculated here in an arbitrary covariant gauge. The gauge-dependent parts are found to vanish identically, and the divergences arising from the loop diagrams cancel amongst each other, making renormalization unnecessary. However, it is shown here that one can, if it is necessary, remove the divergences from the cavity diagrams by subtracting from them a singular factor which is found using dimensional regularization in the analogous free-space diagrams.

In this calculation, the proton and neutron magnetic moments are found to be

$$\begin{aligned} \mu_{\rm p} &= 1.924 - 0.753\alpha_s \\ \mu_{\rm n} &= -1.284 + 0.566\alpha_s \end{aligned}$$

where the cavity radius has been set to $R = 1$ fm.

Contents

Chapter 1

Introduction

It is generally believed that the dynamics of strongly interacting particles are correctly described by the theory of quantum chromodynamics [1]. Certainly, QCD can explain a wealth of experimental observations, such as asymptotic freedom at high energies, and most people expect that confinement, which describes the fact that quarks and gluons are never observed in isolation, is contained within the theory at low energies. This expectation is encouraged by the results obtained from lattice calculations.

However, most of the agreement between experiment and theory, in the physics of strongly interacting particles, is of a rather qualitative nature: to date, there have been *no* precision tests of QCD, which would necessarily take place at low energy. This is contrasted by the remarkably successful Abelian gauge theory, QED, where the experimental and theoretical results for the anomalous magnetic moment of the electron agree to 12 digits! One of the reason for the success of QED is that the perturbative expansion of the theory converges asymptotically, whereas this does not appear to be the case in QCD, at least at low energies. Also, the number of graphs to be considered increases much more rapidly with the order of the perturbative expansion in QCD, and these graphs are usually more difficult to calculate than the corresponding ones in QED, due to their non-Abelian nature. Moreover, it seems that confinement is an inherently non-perturbative phenomenon, and cannot be generated as a power series in the coupling constant. Thus, as long as it is not understood, one has to resort to some simplifying assumptions about the confinement mechanism before QCD calculations are possible, which lead to results which are usually only of a qualitative nature, or at best are model-dependent.

One particular model which enjoyed a great vogue for a while was the MIT bag model [2]. Since confinement was required by experiment, and since it could not be coaxed out of the theory, it was simply introduced by hand with the imposition of boundary conditions on the colour-carrying particles. Confining particles to a static sphere breaks both the translational and Lorentz invariance, as well as the chiral symmetry of the theory, but it does make it possible to calculate the hadron mass spectrum, etc., within the model. The results, to lowest order in perturbation theory, are generally in good agreement with experiment. One therefore expects that higher order QCD corrections should improve the agreement, if perturbation theory

and the model for confinement are valid. Unfortunately, higher order calculations within the M.I.T. bag model are rather difficult, especially if they involve divergent loop diagrams. The difficulties with higher order graphs are of an even more serious nature in the 'improved', but non-renormalizable, bag models such as the chiral [3] and cloudy [4] bags, where in addition to the pion-like $q\bar{q}$ excitations already present in the theory, an elementary pion field is introduced to restore chiral symmetry (see also [5] and references therein).

Recently, confined QCD has been approached from a somewhat different perspective. Buser *et al.* [6] have shown that a consistent theory of QCD can be formulated in a finite region of space, and Stoddart *et. al.* [7] have introduced standard renormalization techniques to this cavity field theory. Hence, a fully fledged theory of QCD in a cavity has evolved from the original, semi-classical bag model, with the advantage that one is now able to calculate the loop diagrams in a reliable manner. This theory of cavity QCD can be viewed either as a viable gauge theory, in which the effects of confining fields to a finite region of space can be studied, or it can be seen as a reasonable approximation to the observable world.

The basic motivation for this thesis is to make a start towards a precision test of QCD. An obvious candidate for such a test is the ratio of the magnetic moments of the proton to neutron, which is known to some 8 digits from experiment, but present calculations are only at the 3% level. However, there is no hope at present that a precise, or even reliable calculation of this quantity can be performed using the full machinery of QCD, so a more modest approach is required. Therefore, in this paper, we shall restrict ourselves to perturbative QCD in a cavity, and propose to calculate all the order α_s corrections to the proton and neutron magnetic moments. The purpose of this calculation can be viewed in several ways, such as:

- a model calculation using cavity QCD;
- a pedagogical example which hopefully provides some insight into the behaviour of confined quarks;
- a gratuitous Ph.D thesis.

If one is inclined to the first interpretation (although the author is not), then there are some problems, such as dealing with the centre-of-mass motion in a reliable way. The usual Peierl-Yoccoz method of calculating the centre-of-mass corrections to baryon magnetic moments appears to be somewhat untrustworthy (see ref. [4] for a discussion of this point), and no attempt has been made here to calculate them. Furthermore, the mechanism of confinement is not at all understood, so the method of confining particles used in cavity QCD is necessarily *ad hoc*, and while it does maintain the important BRST symmetry of the theory, this method is not unique. On the other hand, one might argue that the ratio of μ_n/μ_p is not sensitive to the mechanism of confinement.

As a first step towards the calculation, perturbative QCD in a cavity is developed using a generalized form of the Gell-Mann and Low theorem. This allows us to

systematically generate all corrections to a given order in α_s. In particular, the energy shift for first-order interactions is derived explicitly in two slightly different forms, one of which leads to an expansion of the interaction in time-ordered diagrams. The other form is closer to the more familiar expansion into Feynman diagrams, and allows some free-space techniques to be used.

The Feynman diagrams relevant to the anomalous magnetic moment of the quark are then closely reviewed, since many of the mathematical methods used in the free-space calculation, and some of the results, will be taken over in the cavity calculation. An important consideration is that observable quantities should be gauge independent, and this question is examined in free space. It is shown that the graphs which lead to a gauge independent result in free space are also gauge independent in the cavity.

Once it is known which diagrams must be included in the calculation, the expressions for the energy shifts of these diagrams can be derived. For the vertex correction diagram, this is done using both the time-ordered diagram approach, and a quasi-free space method. For all the diagrams involved, the energy shift is derived using the gluon propagator in an arbitrary gauge.

The numerical computation of the radial and angular matrix elements forms a large part of the total work involved in the calculation, so this aspect merits at least some discussion. Finally, the magnetic moment of the proton, μ_p, can be found from the energy shift using $\Delta E = -\vec{\mu} \cdot \vec{B}$.

Chapter 2

Quantum Chromodynamics in a Cavity

As an introduction to this chapter, a review of the some of the familiar properties of QCD in free space will be given. This will serve to establish the notation used, and hopefully will also provide a convenient reference for the reader.

Once the free-space theory has been introduced, QCD in a cavity follows on quite easily since the changes to be made are mainly in the boundary conditions characterizing the two theories. These changes do not affect the basic algebra of the fields, but merely change the functional form and some of the internal properties of wave functions. However, the loss of translational and Lorentz invariance in the cavity does mean that the approach to particular calculations, e.g. scattering amplitudes in a cavity, might appear to be rather different to the more familiar free-space methods. The differences, and more particularly the frequent similarities between the free-space and cavity theories will be emphasized as a general principle throughout this work. The notation in this section closely follows that of ref. [6].

2.1 The QCD Lagrange Density

The QCD Lagrange density is given by

$$\begin{aligned} \mathcal{L} &= \bar{\psi}\left(i\gamma_\mu D^\mu - m_f\right)\psi - \tfrac{1}{2}\,i\partial_\mu\left(\bar{\psi}\,\gamma^\mu\psi\right) - \tfrac{1}{4}\boldsymbol{F}_{\mu\nu}\cdot\boldsymbol{F}^{\mu\nu} \\ &\quad -\tfrac{1}{2}\,\lambda\partial_\mu\boldsymbol{A}^\mu\cdot\partial_\nu\boldsymbol{A}^\nu - i\partial_\mu\boldsymbol{\chi}\cdot\mathcal{D}^\mu\boldsymbol{\omega} \end{aligned} \tag{2.1}$$

where ψ is the quark field and m_f is the (diagonal) mass matrix for the different flavours of quarks. $\boldsymbol{A}^\mu$ is the gauge field describing the gluons, and $\boldsymbol{\chi}$ and $\boldsymbol{\omega}$ are the Faddeev-Popov ghost fields. D^μ and $\mathcal{D}^\mu$ are the covariant derivatives:

$$D^\mu\psi = \left(\partial^\mu - \tfrac{1}{2}\,ig\boldsymbol{\lambda}\cdot\boldsymbol{A}^\mu\right)\psi \quad ; \quad \mathcal{D}^\mu\boldsymbol{\omega} = \partial^\mu\boldsymbol{\omega} + g\boldsymbol{A}^\mu\times\boldsymbol{\omega} \tag{2.2}$$

with the vector dot- and cross products in colour space defined as

$$\boldsymbol{A}\cdot\boldsymbol{B}=\sum_{a=1}^{8}A_aB_a \qquad ; \qquad (\boldsymbol{A}\times\boldsymbol{B})_a=\sum_{b,c=1}^{8}f_{abc}A_bB_c \tag{2.3}$$

The $\boldsymbol{\lambda}$'s are the 8 Gell-Mann matrices, the f_{abc} are the structure constants of $SU(3)_{\text{colour}}$ and λ parametrizes the gauge.

The Hamilton density can be derived from the Lagrangean using the Euler-Lagrange equations (for example, see [6]), and may be written as the sum of two terms, $\mathcal{H}=\mathcal{H}_0+\mathcal{H}_{int}$. The first term $\mathcal{H}_0$ is independent of the strong coupling constant g and describes the non-interacting fields. It is given by

$$\begin{aligned}\mathcal{H}_0 \;=\; & \bar{\psi}\left(-\tfrac{1}{2}i\gamma_k\overleftrightarrow{\partial^k}+m_f\right)\psi+\tfrac{1}{4}\left(\partial_kA^l-\partial_lA^k\right)\cdot\left(\partial_kA^l-\partial_lA^k\right)+\tfrac{1}{2}\boldsymbol{\Pi}^k\cdot\boldsymbol{\Pi}^k \\ & -\frac{1}{2\lambda}\boldsymbol{\Pi}^0\cdot\boldsymbol{\Pi}^0+\boldsymbol{\Pi}^k\cdot\partial_kA^0-\boldsymbol{\Pi}^0\cdot\partial_kA^k-i\boldsymbol{\Omega}\cdot\boldsymbol{X}-i\partial_k\boldsymbol{\chi}\cdot\partial_k\boldsymbol{\omega}\end{aligned} \tag{2.4}$$

In the above, $\boldsymbol{\Pi}^\mu$, $\boldsymbol{\Omega}$ and $\boldsymbol{X}$ are the canonically conjugate momenta to the gluon and two ghost fields respectively. The second term, $\mathcal{H}_{int}$, describes the interaction between the fields, and depends linearly and quadratically on g. The explicit form of this term is

$$\begin{aligned}\mathcal{H}_{int} \;=\; & -\tfrac{1}{2}g\bar{\psi}\gamma_\mu\boldsymbol{\lambda}\psi\cdot\boldsymbol{A}^\mu-\tfrac{1}{2}g\left(\partial_kA^l-\partial_lA^k\right)\cdot\left(\boldsymbol{A}^k\times\boldsymbol{A}^l\right)-g\boldsymbol{\Pi}^k\cdot(\boldsymbol{A}^k\times\boldsymbol{A}^0) \\ & +\tfrac{1}{4}g^2\left(\boldsymbol{A}^k\times\boldsymbol{A}^l\right)\cdot\left(\boldsymbol{A}^k\times\boldsymbol{A}^l\right)+g\boldsymbol{\Omega}\cdot\left(\boldsymbol{A}^0\times\boldsymbol{\omega}\right)+ig\partial_k\boldsymbol{\chi}\cdot\left(\boldsymbol{A}^k\times\boldsymbol{\omega}\right)\end{aligned} \tag{2.5}$$

The various terms in $\mathcal{H}_{int}$ describe: the interaction of two quarks and a gluon; the elementary three-gluon vertex; the elementary four-gluon vertex; and the interaction of two ghosts and a gluon respectively.

The Hamilton density is quantized by interpreting the arguments ψ, $\boldsymbol{A}^\mu$, etc. as field operators on which are imposed the following equal-time commutation and anti-commutation relations:

$$\left\{\psi_{cf\alpha}(\vec{x},t),\psi^\dagger_{c'f'\beta}(\vec{y},t)\right\}=\delta_{cc'}\,\delta_{ff'}\,\delta_{\alpha\beta}\,\delta^{(3)}(\vec{x}-\vec{y}) \tag{2.6}$$

The subscripts c, f and α on $\psi_{cf\alpha}$ denote the colour, flavour and spinor indices of the quark respectively. Similarly, the commutators for the gluon fields are

$$[\,A^\mu_a(\vec{x},t),\Pi^\nu_b(\vec{y},t)\,]=ig^{\mu\nu}\delta_{ab}\,\delta^{(3)}(\vec{x}-\vec{y}) \tag{2.7}$$

Although the ghosts fields have integer spin, they satisfy anti-commutation relations, and these are given by

$$\{\,\omega_a(\vec{x},t),\Omega_b(\vec{y},t)\,\}\;=\;\{\,\chi_a(\vec{x},t),X_b(\vec{y},t)\,\}\;=\;-i\delta_{ab}\,\delta^{(3)}(\vec{x}-\vec{y}) \tag{2.8}$$

Transforming the field operators and state vectors into the Dirac picture with the time evolution operator $U(t,t_0)$, and denoting quantities in this picture with a hat, one arrives at the following differential equation for this operator

$$U(t,t_0) = e^{-i\mathcal{H}_0(t-t_0)}$$

$$i\frac{\partial}{\partial t}U(t,t_0) = \hat{H}_{int}(t)\,U(t,t_0) \tag{2.9}$$

$\hat{H}_{int}(t)$ satisfies the same differential equation as $H_{int}(t)$ if all the arguments in (2.5) are transformed into the Dirac picture. The field operators in the Dirac picture satisfy the non-interacting field equations, given by

$$(i\gamma_\mu\partial^\mu - m)\,\hat{\psi} \;=\; \hat{\bar{\psi}}\left(i\gamma_\mu\,\overleftarrow{\partial^\mu} + m\right) \;=\; 0 \tag{2.10}$$

$$\Box\hat{\boldsymbol{A}}^\mu + (\lambda-1)\partial^\mu\partial_\nu\hat{\boldsymbol{A}}^\nu = 0 \tag{2.11}$$

$$\Box\hat{\omega} = \Box\hat{\chi} = 0 \tag{2.12}$$

The properties of QCD which have been discussed so far have been of a rather general nature, and apply regardless of the volume of space occupied by the fields. It is appropriate at this point to consider only a finite volume of space and specialize to cavity QCD. Effectively, this amounts to the introduction of confinement by hand, and is done by imposing boundary conditions on the fields at some surface S. The boundary conditions must be compatible with the field equations, and are chosen by requiring that no colour charge leaks through the surface S. In the case of a static, spherically symmetric cavity, these boundary conditions are simply those of the MIT bag model [2]:

$$\left(in_k\gamma^k - 1\right)\hat{\psi}\Big|_S \;=\; \hat{\bar{\psi}}\left(in_k\gamma^k + 1\right)\Big|_S \;=\; 0 \tag{2.13}$$

$$n_k\left(\partial^k\hat{\boldsymbol{A}}^\nu - \partial^\nu\hat{\boldsymbol{A}}^k\right)\Big|_S \;=\; n_k\hat{\boldsymbol{A}}^k\Big|_S \;=\; n_k\partial^k\left(\partial_\nu\hat{\boldsymbol{A}}^\nu\right)\Big|_S \;=\; 0 \tag{2.14}$$

$$n_k\partial^k\hat{\omega}\,\Big|_S = n_k\partial^k\hat{\chi}\,\Big|_S = 0 \tag{2.15}$$

The solutions to eqs. (2.10) and (2.11) with the boundary conditions (2.13) and (2.14) are the well-known quark and gluon cavity modes, which may be found in appendix A.

2.2 The Quark Propagator

The quark field ψ may be expanded in the complete set of cavity modes

$$\hat{\psi}_{cf}(x) = \sum_{\substack{\kappa\mu\\ \nu>0}}\left[\hat{a}_{cfn}u_n(\vec{x})e^{-i\varepsilon_n t} + \hat{b}^\dagger_{cfn}u_{-n}(\vec{x})e^{i\varepsilon_n t}\right] \tag{2.16}$$

where $n \equiv \{\nu, \kappa, \mu\}$ is the set of quantum numbers characterizing the radial, angular momentum and magnetic quantum numbers of the quark respectively. The expansion coefficients $\hat{a}$ and $\hat{b}^\dagger$ are quark annihilation and antiquark creation operators respectively. The spinors $\bar{u}_n(\vec{x})$ and $u_n(\vec{x})$ are solutions to the non-interacting field equations (2.10) with the MIT boundary conditions (i.e. the quark cavity modes), and ε_n is the energy of the mode.

The propagator is defined as the time-ordered product of the fields

$$iS(x_1, x_2) = \left\langle \hat{0} \left| T\left[\hat{\psi}_{cf}(x_1)\hat{\bar{\psi}}_{c'f'}(x_2)\right] \right| \hat{0} \right\rangle \tag{2.17}$$

$$= \delta_{cc'}\,\delta_{ff'} \sum_{\substack{\kappa\mu \\ \nu>0}} \left[u_n(\vec{x}_1)\bar{u}_n(\vec{x}_2)\Theta(t_1 - t_2) - u_{-n}(\vec{x}_1)\bar{u}_{-n}(\vec{x}_2)\Theta(t_2 - t_1)\right] e^{-i\varepsilon_n|t_1 - t_2|}$$

where the spinor indices have been suppressed. Using the integral representation of the theta function,

$$\Theta(t) = \lim_{\epsilon \to 0} \frac{-1}{2\pi i} \int_{-\infty}^{\infty} d\omega \, \frac{e^{-i\omega t}}{\omega + i\epsilon} \tag{2.18}$$

the propagator may be written in the following way:

$$iS(x_1, x_2) = i\delta_{cc'}\,\delta_{ff'} \sum_n u_n(\vec{x}_1)\bar{u}_n(\vec{x}_2) \int \frac{d\omega}{2\pi} \frac{e^{-i\omega(t_1 - t_2)}}{\omega - \varepsilon_n \pm i0} \tag{2.19}$$

The sum over n now includes both positive and negative radial quantum numbers. The usual Feynman prescription for the poles should be employed when performing the contour integral, as indicated by the $\pm i0$. In other words, poles with positive energy are given a small, imaginary negative part while the negative energy poles acquire a positive imaginary part. Of course, the propagator is a Green's function of the Dirac equation

$$(i\partial\!\!\!/_x - m)\, S(x, y) = \delta^{(4)}(x, y) \ . \tag{2.20}$$

2.3 The Gluon Propagator

In a similar way, the gluon field may be expanded in the complete set of cavity modes

$$\hat{A}^\mu_a(x) = \sum_{m\Sigma} \frac{1}{\sqrt{2\Omega^\Sigma_m}} \left[\hat{c}^\Sigma_{am} a^\mu_{m\Sigma}(\vec{x}) e^{-i\Omega^\Sigma_m t} + \hat{c}^{\Sigma\dagger}_{am} a^{\mu\,*}_{m\Sigma}(\vec{x}) e^{i\Omega^\Sigma_m t}\right] \tag{2.21}$$

Here, the functions $a^\mu_{m\Sigma}(\vec{x})$ are the gluon cavity modes, where $m \equiv \{N, J, M\}$ denotes the radial, angular momentum and magnetic quantum numbers, and the label $\Sigma \equiv \mathcal{S}, \mathcal{L}, \mathcal{M}, \mathcal{E}$ denotes the scalar, longitudinal, transverse magnetic and transverse electric polarizations of the gluon respectively. The propagator in the Feynman gauge

($\lambda = 1$) is then

$$iD^{\mu\nu}_{ab}(x_1,x_2) = \left\langle \hat{0} \left| T\left\{ \hat{A}^{\mu}_{a}(x_1)\hat{A}^{\nu}_{b}(x_2) \right\} \right| \hat{0} \right\rangle \tag{2.22}$$

$$= -\delta_{ab} \sum_{m\Sigma} \frac{g^{\Sigma\Sigma}}{2\Omega^{\Sigma}_{m}} a^{\mu}_{m\Sigma}(\vec{x}_1) a^{\nu\,*}_{m\Sigma}(\vec{x}_2)\, e^{-i\Omega^{\Sigma}_{m}|t_1-t_2|}$$

where $g^{\Sigma\Sigma}$ is the metric tensor in polarization space given by

$$g^{\mathcal{SS}} = -g^{\mathcal{LL}} = -g^{\mathcal{MM}} = -g^{\mathcal{EE}} = 1$$

$$g^{\Sigma\Sigma'} = 0\,, \qquad \Sigma \neq \Sigma' \tag{2.23}$$

At this point, it is useful to introduce a vector q^{Σ} in polarization space, which may be defined as

$$q^{\Sigma} \equiv (q^{\mathcal{S}}, q^{\mathcal{L}}, q^{\mathcal{M}}, q^{\mathcal{E}}) = (\omega, \Omega^{\Sigma}_{m}, 0, 0) \tag{2.24}$$

$$q_{\Sigma} = (\omega, -\Omega^{\Sigma}_{m}, 0, 0)$$

The vector, defined in this way, satisfies the requirement that

$$q^2 = \omega^2 - \left(\Omega^{\Sigma}_{m}\right)^2 \tag{2.25}$$

Using this definition of q^{Σ} and the integral representation of $\Theta(t)$, eq. (2.18), the Feynman gauge propagator may be written as

$$iD^{\mu\nu}_{ab}(x_1,x_2) = -i\delta_{ab} \sum_{m\Sigma} g^{\Sigma\Sigma}\, a^{\mu}_{m\Sigma}(\vec{x}_1) a^{\nu\,*}_{m\Sigma}(\vec{x}_2) \int \frac{d\omega}{2\pi} \frac{e^{i\omega(t_2-t_1)}}{q^2+i0} \tag{2.26}$$

The functions $D^{\mu\nu}_{ab}(x,y)$ satisfy the inhomogenous d'Alembert equations

$$\Box_x D^{\mu\nu}_{ab}(x,y) = \delta_{ab}\, g^{\mu\nu}\, \delta^{(4)}(x,y) \tag{2.27}$$

The gluon propagator in an arbitrary gauge plays an important part in many of the calculations performed here. The cavity version of the propagator in an arbitrary gauge was derived by Stoddart [8]

$$iD^{\mu\nu}_{ab}(x_1,x_2) = i\delta_{ab} \sum_{m\Sigma\Sigma'} a^{\mu}_{m\Sigma}(\vec{x}_1) a^{\nu\,*}_{m\Sigma'}(\vec{x}_2) \int \frac{d\omega}{2\pi} \left[\frac{-g^{\Sigma\Sigma'}}{q^2} - \frac{1-\lambda}{\lambda} \frac{q^{\Sigma} q^{\Sigma'}}{q^4} \right] e^{i\omega(t_2-t_1)} \tag{2.28}$$

2.4 The Gell-Mann and Low Theorem

The amplitude for some transition in the cavity, e.g. one-gluon exchange between quarks, is often expressed as the shift in energy induced by an interaction. In the

case of one-gluon exchange, say, the energy shift calculated would be the difference in energy between a state consisting of two non-interacting quarks, and the state in which the two quarks exchange a gluon. See Close and Horgan [9] for a discussion of this particular example.

The usual path to an expression for the energy level shifts is via the Gell-Mann and Low theorem [10], and the expression which is used most frequently is that given by Fetter and Walecka in their well-known book [11]. When energy shifts are calculated in this way, the Feynman diagrams representing the process are expanded in a series of time-ordered diagrams, and each time-ordered diagram has to be evaluated separately[1].

From the Gell-Mann and Low theorem, the energy shift is

$$E_k - E_k^{(0)} = \lim_{\epsilon \to 0} \frac{\langle\, \hat{\phi}_k \,|\, \hat{H}^{\epsilon}_{int}(0) U^{\epsilon}(-\infty, 0) \,|\, \hat{\phi}_k \,\rangle_c}{\langle\, \hat{\phi}_k \,|\, U^{\epsilon}(-\infty, 0) \,|\, \hat{\phi}_k \,\rangle_c} \tag{2.29}$$

where $U(t, t_0)$ is the time evolution operator defined in terms of the interaction Hamiltonian $H_{int}(t)$ and Wick's time-ordered product T by

$$U^{\epsilon}(-\infty, 0) \;=\; \sum_{n=0}^{\infty} \frac{(-i)^n}{n!} \int_{-\infty}^{0} dt_1 \cdots \int_{-\infty}^{0} dt_n T\left[\hat{H}^{\epsilon}_{int}(t_1) \cdots \hat{H}^{\epsilon}_{int}(t_n)\right] \tag{2.30}$$

In the equations above, the usual adiabatic damping of the interaction has been introduced, as indicated by the superscript ϵ. Explicitly, the damping factor is $\hat{H}^{\epsilon}_{int}(t) \equiv e^{-\epsilon|t|}\, \hat{H}_{int}(t)$. The subscript "c" indicates that only connected diagrams need be included in the sum, and $\hat{\phi}_k$ is an eigenvector of the non-interacting Hamiltonian; for example

$$\left|\, \hat{\phi}_k \right\rangle \sim \hat{a}^{\dagger}_{c_1 f_1 n_1} \hat{a}^{\dagger}_{c_2 f_2 n_2} \hat{a}^{\dagger}_{c_3 f_3 n_3} \left|\, \hat{0} \right\rangle$$

for a three-body wave function such as the proton. There is an equivalent form of the Gell-Mann and Low theorem, due to Sucher [12], which does not appear to be have been exploited before in cavity calculations. However, Mohr [13] has given a most satisfying account of the self-energy of an electron and the vacuum polarization in the strong electromagnetic field of a high-Z atom using this formulation. His work shows that this approach is eminently suitable for cavity calculations.

The energy shift in the Sucher formulation, given in terms of the dummy variable ξ, is

$$E_k - E_k^{(0)} \;=\; \lim_{\substack{\xi \to 1 \\ \epsilon \to 0}} \frac{i\epsilon}{2} \frac{\partial \langle\, \hat{\phi}_k \,|\, S_{\epsilon,\xi} \,|\, \hat{\phi}_k \,\rangle_c / \partial \xi}{\langle\, \hat{\phi}_k \,|\, S_{\epsilon,\xi} \,|\, \hat{\phi}_k \,\rangle_c} \tag{2.31}$$

$S_{\epsilon,\xi}$ is the adiabatic S-matrix and is closely related to the time evolution operator of eq. (2.30). Expanding $S_{\epsilon,\xi}$ in terms of the dummy variable ξ,

$$S_{\epsilon,\xi} \;=\; 1 + \sum_{n=1}^{\infty} S^{(n)}_{\epsilon,\xi}$$

[1] At the very least, the time integrals of each diagram must be evaluated separately.

the similarity to $U^\epsilon(t,t_0)$ is obvious:

$$S^{(n)}_{\epsilon,\xi} = \frac{(-i\xi)^n}{n!}\int_{-\infty}^{\infty} dt_1 \cdots \int_{-\infty}^{\infty} dt_n\, e^{-\epsilon|t_1|}\cdots e^{-\epsilon|t_n|}\, T\left[\hat{H}_{int}(t_1)\cdots\hat{H}_{int}(t_n)\right] \tag{2.32}$$

The benefit of using this expression is that the Feynman diagrams are no longer decomposed into time-ordered diagrams. This may be seen immediately from the symmetry of the limits in the time integrations appearing in the S matrix. However, the price one pays for this luxury is that the time integrations are often tedious and more difficult.

2.5 The Energy Shift to Order eg^2

The magnetic moment μ of a particle may be defined as the shift in energy $\Delta E = \vec{\mu}\cdot\vec{B}$ which it experiences when it is placed in an external electromagnetic field $\vec{B}$. With this definition of μ in terms of energy shifts, eq. (2.31) is particularly useful for calculating, up to any order in g, the radiative corrections to the magnetic moments of the proton and neutron. It is the first order in the strong coupling constant, or $O(eg^2)$, which is of interest here.

To this order, there are no gluon-gluon or ghost-gluon couplings which can be connected to the proton wave function, so the Hamiltonian describing the quark-gluon and quark-photon interactions is simply given by

$$\hat{H}_{int}(t) = -\int d^3x\, \bar{\psi}(\vec{x})\left[g\frac{\lambda_a}{2}\not{A}_a(\vec{x}) + Q\not{A}_{\rm ext}(\vec{x})\right]\psi(\vec{x}) \tag{2.33}$$

Q is the (electro-magnetic) charge matrix of the flavoured quarks, $A^\mu_{\rm ext}(x)$ is the potential due to the external magnetic field, $A^\mu_a(x)$ is a vector in 8-dimensional colour space describing the colour potential of the gluons and the λ_a's are the Gell-Mann matrices.

The energy shift, correct to $O(eg^2)$, may be obtained from eqs. (2.31), (2.32) and (2.33). Taking the limit $\xi \to 1$, one obtains

$$\Delta E = \lim_{\epsilon\to 0}\frac{i\epsilon}{2}\left[\langle S^{(1)}_\epsilon\rangle_{\rm c} + 2\langle S^{(2)}_\epsilon\rangle_{\rm c} + 3\langle S^{(3)}_\epsilon\rangle_{\rm c} - \langle S^{(1)}_\epsilon\rangle^2_{\rm c} + \langle S^{(1)}_\epsilon\rangle^3_{\rm c} - 3\langle S^{(1)}_\epsilon\rangle_{\rm c}\langle S^{(2)}_\epsilon\rangle_{\rm c}\right] \tag{2.34}$$

The terms of order eg^2 in the expression above which contribute to the baryon magnetic moment are

$$\Delta E^{(3)} = \lim_{\epsilon\to 0}\frac{3i\epsilon}{2}\left[\langle S^{(3)}_\epsilon\rangle_{\rm c} - \langle S^{(1)}_\epsilon\rangle_{\rm c}\langle S^{(2)}_\epsilon\rangle_{\rm c}\right] \tag{2.35}$$

since the other terms are not connected to the wave function of the baryons. The second term in eq. (2.35), $\langle S^{(1)}_\epsilon\rangle_{\rm c}\langle S^{(2)}_\epsilon\rangle_{\rm c}$, comes from the denominator of (2.31) and is possibly singular. It usually serves to cancel divergences in the first term which arise

from connected loop diagrams, or from poles which occur when energy denominators in convergent graphs vanish.

Concentrating on the first term contributing to $\Delta E^{(3)}$ in eq. (2.35), and omitting the spinor and colour indices, the energy shift is

$$\Delta E^{(3)} = -\lim_{\epsilon\to 0} \frac{3i\epsilon}{2}\frac{(-i)^3}{3!}\int d^4x_1 \int d^4x_2 \int d^4x_3\, e^{-\epsilon(|t_1|+|t_2|+|t_3|)} \times \tag{2.36}$$

$$\left\langle T\left[\left(\bar\psi(g\frac{\lambda_a}{2}\not{A}_a + Q\not{A}_{\rm ext})\psi\right)_{x_1}\left(\bar\psi(g\frac{\lambda_b}{2}\not{A}_b + Q\not{A}_{\rm ext})\psi\right)_{x_2}\left(\bar\psi(g\frac{\lambda_c}{2}\not{A}_c + Q\not{A}_{\rm ext})\psi\right)_{x_3}\right]\right\rangle_c$$

The time-ordered product in eq. (2.36) can now be decomposed into normal-ordered products using Wick's theorem. Leaving the details until chapter 4, we merely note here that the expression above contains 5 Feynman diagrams of $O(eg^2)$ and one of $O(e^3)$. The last diagram is purely a QED contribution, corresponding to a vacuum polarization insert in the vertex graph. Since it is a QED diagram, it is suppressed by a factor of $\alpha \approx 1/137$, and is not included here.

Chapter 3

The Vertex Correction in Free Space

It is well known that the vertex correction and self-energy graphs contain ultra-violet divergences (see, for example, [14] and [15]) which must be regularized before they yield physically meaningful results. In this chapter, the calculation of the the vertex correction in free space will be reviewed, with special emphasis being placed on the method of regularizing the divergences. This free-space calculation will provide a model which will be closely followed when the cavity calculation of this graph is performed.

An important point to note here is that some of the quantitative results obtained in free space may be used in the cavity. The ultra-violet divergences are a large momentum, and thus short distance, phenomenon. On the other hand, the radius of the cavity is comparatively very large, and one does not expect the boundary conditions on the surface to affect the short distance singularities. In other words, the ultra-violet divergences should be precisely the same in the cavity as in free space. Thus, if one can parametrize the free space divergence in some fashion, e.g. $1/\epsilon$ for some parametric variable $\epsilon \to 0$, then exactly the same parametrization of the divergence should hold in the cavity.

In some recent work by A. J. Stoddart, the idea of using free-space expressions in the cavity has been developed upon to yield quantitative results. After isolating and parametrizing the free-space ultra-violet divergences for some diagrams using dimensional regularization, Stoddart uses these parametric forms to renormalize the less tractable cavity diagrams. For a full discussion of this technique, see [7] and [8]. This procedure will not be used here—instead, the free-space results will be used to check the cavity calculation.

Figure (3.1) shows the three $O(eg^2)$ contributions to the anomalous magnetic moment of a quark. It will be shown in the following sections that the divergences occurring in these three graphs cancel when they are summed, and that the sum is also gauge-independent.

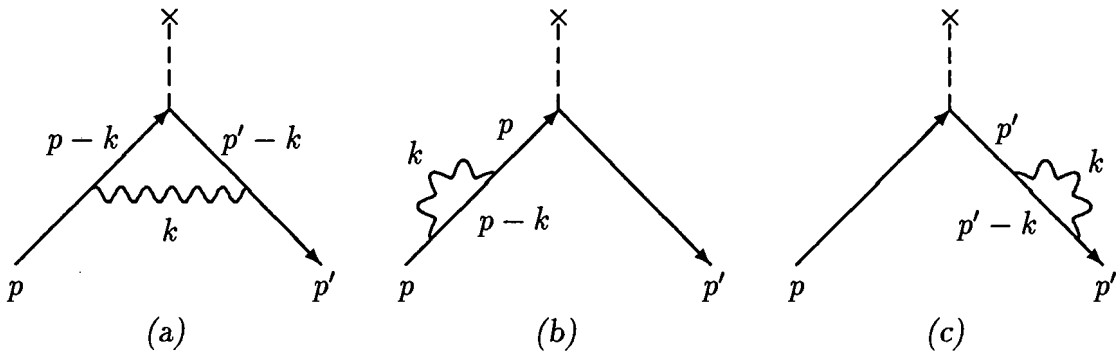

Figure 3.1: *Feynman diagrams contributing to the anomolous magnetic moment of a quark. The cross and dashed line denote the external electromagnetic source, and the gluons are indicated by the wavy lines.*

3.1 Cancellation of Divergences

A convenient starting point for demonstrating explicitly how the divergences in the loop diagrams of fig. (3.1) cancel is with the Feynman amplitudes for these graphs. The Feynman amplitudes are given by

$$\mathcal{M}^a = eg^2 C\, \bar{u}(p')\, \Lambda_\mu(p', p, q)\, u(p) A^\mu_{\rm ext}(q) \tag{3.1}$$

$$\mathcal{M}^b = eg^2 C\, \bar{u}(p')\, i\gamma_\mu\, iS(p)\Sigma(p)\, u(p) A^\mu_{\rm ext}(q) \tag{3.2}$$

$$\mathcal{M}^c = eg^2 C\, \bar{u}(p')\, \Sigma(p')\, iS(p')\, i\gamma_\mu\, u(p) A^\mu_{\rm ext}(q) \tag{3.3}$$

where $A^\mu_{\rm ext}(q)$ is the potential due the external magnetic field and C is a colour factor given by

$$C = \sum_a \left(\frac{\lambda_a}{2}\right)_{\alpha\beta} \left(\frac{\lambda_a}{2}\right)_{\beta\gamma} = \frac{4}{3}\delta_{\alpha\gamma} \tag{3.4}$$

The vertex function $\Lambda^\mu(p', p, q)$ and the quark self energy $\Sigma(p)$ in D-dimensions are:

$$\Lambda^\mu(p', p, q) = \int \frac{d^D k}{(2\pi)^D} (i\gamma_\alpha)\, iS(p' - k)(i\gamma^\mu)\, iS(p - k)(i\gamma_\beta)\, iD^{\alpha\beta}(k) \tag{3.5}$$

$$\Sigma(p) = \int \frac{d^D k}{(2\pi)^D} (i\gamma_\alpha)\, iS(p - k)(i\gamma_\beta)\, iD^{\alpha\beta}(k) \tag{3.6}$$

We have been a bit sloppy in the expressions above in that the arbitrary mass parameter μ^{4-D}, which is required if the coupling constant g is to remain dimensionless, has been omitted. However, the only results which are needed are in $D = 4$ dimensions, where this factor approaches 1 when the overall diagram is finite. Hopefully, the

omission of this intermediate factor will make formulae more transparent to the eye. In terms of the gauge parameter λ, the gluon propagator is

$$D^{\mu\nu}(k) = -\frac{g^{\mu\nu}}{k^2 + i0} - \frac{1-\lambda}{\lambda}\frac{k^\mu k^\nu}{k^4 + i0} \tag{3.7}$$

We shall often talk about the gauge-independent (or gauge-dependent) part of an expression. By this, we mean the part of the expression containing the first (or second) term of the gluon propagator (3.7). We have tried to avoid using the term 'Feynman propagator' ($\lambda = 1$) for the first term since it implies that we are working in a specific gauge. However, the full propagator will be used in *all* calculations performed in this work.

In order to show that the gauge-independent, divergent parts of eqs. (3.1), (3.2) and (3.3) cancel, the divergent pieces of $\Lambda^\mu(p', p, q)$ and $\Sigma(p)$ must first be extracted using dimensional regularization. It turns out that the divergent part of the vertex function is independent of both the mass of the quark and the momentum transfer q of the external field. To simplify the derivation here, m and q are set to zero at the outset. The quark mass will remain at zero for the rest of this chapter. Note: the definitions of Λ^μ and Σ above may differ by a factor of $-i$ from some other definitions used in the literature.

Substituting the quark propagator and the gauge-independent part of the gluon propagator into (3.5), one has

$$\Lambda^\mu(p,p) = \int \frac{d^Dk}{(2\pi)^D}\gamma_\alpha \frac{1}{\not p - \not k}\gamma^\mu \frac{1}{\not p - \not k}\gamma_\beta \frac{g^{\alpha\beta}}{k^2} = \int \frac{d^Dk}{(2\pi)^D}\frac{\gamma_\nu(\not p - \not k)\gamma^\mu(\not p - \not k)\gamma^\nu}{(p-k)^2(p-k)^2k^2} \tag{3.8}$$

where the factors of $(p-k)^2$ in the denominator are written separately since they are potentially different (recall that we have let $p' = p$ for the purpose of this calculation). With the help of some Diracology,

$$\gamma_\nu \not a \gamma^\mu \not a \gamma^\nu = (2-D)(2a^\mu \not a - \gamma^\mu a^2) \tag{3.9}$$

the vertex function becomes

$$\Lambda^\mu(p,p) = (2-D)\int \frac{d^Dk}{(2\pi)^D}\left[\frac{2(\not p - \not k)(p-k)^\mu - \gamma^\mu(\not p - \not k)^2}{(p-k)^2(p-k)^2k^2}\right] \tag{3.10}$$

The usual trick now is to rotate k and p to Euclidean space, $k^0 \to ik^0$ and $p^0 \to ip^0$, then elevate the denominators into an exponential factor using

$$\frac{1}{(p-k)^2} = \int_0^\infty dz\, e^{-z(p-k)^2} \tag{3.11}$$

for each factor in the denominator. Λ^μ can now be written as

$$\Lambda^\mu(p,p) = -i(2-D)\int \frac{d^Dk}{(2\pi)^D}\int_0^\infty dr \int_0^\infty ds \int_0^\infty dt \times \tag{3.12}$$

$$\left[2(\not p - \not k)(p-k)^\mu + \gamma^\mu(\not p - \not k)^2\right] e^{-rk^2 - (s+t)(k-p)^2}$$

It is convenient to make two successive shifts of variables, which bring the argument of the exponent into a more useful form

$$k \to k' + \frac{p(s+t)}{r+s+t} = k' + p - \frac{pr}{r+s+t} \tag{3.13}$$

$$r \to z(1-x-y) \quad , \qquad s \to zx \quad , \qquad t \to zy \tag{3.14}$$

The exponent in eq. (3.12) becomes $zk'^2 + p^2 z(x+y)(1-x-y)$ using these transformations. The integral over k' is now a standard Gaussian integral and may be performed immediately to yield

$$\Lambda^\mu(p,p) = -i(2-D)\int_0^1 dx \int_0^{1-x} dy \int_0^\infty dz\, z^2 \left(\frac{1}{4\pi z}\right)^{D/2} \left[\frac{\gamma^\mu}{z}\left(1-\frac{D}{2}\right)\right. \tag{3.15}$$

$$\left. + (1-x-y)^2(2\not{p}p^\mu - \gamma^\mu p^2)\right] e^{-zp^2(x+y)(x+y-1)}$$

where the result has been rotated back into Minkowski space. The z-integration is in the form of another standard integral, the gamma function Γ, and also may be evaluated immediately

$$\Lambda^\mu(p,p) = \frac{-i(2-D)}{(4\pi)^{D/2}} \int_0^1 dx \int_0^{1-x} dy \tag{3.16}$$

$$\left[\gamma^\mu\left(1-\frac{D}{2}\right)\left[p^2(x+y)(x+y-1)\right]^{D/2-2}\Gamma(2-D/2)\right.$$

$$\left. + (1-x-y)^2(2\not{p}p^\mu - \gamma^\mu p^2)\left[p^2(x+y)(x+y-1)\right]^{D/2-3}\Gamma(3-D/2)\right]$$

Setting $D = 4-2\epsilon$ where ϵ is small (we are discarding powers of ϵ^n, $n \geq 1$), and evaluating the remaining integrals, one arrives at

$$\Lambda^\mu(p,p) = -\frac{i}{16\pi^2}\left[\gamma^\mu\left(\frac{1}{\epsilon} - \gamma + 1 - \ln(-p^2/4\pi)\right) - \frac{2\not{p}p^\mu}{p^2}\right] \tag{3.17}$$

where γ is Euler's constant. The troublesome term $1/\epsilon$, originating from the factor $\Gamma(2-D/2) = \Gamma(\epsilon)$ in the first term of (3.17), has now been isolated. Restoring the integral representation of the gamma function, the singular part (denoted by a subscript S) of Λ^μ in 4-dimensional space may be parametrized as

$$\Lambda^\mu_S = -\frac{i\gamma^\mu}{16\pi^2}\int_0^\infty dz\, \frac{e^{-z}}{z} \tag{3.18}$$

In other words, if $\Lambda^\mu(p',p,q)$ was calculated as a function of the parameter z, then one would see that $\Lambda^\mu(z)$ diverges as $1/z$ for small z. Furthermore, if the vertex function in a cavity is calculated, then it should also diverge according to (3.18). This will turn out to be an important diagnostic for the cavity calculation.

The quark self-energy $\Sigma(p)$ can be calculated in exactly the same manner. Sparing the reader the details, it is given by

$$\Sigma(p) = -\frac{i\not{p}}{16\pi^2}\left[\frac{1}{\epsilon} - \gamma + 1 - \ln(-p^2/4\pi)\right] \tag{3.19}$$

The singular part $\Sigma_S(p)$ of (3.19) is the same as Λ^μ_S, given in (3.18), if γ^μ is replaced by $\not{p}$. This is to be expected since, for zero momentum transfer, the vertex function $\Lambda^\mu(p', p, q = 0) = \Lambda^\mu(p, p)$ is related to $\Sigma(p)$ through the Ward identity

$$\Lambda^\mu(p, p) = \frac{\partial \Sigma(p)}{\partial p_\mu} \tag{3.20}$$

Armed with the explicit forms of Λ^μ_S and Σ_S, we are now in a position to show that the singular, gauge-independent parts of $\mathcal{M}^a + \mathcal{M}^b + \mathcal{M}^c$ vanish. Substituting the singular part of $\Sigma(p)$ into (3.2), and remembering that we are working with massless quarks for the present, the singular part $\mathcal{M}^b_S$ becomes

$$\mathcal{M}^b_S = ieg^2 C\, \bar{u}(p')\, \gamma_\mu \frac{1}{\not{p}}\, B\, \not{p}\, u(p) A^\mu_{\text{ext}}(q) \tag{3.21}$$

where B is the divergent constant $\Gamma(\epsilon)/16\pi^2$, and the finite contributions have been neglected. Unfortunately, eq. (3.21) is indeterminate as it stands. This is easily seen since the result of $\not{p}$ acting on a free particle spinor $u(p)$ is zero, but if the $\not{p}$'s in the numerator and denominator are allowed to cancel before acting on the spinor, the result is proportional to $u(p)$. This particular problem was solved by Feynman [16] with the introduction of adiabatic damping of the interaction—a factor so far omitted in this section, although it was included when the energy shifts in cavity QCD were discussed. We more or less follow Feynman's argument here.

The damping factor $e^{-\epsilon|t|}$ of the last chapter has the properties that it tends to zero as $t \to \pm\infty$, and is ~ 1 for a time T which is much longer than the interaction time. It is these properties of the damping factor which are important, not the actual form, so we may generalize to a function $g(t)$ with these properties. Fourier transforming $g(t)$ into momentum space,

$$g(t) = \int_{-\infty}^{\infty} dE\, G(E) e^{iEt} = \int_{-\infty}^{\infty} dE\, G(E) e^{isx} \tag{3.22}$$

with $s \equiv (E, \vec{0})$, one sees that $G(E)$ is almost a δ-function, and is normalized such that $g(0) = \int dE\, G(E) = 1$. When the Fourier-transformed damping factor is included in the interaction Hamiltonian, the self-energy and quark propagator are replaced by

$$\Sigma(p) \to \Sigma(p - s) \qquad , \qquad \frac{1}{\not{p}} \to \frac{1}{\not{p} - \not{s} - \not{s}'}$$

The propagator has one factor of s more than the self-energy since it is of order eg^2. The Feynman amplitude (3.21) becomes

$$\mathcal{M}^b_S = ieg^2 C \bar{u}(p') \int dE\, dE'\, G(E) G(E')\, \gamma_\mu \frac{1}{\not{p} - \not{s} - \not{s}'} B(\not{p} - \not{s})\, u(p) A^\mu_{\text{ext}}(q) \tag{3.23}$$

One of the ways of evaluating the integral is to subtract a factor of $\frac{1}{2}\not{p}u(p)$ from the numerator, which may be done since $\not{p}u(p) = 0$. This allows one to make the substitution

$$(\not{p}-\not{k}) \rightarrow (\not{p}-\not{k}) - \tfrac{1}{2}\not{p} = \tfrac{1}{2}(\not{p} - 2\not{k})$$

Furthermore, the factor of $2\not{k}$ may be symmetrized by making the replacement $2\not{k} \rightarrow \not{k}+\not{k}'$. The integral is now straight-forward, and yields

$$\mathcal{M}_S^b = ieg^2C\,\bar{u}(p')\,\frac{\gamma_\mu B}{2}\,u(p)A^\mu_{\rm ext}(q) \tag{3.24}$$

The factor of $\frac{1}{2}B$ is particularly important and should be noted. The same result holds for $\mathcal{M}_S^c$, so that the sum of these two terms contains a factor of exactly B.

The Feynman amplitude $\mathcal{M}_S^a$ for the singular part of the vertex correction follows immediately from (3.1) and (3.18), and is given by

$$\mathcal{M}_S^a = -ieg^2C\,\bar{u}(p')\,\gamma_\mu B\,u(p)A^\mu_{\rm ext}(q) \tag{3.25}$$

This is exactly cancelled by the singularities arising from the two graphs containing self-energy inserts, i.e. the gauge-independent part of $\mathcal{M}_S^a + \mathcal{M}_S^b + \mathcal{M}_S^c$ is zero.

3.2 Gauge Dependence

The problem of the gauge-dependent contributions to the graphs shown in figure (3.1) remains to be investigated. That will be done in this section, where it will be shown that these contributions vanish identically. This is rather nice since the observables calculated from these three graphs are independent of the gauge used[1].

The Feynman amplitude for the gauge-dependent part of the vertex correction graph is

$$\mathcal{M}^a = eg^2C\left(\frac{1-\lambda}{\lambda}\right)\int\frac{d^Dk}{(2\pi)^D}\,\bar{u}(p')\,\gamma_\alpha\frac{1}{\not{p}'-\not{k}}\gamma_\mu\frac{1}{\not{p}-\not{k}}\gamma_\beta\frac{k^\alpha k^\beta}{k^4}\,u(p)A^\mu_{\rm ext}(q) \tag{3.26}$$

The integral above is much simplified if the $\not{p}$'s are first allowed to act on the free particle spinors, since $\not{p}u(p) = 0$ and $p^2 = 0$. Concentrating on the Dirac algebra in (3.26) for the moment, we have

$$\begin{aligned}\bar{u}(p')\,\gamma_\alpha\frac{1}{\not{p}'-\not{k}}\gamma_\mu\frac{1}{\not{p}-\not{k}}\gamma_\beta\frac{k^\alpha k^\beta}{k^4}\,u(p) &= \bar{u}(p')\,\frac{\not{k}(\not{p}'-\not{k})\gamma_\mu(\not{p}-\not{k})\,\not{k}}{(p'-k)^2(p-k)^2k^4}\,u(p)\\ &= \bar{u}(p')\,\frac{(2k\cdot p'-\not{p}'\not{k}-k^2)\,\gamma_\mu\,(2k\cdot p-\not{k}\not{p}-k^2)}{(k^2-2k\cdot p')(k^2-2k\cdot p)k^4}\,u(p)\end{aligned} \tag{3.27}$$

[1] I would like to thank Dr. Gary Tupper for pointing this out to me.

where p^2 has been set to zero. Letting $\not{p}'$ act to the left on the spinor $\bar{u}(p')$, and $\not{p}$ to the right on $u(p)$ in (3.27) produces a result of zero, and that allows one to cancel the remaining terms in the numerator and denominator, leaving only the factor of $1/k^4$. Hence, after rotating to Euclidean space, eq. (3.26) reduces to

$$\begin{aligned}\mathcal{M}^a &= ieg^2C\left(\frac{1-\lambda}{\lambda}\right)\bar{u}(p')\,\gamma_\mu\,u(p)A^\mu_{\rm ext}(q)\int\frac{d^Dk}{(2\pi)^D}\,\frac{1}{k^4}\\ &= i\left(\frac{1-\lambda}{\lambda}\right)\left(\frac{eg^2C}{16\pi^2}\right)\bar{u}(p')\,\gamma_\mu\,u(p)A^\mu_{\rm ext}(q)\int dz\,\frac{1}{z}\end{aligned}\tag{3.28}$$

3.2.1 The Gauge-Dependent Part of the Self-Energy Insert

The gauge-dependent part of the graph which contains a self-energy insert, fig. (3.1b), may readily be calculated. It is given by

$$\Sigma(p) = -\left(\frac{1-\lambda}{\lambda}\right)\int\frac{d^Dk}{(2\pi)^D}\,\gamma_\alpha\frac{1}{\not{p}-\not{k}}\gamma_\beta\frac{k^\alpha k^\beta}{k^4} = -\left(\frac{1-\lambda}{\lambda}\right)\int\frac{d^Dk}{(2\pi)^D}\,\frac{\not{k}(\not{p}-\not{k})\not{k}}{(k-p)^2k^4}\tag{3.29}$$

Using the properties of the Dirac matrices to reduce the numerator, and rotating to Euclidean space, (3.29) becomes

$$\Sigma(p) = i\left(\frac{1-\lambda}{\lambda}\right)\int\frac{d^Dk}{(2\pi)^D}\,\frac{p^2\not{k}+k^2\not{p}}{(k-p)^2k^4}\tag{3.30}$$

where terms which integrate to zero have been dropped. The procedure now is similar to that used when evaluating $\Lambda^\mu(p,p)$: i.e. elevate the denominators into exponential factors; shift the variables with (3.13) and (3.14); and evaluate the Gaussian integral. Hence, (3.30) becomes

$$\Sigma(p) = i\left(\frac{1-\lambda}{\lambda}\right)\not{p}\int_0^\infty dz\,z^2\int_0^1 dt\,(1-t)\left[\frac{D}{2z}+p^2t(t-1)\right]\left(\frac{1}{4\pi z}\right)^{D/2}e^{-zp^2t(1-t)}\tag{3.31}$$

Once again, $\Sigma(p)$ has the form $\not{p}A$, where A contains a singular piece independent of p^2, and a finite piece which depends explicitly on p^2. This differs from the gauge-independent part only in the factor $(1-\lambda)/\lambda$. Hence, when (3.31) is substituted into (3.2), the result is indeterminate for the reasons given in the previous section. The cure for this problem is the introduction of adiabatic damping factors. Following the previous arguments, we immediately arrive at, in $D = 4$ dimensions

$$\begin{aligned}\mathcal{M}^b &= -eg^2C\,\bar{u}(p')\,\gamma_\mu\frac{A}{2}\,u(p)A^\mu_{\rm ext}(q)\\ &= -i\left(\frac{1-\lambda}{\lambda}\right)\left(\frac{eg^2C}{16\pi^2}\right)\bar{u}(p')\,\gamma_\mu\int_0^\infty dz\int_0^1 dt\,(1-t)\left[\frac{1}{z}+\frac{p^2t(t-1)}{2}\right]\\ &\quad e^{-zp^2t(1-t)}\,u(p)A^\mu_{\rm ext}(q)\end{aligned}\tag{3.32}$$

Since $p^2 = 0$ for the on-shell quarks, this reduces to

$$\mathcal{M}^b = -\frac{i}{2}\left(\frac{1-\lambda}{\lambda}\right)\left(\frac{eg^2C}{16\pi^2}\right)\bar{u}(p')\,\gamma_\mu\,u(p)A^\mu_{\text{ext}}(q)\int_0^\infty dz\,\frac{1}{z} \tag{3.33}$$

This result also holds for the gauge-dependent part of $\mathcal{M}^c$. Thus, inspection of (3.28) and (3.33) shows that $\mathcal{M}^b + \mathcal{M}^c$ exactly cancels $\mathcal{M}^a$.

In summary, it has been shown here that all the divergences appearing in the one-loop vertex graphs cancel in free space. Furthermore, the gauge-dependent parts vanish identically. These results are well known, but have been repeated here to remind the reader of the mathematical methods used to control the singularities in free space, since they will be used again in the cavity calculation.

Chapter 4

Loop Diagrams in Cavity QCD

The full expression for the $O(eg^2)$ energy shift in the cavity was given in eq. (2.36) in chapter 2. Using Wick's theorem, the time-ordered product of the fields in that expression may be contracted in all possible ways to yield the sum of normal-ordered products. Of these, some are not connected to our asymptotic three-body states and must be discarded. The remaining terms with the same spatial structure can then be gathered together in groups of 6 and represented by the Feynman diagrams shown in figure (4.1).

The three divergent graphs shown in figure (4.1a–c) will be examined closely in this chapter. Discussion of the two finite, one-gluon exchange graphs (4.1d) and (4.1e) will be deferred until the next chapter.

4.1 The Cavity Vertex Correction

Recall that two equivalent forms of the Gell-Mann and Low theorem for energy shifts were given in §2.4. While the first expression (2.29) leads to a series of time-ordered diagrams for each Feynman graph, this can be avoided if the second form, eq. (2.31), is used. The latter does not appear to have been used before in cavity QCD. In this section, both forms shall be used as a demonstration of the relative merits of each method.

Let us start with the Sucher form of the Gell-Mann and Low theorem. The energy shift for the Feynman graph (4.1a) corresponding to the vertex correction is given by

$$\Delta E_{\rm a} = -\lim_{\epsilon\to 0}\frac{3i\epsilon}{2}\frac{(-i)^3}{3!}\int d^4x_1\int d^4x_2\int d^4x_3\, e^{-\epsilon(|t_1|+|t_2|+|t_3|)} \tag{4.1}$$

$$\times\left\langle N\left[\left(\bar\psi g\frac{\lambda_a}{2}\not{A}_a\psi\right)_{x_1}\left(\bar\psi\, Q\not{A}_{\rm ext}\psi\right)_{x_2}\left(\bar\psi g\frac{\lambda_b}{2}\not{A}_b\psi\right)_{x_3}\right]\right\rangle_{\rm c}$$

where one of the possible contractions has been indicated. Since the limits of the time

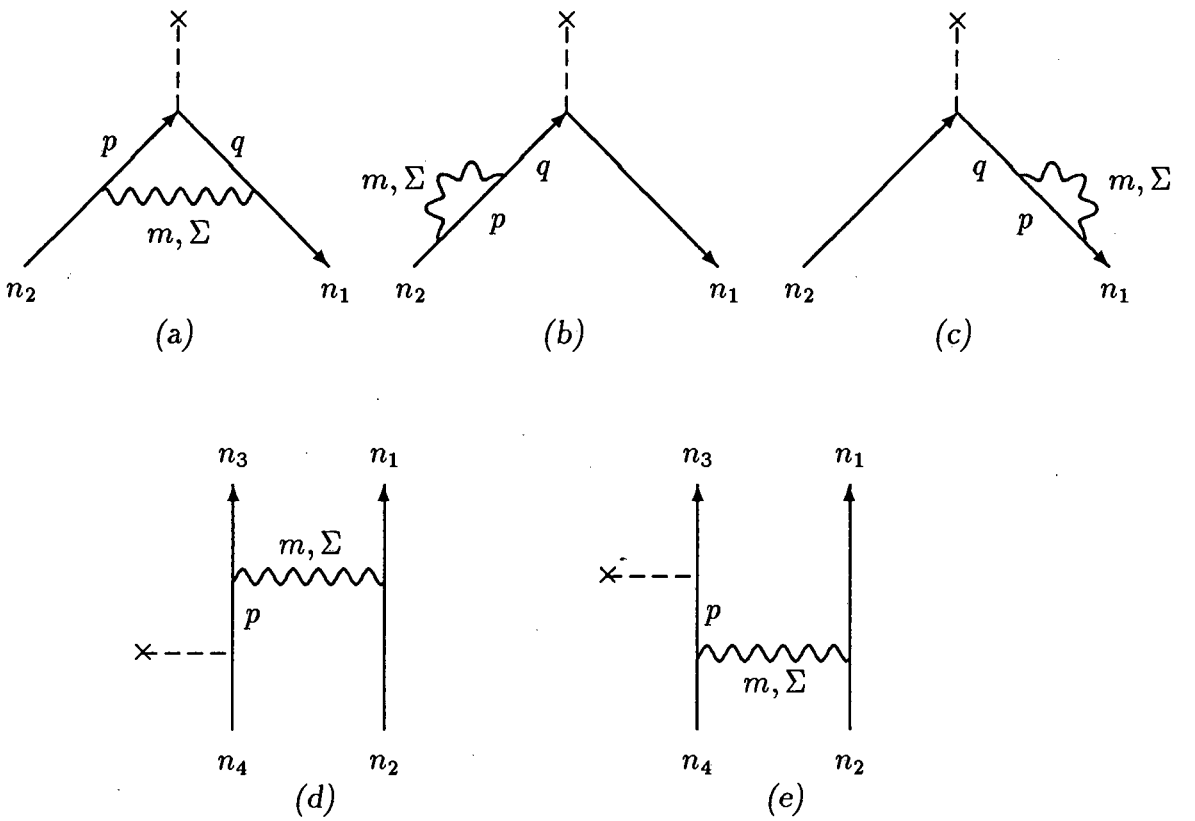

Figure 4.1: *Feynman diagrams contributing to the baryon magnetic moments. The intermediate quarks are labelled by p and q, and the gluon by* m, Σ.

integrals are symmetric, there are 6 equivalent permutations of the space-time labels x_1, x_2 and x_3, so we may use the one contraction shown above and omit the factor of 1/3!, thus including all the permutations. One should note that this expression is essentially $-i$ times the Feynman amplitude for the process, with the adiabatic damping factors written out explicitly.

Substituting in the cavity mode expansion of the fields, and inserting the cavity quark propagator (2.19) and the gauge-independent part of the gluon propagator, (2.26), this becomes

$$\Delta E_{\rm a} = \lim_{\epsilon\to 0} \frac{3i\epsilon}{2} g^2 \left\langle \hat{a}^\dagger_{c'f'n_1} \left(\frac{\lambda^a}{2}\right)_{c'd} \left(\frac{\lambda^a}{2}\right)_{dc} Q\, \hat{a}_{cfn_2} \right\rangle \sum_{pqm\Sigma} g^{\Sigma\Sigma} \int dt_1\, dt_2\, dt_3 \int \frac{d\omega}{2\pi} \frac{d\omega'}{2\pi} \frac{d\omega''}{2\pi}$$

$$\frac{e^{-\epsilon(|t_1|+|t_2|+|t_3|)}\, e^{it_1(\varepsilon_1+\omega-\omega')}\, e^{it_2(\omega'-\omega'')}\, e^{it_3(\omega''-\omega-\varepsilon_2)}}{(\omega'-\varepsilon_p \pm i0)(\omega''-\varepsilon_q \pm i0)(\omega^2-\Omega^{\Sigma\,2}_m + i0)} \int d^3x_1\, \bar{u}_{n_1}(x_1)\gamma_\mu u_p(x_1) a^{\mu\,*}_{m\Sigma}(x_1)$$

$$\int d^3x_2\, \bar{u}_p(x_2)\gamma_\lambda u_q(x_2) A^\lambda_{\rm ext}(x_2) \int d^3x_3\, \bar{u}_q(x_3)\gamma_\nu u_{n_2}(x_3) a^\nu_{m\Sigma}(x_3) \qquad (4.2)$$

To reduce somewhat the proliferation of indices, the energy of the outgoing quark has been written as ε_1 instead of ε_{n_1}, and for the same reason, the energy of the intermediate gluon will henceforth be written as Ω instead of Ω_m^Σ. No confusion should result since there is only one intermediate gluon in the diagram. The $\pm i0$ prescription will be assumed implicit in the propagators, and the summation over the labels $c'f'n_1$ and cfn_2 (i.e. colour, flavour and cavity modes) is also assumed. The expectation value of the colour, charge and creation/annihilation operators is given in appendix E, and will henceforth be discarded from the formulae until needed. The vertex integrals over the space co-ordinates will be written in the short-hand form introduced in appendix B, eq. (B.1). The energy shift (4.2) can now be written in a more compact form as

$$\Delta E_{\mathrm{a}} = \lim_{\epsilon\to 0} -\frac{3i\epsilon}{2}\frac{1}{(2\pi)^3} g^2 \sum_{pqm\Sigma} g^{\Sigma\Sigma}\, \tilde{Q}^{m\Sigma}_{n_1 p}\, M_{pq}\, Q^{m\Sigma}_{qn_2} \times \tag{4.3}$$

$$\int_{-\infty}^{\infty} dt_1\, dt_2\, dt_3 \int_{-\infty}^{\infty} d\omega\, d\omega'\, d\omega'' \frac{e^{-\epsilon(|t_1|+|t_2|+|t_3|)}\, e^{it_1(\varepsilon_1+\omega-\omega')}\, e^{it_2(\omega'-\omega'')}\, e^{it_3(\omega''-\omega-\varepsilon_2)}}{(\omega'-\varepsilon_p)(\omega''-\varepsilon_q)(\omega^2-\Omega^2)}$$

The integrals $\int dt_i \int d\omega'\, d\omega''$ are fairly straight-forward to evaluate—they may be done in several different ways, all of which are more or less tiresome. The integral $\int d\omega$ is analogous to the free-space integral over the gluon momentum k, and is left until last.

To evaluate the integrals rigorously, we proceed as follows: perform the contour integrals over $d\omega'$ and $d\omega''$ to get the sum of 4 step functions involving the energy and time variables. It turns out that each term gives the same result (up to an energy Θ function) after integrating out all the time dependence, so we may concentrate on a particular term. For example, one of these terms is

$$I_1 = \lim_{\epsilon\to 0} \frac{3i\epsilon}{2} \int \frac{d\omega}{2\pi} \frac{\Theta(\varepsilon_p)\Theta(\varepsilon_q)}{\omega^2-\Omega^2} \int_{-\infty}^{\infty} dt_3 \int_{t_3}^{\infty} dt_2 \int_{t_2}^{\infty} dt_1 \times \tag{4.4}$$

$$e^{-\epsilon(|t_1|+|t_2|+|t_3|)}\, e^{it_1(\varepsilon_1+\omega-\varepsilon_p)}\, e^{it_2(\varepsilon_p-\varepsilon_q)}\, e^{it_3(\varepsilon_q-\omega-\varepsilon_2)}$$

After evaluating the three time integrals, and discarding terms which vanish in the limit $\epsilon \to 0$, this yields

$$I_1 = \lim_{\epsilon\to 0} \frac{3i\epsilon}{2} \int \frac{d\omega}{2\pi} \left[\frac{1}{[i(\varepsilon_1+\omega-\varepsilon_p)+\epsilon]\,[i(\varepsilon_1+\omega-\varepsilon_q)+2\epsilon]\,[i(\varepsilon_1-\varepsilon_2)+3\epsilon]} \right. \tag{4.5}$$

$$\left. - \frac{1}{[i(\varepsilon_1+\omega-\varepsilon_p)-\epsilon]\,[i(\varepsilon_1+\omega-\varepsilon_q)-2\epsilon]\,[i(\varepsilon_1-\varepsilon_2)-3\epsilon]} \right] \frac{\Theta(\varepsilon_p)\Theta(\varepsilon_q)}{\omega^2-\Omega^2}$$

When the limit $\epsilon \to 0$ is taken, this expression is clearly non-zero only if $\varepsilon_1 = \varepsilon_2$. Expressing the result in terms of the Kronecker delta $\delta(\varepsilon_1, \varepsilon_2)$ for the discrete cavity

eigen-energies, one obtains

$$I_1 = -i\Theta(\varepsilon_p)\Theta(\varepsilon_q)\int\frac{d\omega}{2\pi}\frac{\delta(\varepsilon_1,\varepsilon_2)}{(\varepsilon_1+\omega-\varepsilon_p)(\varepsilon_2+\omega-\varepsilon_q)(\omega^2-\Omega^2)} \tag{4.6}$$

where

$$\delta(\varepsilon_1,\varepsilon_2) = \begin{cases} 1 & \text{if } \varepsilon_1 = \varepsilon_2 \\ 0 & \text{otherwise} \end{cases} \tag{4.7}$$

Note that the factor of 3/2 from the Gell-Mann and Low theorem has cancelled in eq. (4.6).

The other three terms arising from the contour integration can be evaluated in the same way and combined to give the complete energy shift as

$$\Delta E_{\rm a} = -ig^2\sum_{pqm\Sigma} g^{\Sigma\Sigma}\,\tilde{Q}^{m\Sigma}_{n_1p}\,M_{pq}\,Q^{m\Sigma}_{qn_2}\int\frac{d\omega}{2\pi}\frac{\delta(\varepsilon_1,\varepsilon_2)}{(\varepsilon_1+\omega-\varepsilon_p)(\varepsilon_2+\omega-\varepsilon_q)(\omega^2-\Omega^2)} \tag{4.8}$$

This expression should be compared with the corresponding free-space result given in eq. (3.8). The analogy between $\int dk^0$ and $\int d\omega$ is immediately apparent, which is to be expected since both of these arise from time integrals, and the time component has not been altered in any way in going to the cavity theory. The important point here is that the close correspondence between the free space and cavity expressions suggests that the free-space techniques outlined in §3.1 can be applied to the evaluation of (4.8).

Before attempting to apply standard free-space methods to this expression, there are a few remarks which can be made about eq. (4.8). Firstly, the contour integral can be evaluated to yield

$$I^{m\Sigma}_{pq} \equiv -i\int\frac{d\omega}{2\pi}\frac{1}{(\varepsilon_1+\omega-\varepsilon_p)(\varepsilon_1+\omega-\varepsilon_q)(\omega^2-\Omega^2)} \tag{4.9}$$

$$= \begin{cases} \dfrac{1}{2\Omega(\varepsilon_1-\Omega\,\mathrm{sgn}\varepsilon_p-\varepsilon_p)(\varepsilon_1-\Omega\,\mathrm{sgn}\varepsilon_q-\varepsilon_q)} & \text{if } \mathrm{sgn}\varepsilon_p = \mathrm{sgn}\varepsilon_q \\ \dfrac{2\Omega+\varepsilon_p+\varepsilon_q}{2\Omega(\varepsilon_1-\Omega\,\mathrm{sgn}\varepsilon_p-\varepsilon_p)(\varepsilon_1-\Omega\,\mathrm{sgn}\varepsilon_q-\varepsilon_q)(\varepsilon_p+\varepsilon_q)} & \text{if } \mathrm{sgn}\varepsilon_p \neq \mathrm{sgn}\varepsilon_q \end{cases} \tag{4.10}$$

where the superscript in $I^{m\Sigma}_{pq}$ reminds the reader that the gluon energy depends implicitly on these indices. When this result is inserted into (4.8), the energy shift is expressed purely as a sum of vertex integrals weighted with some energy denominators. This is the form in which cavity energy shifts are usually evaluated. It will be shown later that this form arises naturally when the unsymmetric version of the Gell-Mann and Low theorem (2.29) is used. In this particular case, $\Delta E_{\rm a}$ diverges

logarithmically, by which we mean: if it is evaluated up to some cut-off energy Λ (*à la* Pauli-Villars), the result increases logarithmically as as a function of Λ.

Let us now proceed to evaluate the integral (4.9) as it would be done in free space. Reducing the $\pm i0$ prescription to $+i0$ in the denominator by squaring the quark propagator pieces, and Wick-rotating to Euclidean space with the shifts $\omega \to i\omega$ and $\varepsilon_1 \to i\varepsilon_1$, the integral $I_{pq}^{m\Sigma}$ becomes

$$I_{pq}^{m\Sigma} = -\int \frac{d\omega}{2\pi} \frac{[\varepsilon_p + i(\omega+\varepsilon_1)]\,[\varepsilon_q + i(\omega+\varepsilon_1)]}{\left[(\varepsilon_1+\omega)^2+\varepsilon_p^2\right]\left[(\varepsilon_1+\omega)^2+\varepsilon_q^2\right](\omega^2+\Omega^2)} \tag{4.11}$$

Elevating the denominators, this becomes

$$I_{pq}^{m\Sigma} = -\int \frac{d\omega}{2\pi} [\varepsilon_p + i(\omega+\varepsilon_1)]\,[\varepsilon_q + i(\omega+\varepsilon_1)] \tag{4.12}$$

$$\times \int_0^\infty dr \int_0^\infty ds \int_0^\infty dt e^{-r(\omega^2+\Omega^2)}\, e^{-s[(\varepsilon_1+\omega)^2+\varepsilon_p^2]}\, e^{-t[(\varepsilon_1+\omega)^2+\varepsilon_q^2]}$$

Making the following shifts of variables (c.f. the shifts defined by eqs. (3.13) and (3.14) in §3.1),

$$r \to z(1-x-y) \quad , \quad s \to zx \quad , \quad t \to zy \quad , \quad \omega \to \omega - \varepsilon_1(x+y) \tag{4.13}$$

we arrive at

$$I_{pq}^{m\Sigma} = -\int \frac{d\omega}{2\pi} \int_0^\infty dz\, z^2 \int_0^1 dx \int_0^{1-x} dy\, [\varepsilon_p + i\varepsilon_1(1-x-y) + i\omega] \times \tag{4.14}$$

$$[\varepsilon_q + i\varepsilon_1(1-x-y) + i\omega]\; e^{-z\left[\omega^2+\Omega^2(1-x-y)+\varepsilon_1^2(x+y)(1-x-y)+x\varepsilon_p^2+y\varepsilon_q^2\right]}$$

The ω integral is a standard Gaussian, and yields, after rotating back to Minkowski space

$$I_{pq}^{m\Sigma} = -\int_0^\infty dz \int_0^1 dx \int_0^{1-x} dy \left[\Big(\varepsilon_p + \varepsilon_1(1-x-y)\Big)\Big(\varepsilon_q + \varepsilon_1(1-x-y)\Big)\, z - \frac{1}{2}\right]$$

$$\times \sqrt{\frac{z}{4\pi}}\; e^{-z\left[\Omega^2(1-x-y)-\varepsilon_1^2(x+y)(1-x-y)+x\varepsilon_p^2+y\varepsilon_q^2\right]} \tag{4.15}$$

The result obtained from the contour integration of (4.9) could now be recovered by first performing the z integral, then integrating over x and y in the expression above. However, we want to have a form in which the ultra-violet singularity is parametrized, and that results from performing the x and y integrals first, with the integral over z being left as the very last step in the calculation. The divergence then appears as a non-integrable singularity in z.

After a somewhat tedious calculation, the integrals over x and y can be expressed in terms of the error function. The result, unhappily, is not terribly elegant. Writing

$$I_{pq}^{m\Sigma} = \int_0^\infty dz\, I_{pq}^{m\Sigma}(z)$$

we have

$$I_{pq}^{m\Sigma}(z) = \frac{(\varepsilon_1+\varepsilon_q)^2-\Omega^2+2\varepsilon_1\varepsilon_p}{8\varepsilon_1^2(\varepsilon_q^2-\varepsilon_p^2)\sqrt{\pi z}}\,e^{-z\varepsilon_q^2} - \frac{(\varepsilon_1+\varepsilon_p)^2-\Omega^2+2\varepsilon_1\varepsilon_q}{8\varepsilon_1^2(\varepsilon_q^2-\varepsilon_p^2)\sqrt{\pi z}}\,e^{-z\varepsilon_p^2} - \frac{e^{-z\Omega^2}}{8\varepsilon_1^2\sqrt{\pi z}}$$

$$+\frac{\left(\varepsilon_1^2+\varepsilon_q^2-\Omega^2+2\varepsilon_1\varepsilon_p\right)\left[(\varepsilon_1+\varepsilon_q)^2-\Omega^2\right]}{16\varepsilon_1^3(\varepsilon_q^2-\varepsilon_p^2)}\left[e^{-z\Omega^2}\mathrm{nerf}\left(\sqrt{z}\,A_+\right)+e^{-z\varepsilon_q^2}\mathrm{nerf}\left(\sqrt{z}\,A_-\right)\right]$$

$$-\frac{\left(\varepsilon_1^2+\varepsilon_p^2-\Omega^2+2\varepsilon_1\varepsilon_q\right)\left[(\varepsilon_1+\varepsilon_p)^2-\Omega^2\right]}{16\varepsilon_1^3(\varepsilon_q^2-\varepsilon_p^2)}\left[e^{-z\Omega^2}\mathrm{nerf}\left(\sqrt{z}\,B_+\right)+e^{-z\varepsilon_p^2}\mathrm{nerf}\left(\sqrt{z}\,B_-\right)\right] \tag{4.16}$$

where the normalized error function $\mathrm{nerf}(x)$ is defined by

$$\mathrm{nerf}(x) = \frac{2}{\sqrt{\pi}}\,e^{x^2}\int_0^x e^{-t^2}\,dt \tag{4.17}$$

and the following shorthand has been introduced

$$A_+ = \left(\varepsilon_1^2+\Omega^2-\varepsilon_q^2\right)/2\varepsilon_1 \quad , \quad A_- = \left(\varepsilon_1^2-\Omega^2+\varepsilon_q^2\right)/2\varepsilon_1$$

$$B_+ = \left(\varepsilon_1^2+\Omega^2-\varepsilon_p^2\right)/2\varepsilon_1 \quad , \quad B_- = \left(\varepsilon_1^2-\Omega^2+\varepsilon_p^2\right)/2\varepsilon_1 \tag{4.18}$$

The apparent singularity which occurs in (4.16) when $\varepsilon_p = \varepsilon_q$ can easily be dealt with by expanding the exponential and error functions. However, this special case occurs again in the diagrams containing a self-energy insert, and will be presented there.

It can be verified numerically that (4.16) is equivalent to the contour-integrated result (4.10). Analytic proof of their equivalence is possibly not too difficult, but did not seem altogether necessary to the author.

The final form of the energy shift for the vertex correction graph, figure (4.1a), is thus given by

$$\Delta E_{\mathrm{a}} = g^2\left\langle \hat{a}^\dagger_{c'f'n_1}\left(\frac{\lambda^a}{2}\right)_{c'd}\left(\frac{\lambda^a}{2}\right)_{dc} Q\,\hat{a}_{cfn_2}\right\rangle \int_0^\infty dz \sum_{pqm\Sigma} g^{\Sigma\Sigma}\,\tilde{Q}^{m\Sigma}_{n_1p}\,M_{pq}\,Q^{m\Sigma}_{qn_2}\,I^{m\Sigma}_{pq}(z) \tag{4.19}$$

A small point to note here is that the integrand $I_{pq}^{m\Sigma}(z)$ still contains the Kronecker delta involving ε_1 and ε_2. This condition effectively limits the outgoing state to be such that $n_1 = n_2$, since the cavity modes are discrete in energy.

4.2 Time-ordered Diagrams

The more usual approach to cavity energy shifts is through the expansion of the interaction in a series of time-ordered diagrams. The vertex correction in the cavity

has, in fact, already been calculated by Maxwell and Vento [17] in the Coulomb gauge using this method. As an illustration of the method, the energy shift due to the vertex correction is presented here. However, the Feynman gauge is used in this calculation, and the formalism is substantially different from that of ref. [17].

Using (2.29) and (2.30), the energy shift to $O(eg^2)$ is given by

$$\Delta E = -\lim_{\epsilon\to 0}\frac{(-i)^2}{2!}\int_{-\infty}^{0}dt_1\int_{-\infty}^{0}dt_2\int d^3x\int d^3y\int d^3z\, e^{-\epsilon(|t_1|+|t_2|)}\ \times \tag{4.20}$$

$$\left\langle T\left[\left(\bar\psi(g\frac{\lambda_a}{2}\not{A}_a+Q\not{A}_{\rm ext})\psi\right)_x\left(\bar\psi(g\frac{\lambda_b}{2}\not{A}_b+Q\not{A}_{\rm ext})\psi\right)_y\left(\bar\psi(g\frac{\lambda_c}{2}\not{A}_c+Q\not{A}_{\rm ext})\psi\right)_z\right]\right\rangle_c$$

where the co-ordinates x, y and z are defined by $x=(0,\vec{x})$, $y=(t_1,\vec{y})$ and $z=(t_2,\vec{z})$ with $0\geq t_1\geq t_2$. The vertex correction may be extracted from this expression by contracting the fields in such a manner that the external operator is always flanked by quark propagators. The six ways of doing this are shown in figure (4.2).

Choosing one of the possible contractions of the time-ordered product, figure (4.2), the energy shift is

$$\Delta E_1 = \lim_{\epsilon\to 0}\frac{g^2}{2!}\int_{-\infty}^{0}dt_1\int_{-\infty}^{0}dt_2\int d^3x\int d^3y\int d^3z\, e^{-\epsilon(|t_1|+|t_2|)}\ \times \tag{4.21}$$

$$\left\langle N\left[\left(\bar\psi(x)\frac{\lambda_a}{2}\not{A}_a(x)\psi(x)\right)\left(\bar\psi(y)\frac{\lambda_b}{2}\not{A}_b(y)\psi(y)\right)\left(\bar\psi(z)Q\not{A}_{\rm ext}(z)\psi(z)\right)\right]\right\rangle_c$$

The appropriate forms of the quark and gluon propagators to use with this expression are those which contain explicit references to the time-ordering, and are given by (2.17) and (2.22) respectively. With these substitutions, (4.21) becomes

$$\Delta E_1 = \lim_{\epsilon\to 0} g^2\sum_{\substack{p,q>0\\ m\Sigma}}\frac{g^{\Sigma\Sigma}}{2\Omega}\int_{-\infty}^{0}dt_1\int_{-\infty}^{t_1}dt_2\, e^{-\epsilon(|t_1|+|t_2|)}\, e^{it_1(\Omega-\varepsilon_q-\varepsilon_2)}\, e^{it_2(\varepsilon_p+\varepsilon_q)} \tag{4.22}$$

$$\int d^3x\,\bar u_{n_1}(x)\gamma_\mu u_p(x)a^\mu_{m\Sigma}(x)\int d^3y\,\bar u_{-q}(y)\gamma_\nu u_{n_2}(y)a^{\nu *}_{m\Sigma}(y)\int d^3z\,\bar u_p(z)\gamma_\lambda u_{-q}(z)A^\lambda_{\rm ext}(z)$$

The time integrals in this case are trivial, leading to

$$\Delta E_1 = g^2\sum_{\substack{p,q>0\\ m\Sigma}}Q^{m\Sigma}_{n_1p}\,M_{p-q}\tilde{Q}^{m\Sigma}_{-qn_2}\,\frac{g^{\Sigma\Sigma}}{2\Omega(\varepsilon_p+\varepsilon_q)(\Omega+\varepsilon_p-\varepsilon_2)} \tag{4.23}$$

The notation $\sum_{p,q>0}$ in (4.23) indicates that the summation over the intermediate quarks p and q includes only the positive radial frequencies.

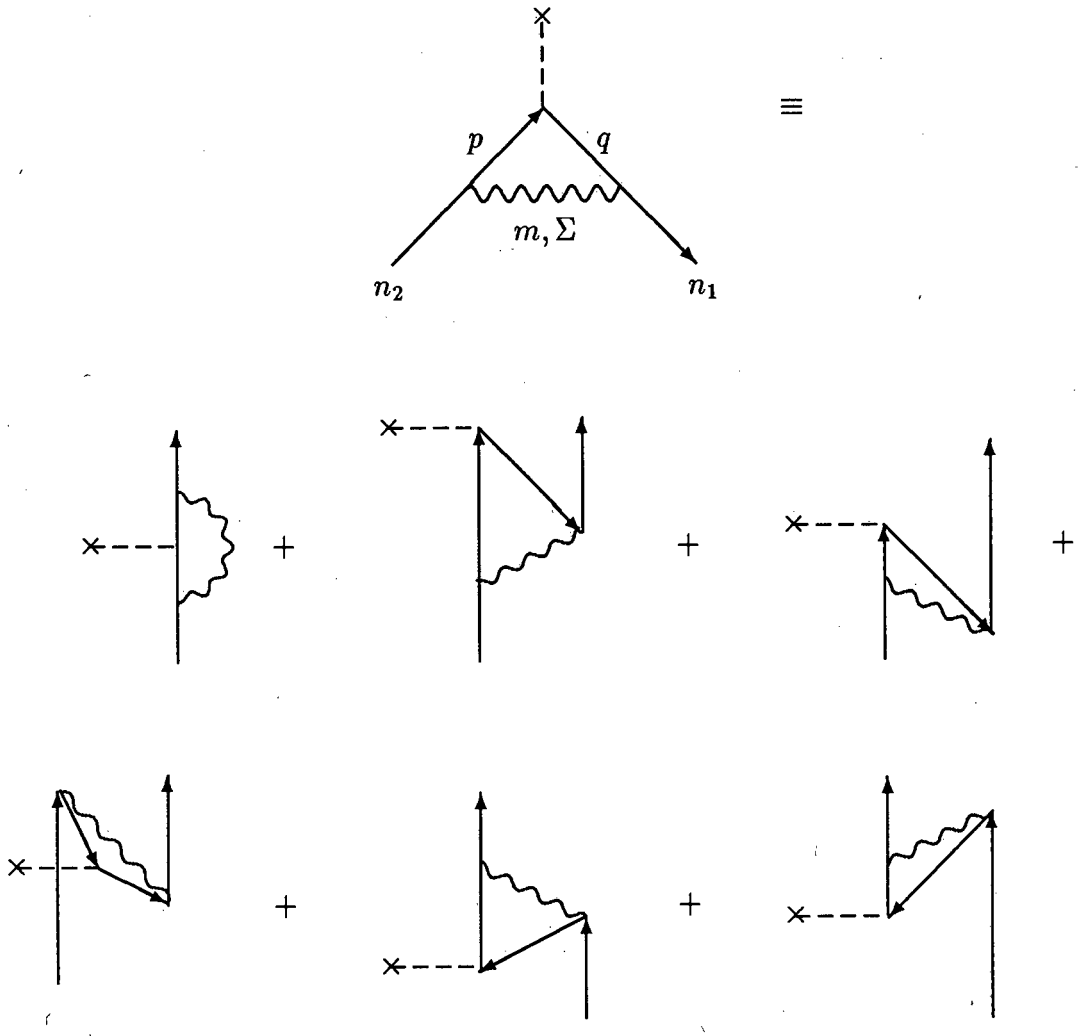

Figure 4.2: *The QCD vertex correction graph as a sum of time-ordered diagrams.*

Closely related to the time-ordered diagram given by ΔE_1 is the last one in figure (4.2). Schematically, the contractions leading to this diagram are

$$\left\langle N\left[\left(\bar{\psi}(x)\frac{\lambda_a}{2}\not{A}_a(x)\psi(x)\right)\left(\bar{\psi}(y)\frac{\lambda_b}{2}\not{A}_b(y)\psi(y)\right)\left(\bar{\psi}(z)\not{A}_{\text{ext}}(z)\psi(z)\right)\right]\right\rangle_c$$

and the energy shift associated with it is readily found to be

$$\Delta E_2 = g^2 \sum_{\substack{p,q\geq 0 \\ m\Sigma}} Q^{m\Sigma}_{n_1 p}\, M_{p\,-q}\, \tilde{Q}^{m\Sigma}_{-q n_2} \frac{g^{\Sigma\Sigma}}{2\Omega(\varepsilon_p+\varepsilon_q)(\Omega+\varepsilon_q+\varepsilon_1)} \tag{4.24}$$

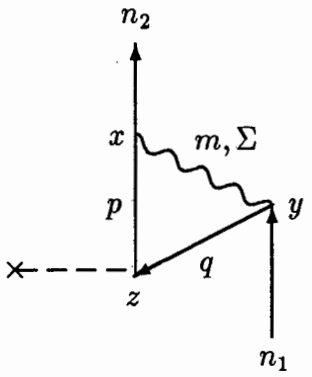

Figure 4.3: *The time-ordered diagram ΔE_1 contributing to the vertex correction.*

Adding together the contributions from these two time-orderings, one obtains

$$\Delta E_{12} = g^2 \sum_{\substack{p,q>0 \\ m\Sigma}} Q^{m\Sigma}_{n_1 p} M_{p-q} \tilde{Q}^{m\Sigma}_{-q n_2} \frac{g^{\Sigma\Sigma}(2\Omega + \varepsilon_p + \varepsilon_q)}{(\varepsilon_p + \varepsilon_q)(\Omega + \varepsilon_q + \varepsilon_1)(\Omega + \varepsilon_p - \varepsilon_2)} \tag{4.25}$$

The sum of these two time-ordered graphs agrees, in part, with the result eq. (4.10) found in the previous section using a different method. The qualifier 'in part' refers to the fact that agreement between the results is limited to those parts containing the quark q propagating backwards in time and quark p going forward, since the two time-orderings calculated contain only this piece. Of course, when the remaining four time-orderings are calculated and added together, complete agreement is reached between the two expressions for the vertex correction energy shift.

4.3 The Self-Energy Inserts

The other two divergent diagrams which we need to consider each contain a self-energy insert on one of the external legs. These are shown in figures (4.1b) and (4.1c). Once again, the gauge-independent part of the energy shift will be calculated here, using the Sucher form of the Gell-Mann and Low theorem.

The energy shift for figure (4.1b) is

$$\Delta E_{\rm b} = \lim_{\epsilon\to 0} \frac{3\epsilon}{2} g^2 \int d^4x_1 \int d^4x_2 \int d^4x_3\, e^{-\epsilon(|t_1|+|t_2|+|t_3|)} \times \tag{4.26}$$

$$\left\langle N\left[\left(\bar\psi(x_1) Q \not{A}_{\rm ext}(x_1)\psi(x_1)\right)\left(\bar\psi(x_2)\frac{\lambda_a}{2}\not{A}_a(x_2)\psi(x_2)\right)\left(\bar\psi(x_3)\frac{\lambda_b}{2}\not{A}_b(x_3)\psi(x_3)\right)\right]\right\rangle_{\rm c}$$

where the factor of 1/3! has been dropped since the 3! permutations of the co-ordinate labels are all equivalent. This immediately yields

$$\Delta E_{\rm b} = \lim_{\epsilon\to 0} -\frac{3i\epsilon}{2}\frac{1}{(2\pi)^3} g^2 \sum_{pqm\Sigma} g^{\Sigma\Sigma}\, M_{n_1 q}\, \tilde{Q}^{m\Sigma}_{qp}\, Q^{m\Sigma}_{pn_2} \;\times \tag{4.27}$$

$$\int_{-\infty}^{\infty} dt_1\, dt_2\, dt_3 \int_{-\infty}^{\infty} d\omega\, d\omega'\, d\omega'' \, \frac{e^{-\epsilon(|t_1|+|t_2|+|t_3|)}\, e^{it_1(\varepsilon_1-\omega')}\, e^{it_2(\omega'-\omega''+\omega)}\, e^{it_3(\omega''-\omega-\varepsilon_2)}}{(\omega'-\varepsilon_q)(\omega''-\varepsilon_p)(\omega^2-\Omega^2)}$$

Some care is needed here when evaluating the time and ω integrals. Recall that when this graph was examined in free space, the Feynman amplitude for the divergent piece was found to be indeterminate because the operator $(1/\not{p})\not{p}$ acting on a free particle spinor produced the undefined quantity 0/0. The ambiguity was resolved with the introduction of adiabatic damping factors, which are already included in the cavity expression, eq. (4.27).

One way (although not the only one) of evaluating these integrals is to Fourier transform the damping factors into momentum space using the transform

$$e^{\epsilon|t|} = \frac{1}{2\pi}\int_{-\infty}^{\infty} dE\, \frac{2\epsilon}{\epsilon^2+E^2}\, e^{iEt} \tag{4.28}$$

With this transform, the integral becomes

$$I^{m\Sigma}_{pq} = \lim_{\epsilon\to 0}\frac{-3i\epsilon}{2}\frac{1}{(2\pi)^3}\int_{-\infty}^{\infty} dt_1\, dt_2\, dt_3 \int_{-\infty}^{\infty} d\omega\, d\omega'\, d\omega''$$

$$\times\; \frac{e^{-\epsilon(|t_1|+|t_2|+|t_3|)}\, e^{it_1(\varepsilon_1-\omega')}\, e^{it_2(\omega'-\omega''+\omega)}\, e^{it_3(\omega''-\omega-\varepsilon_2)}}{(\omega'-\varepsilon_q)(\omega''-\varepsilon_p)(\omega^2-\Omega^2)}$$

$$= \lim_{\epsilon\to 0}\frac{-3i\epsilon}{2}\frac{1}{(2\pi)^6}\int_{-\infty}^{\infty} dE\, dE'\, dE'' \int_{-\infty}^{\infty} dt_1\, dt_2\, dt_3 \int_{-\infty}^{\infty} d\omega\, d\omega'\, d\omega''$$

$$\times\; \frac{2\epsilon}{\epsilon^2+E^2}\,\frac{2\epsilon}{\epsilon^2+E'^2}\,\frac{2\epsilon}{\epsilon^2+E''^2}\,\frac{e^{it_1(\varepsilon_1+E-\omega')}\, e^{it_2(\omega+\omega'+E'-\omega'')}\, e^{it_3(\omega''+E''-\omega-\varepsilon_2)}}{(\omega'-\varepsilon_q)(\omega''-\varepsilon_p)(\omega^2-\Omega^2)} \tag{4.29}$$

After some algebra, and allowing $\epsilon \to 0$, this reduces to

$$I^{m\Sigma}_{pq} = \begin{cases} -i\displaystyle\int \frac{d\omega}{2\pi}\,\frac{\delta(\varepsilon_1,\varepsilon_2)}{(\varepsilon_2-\varepsilon_q)(\omega+\varepsilon_1-\varepsilon_p)(\omega^2-\Omega^2)} & \text{if } \varepsilon_q \neq \varepsilon_2 \\ \\ \dfrac{i}{2}\displaystyle\int \frac{d\omega}{2\pi}\,\frac{\delta(\varepsilon_1,\varepsilon_2)}{(\omega+\varepsilon_1-\varepsilon_p)^2(\omega^2-\Omega^2)} & \text{if } \varepsilon_q = \varepsilon_2 \end{cases} \tag{4.30}$$

The second case of eq. (4.30), $\varepsilon_q = \varepsilon_2$, leads to a logarithmically divergent expression when inserted into (4.27), while the first case remains finite. In fact, when the former condition $\varepsilon_q = \varepsilon_2$ is imposed on (4.27), the result is almost identical to the vertex correction (4.8), but with equal momenta on either side of the external operator. In other words, the divergent piece here looks very much like the function $\Lambda(p,p)$ in free space. One should particularly notice that the divergent term has acquired a factor of $1/2$ relative to the finite term—a requirement for the singularities of the three loop graphs to cancel. This should be compared to the free space calculation, especially eq. (3.24).

The remaining integral may now be evaluated in the standard way, i.e. Wick rotate to Euclidean space, elevate the denominators into the exponent, etc. Changing the notation slightly to distinguish between the two cases $\varepsilon_q \neq \varepsilon_2$ and $\varepsilon_q = \varepsilon_2$

$$I_{pq}^{m\Sigma} = \begin{cases} \displaystyle\int_0^\infty dz\, K_{pq}^{m\Sigma}(z) & \text{if } \varepsilon_q \neq \varepsilon_2 \\ \displaystyle\int_0^\infty dz\, L_p^{m\Sigma}(z) & \text{if } \varepsilon_q = \varepsilon_2 \end{cases} \tag{4.31}$$

and leaving the technical details aside, the result in this notation is

$$K_{pq}^{m\Sigma}(z) = \frac{1}{4\varepsilon_1(\varepsilon_2-\varepsilon_q)\sqrt{\pi z}}\left(e^{-z\varepsilon_p^2} - e^{-z\Omega^2}\right) \tag{4.32}$$

$$+ \frac{(\varepsilon_p+\varepsilon_1)^2-\Omega^2}{8\varepsilon_1^2(\varepsilon_2-\varepsilon_q)}\left\{e^{zB_+^2-z\Omega^2}\operatorname{erf}\left(\sqrt{z}B_+\right) + e^{zB_-^2-z\varepsilon_p^2}\operatorname{erf}\left(\sqrt{z}B_-\right)\right\}$$

for the first possibility. The quantities B_+ and B_- were defined in eq. (4.18). The other possibility, $\varepsilon_q = \varepsilon_2$, is actually a special case of the analogous integral, eq. (4.16), for the vertex correction diagram, and is given by

$$-2L_p^{m\Sigma}(z) = \frac{1}{16\varepsilon_1^4\sqrt{\pi z}}\left[(\varepsilon_1+\varepsilon_p+\Omega)^2(\varepsilon_1+\varepsilon_p-\Omega)^2 z + 2\varepsilon_1^2\right]e^{-z\Omega^2} \tag{4.33}$$

$$+ \frac{1}{16\varepsilon_1^4\sqrt{\pi z}}\left[\left((\varepsilon_1+\varepsilon_p)^2-\Omega^2\right)\left((\varepsilon_1-\varepsilon_p)^2+\Omega^2\right)z + 4\varepsilon_p\varepsilon_1^3 z - 2\varepsilon_1^2\right]e^{-z\varepsilon_p^2}$$

$$+ \frac{1}{32\varepsilon_1^5}\left[\left(\varepsilon_1^2-\varepsilon_p^2+\Omega^2\right)\left((\varepsilon_1+\varepsilon_p)^2-\Omega^2\right)z - 4\varepsilon_1^2\right]\left((\varepsilon_1+\varepsilon_p)^2-\Omega^2\right)$$

$$\times\left[e^{-z\Omega^2}\operatorname{nerf}\left(\sqrt{z}B_+\right) + e^{-z\varepsilon_p^2}\operatorname{nerf}\left(\sqrt{z}B_-\right)\right]$$

Inserting these integrals into (4.27), we arrive at the final form of the energy shift for the vertex diagram containing a self-energy insert

$$\Delta E_{\rm b} = g^2 \int_0^\infty dz \sum_{\substack{pm\Sigma \\ q\neq n_2}} g^{\Sigma\Sigma}\, M_{n_1 q}\, \tilde{Q}^{m\Sigma}_{qp}\, Q^{m\Sigma}_{pn_2}\, K^{m\Sigma}_{pq}(z)$$

$$+ g^2 \int_0^\infty dz\, M_{n_1 n_2} \sum_{pm\Sigma} g^{\Sigma\Sigma}\, \tilde{Q}^{m\Sigma}_{n_2 p}\, Q^{m\Sigma}_{pn_2}\, L^{m\Sigma}_{p}(z) \tag{4.34}$$

Once again, the Kronecker delta implicit in the integrands K and L restricts the modes such that $n_1 = n_2$.

The diagram with the self-energy insert on the other external leg, figure (4.1c), turns out to be the same as (4.34). The former will be included by multiplying (4.34) by a factor of 2.

As a reasonably independent check on the correctness of eq. (4.34), it may be derived from a time-ordered expansion of the interaction. Since this yields the same result, one can be confident that it is correct.

4.4 Gauge-Dependent Terms

Recall that in free space, the sum of the three loop diagrams contributing to the quark anomalous magnetic moment was gauge independent; i.e. the terms containing the gauge parameter λ cancelled identically. One therefore expects that something similar will happen in the cavity. It turns out that these gauge-dependent terms also vanish in the cavity, as will be shown in this section.

The gluon propagator in an arbitrary gauge was given in eq. (2.28). For easy reference, the gauge-dependent part is repeated here

$$iD^{\mu\nu}_{ab}(x_1, x_2) = -i\delta_{ab}\, \frac{1-\lambda}{\lambda} \sum_{m\Sigma\Sigma'} a^{\mu}_{m\Sigma}(\vec{x}_1)\, a^{\nu\,*}_{m\Sigma'}(\vec{x}_2) \int \frac{d\omega}{2\pi}\, \frac{q^{\Sigma} q^{\Sigma'}}{q^4}\, e^{i\omega(t_2 - t_1)} \tag{4.35}$$

where the polarization vector q^{Σ} is defined by

$$\begin{aligned} q^{\Sigma} &\equiv (q^{\mathcal{S}}, q^{\mathcal{L}}, q^{\mathcal{M}}, q^{\mathcal{E}}) = (\omega, \Omega, 0, 0) \\ q_{\Sigma} &= (\omega, -\Omega, 0, 0) \\ q^2 &= \omega^2 - \Omega^2 \end{aligned}$$

The gluon energy Ω is written here without its indices.

4.4.1 The Vertex Correction

Inserting (4.35) into the expression for the energy shift, eq. (4.1), the gauge dependent piece of the vertex correction diagram is found to be

$$\Delta E_{\rm a} = \lim_{\epsilon\to 0} -\frac{3i\epsilon}{2}\frac{1-\lambda}{\lambda}\frac{1}{(2\pi)^3}g^2 \sum_{pqm\Sigma\Sigma'} \tilde{Q}^{m\Sigma'}_{n_1p}\, M_{pq}\, Q^{m\Sigma}_{qn_2}\, q^{\Sigma} q^{\Sigma'} \times \tag{4.36}$$

$$\int_{-\infty}^{\infty} dt_1\, dt_2\, dt_3 \int_{-\infty}^{\infty} d\omega\, d\omega'\, d\omega'' \frac{e^{-\epsilon(|t_1|+|t_2|+|t_3|)}\, e^{it_1(\varepsilon_1+\omega-\omega')}\, e^{it_2(\omega'-\omega'')}\, e^{it_3(\omega''-\omega-\varepsilon_2)}}{(\omega'-\varepsilon_p)(\omega''-\varepsilon_q)(\omega^2-\Omega^2)^2}$$

From the definition of q^{Σ}, one can see that the sum over gluon polarizations above is restricted to the scalar and longitudinal modes only, and since the vertex integrals of these two polarizations are related by current conservation (A.30) and (B.12),

$$Q^{m\mathcal{L}}_{pq} = \frac{\varepsilon_q-\varepsilon_p}{\Omega^{\mathcal{S}}_m} Q^{m\mathcal{S}}_{pq} \quad , \qquad \tilde{Q}^{m\mathcal{L}}_{pq} = -\frac{\varepsilon_q-\varepsilon_p}{\Omega^{\mathcal{S}}_m} \tilde{Q}^{m\mathcal{S}}_{pq}$$

the sum over polarizations may written in terms of scalar modes only.

$$\begin{aligned}\sum_{\Sigma\Sigma'} \tilde{Q}^{m\Sigma'}_{n_1p}\, Q^{m\Sigma}_{qn_2}\, q^{\Sigma} q^{\Sigma'} &= \tilde{Q}^{m\mathcal{S}}_{n_1p}\, Q^{m\mathcal{S}}_{qn_2} \Big[q^{\mathcal{S}} q^{\mathcal{S}} + q^{\mathcal{S}} q^{\mathcal{L}} \frac{\varepsilon_2-\varepsilon_q}{\Omega} + q^{\mathcal{L}} q^{\mathcal{S}} \frac{\varepsilon_1-\varepsilon_p}{\Omega} + \\ &\qquad + q^{\mathcal{L}} q^{\mathcal{L}} (\varepsilon_1-\varepsilon_p)(\varepsilon_2-\varepsilon_q) \Big] \\ &= (\omega+\varepsilon_2-\varepsilon_q)(\omega+\varepsilon_1-\varepsilon_p)\, \tilde{Q}^{m\mathcal{S}}_{n_1p}\, Q^{m\mathcal{S}}_{qn_2} \end{aligned} \tag{4.37}$$

The integrals over the time and ω variables have already been done in §4.1, so we are now able to express the energy shift as

$$\begin{aligned}\Delta E_{\rm a} &= -i\frac{1-\lambda}{\lambda} g^2 \sum_{pqm} \tilde{Q}^{m\mathcal{S}}_{n_1p}\, M_{pq}\, Q^{m\mathcal{S}}_{qn_2} \int_{-\infty}^{\infty} \frac{d\omega}{2\pi} \frac{\delta(\varepsilon_1,\varepsilon_2)(\omega+\varepsilon_1-\varepsilon_p)(\omega+\varepsilon_2-\varepsilon_q)}{(\omega+\varepsilon_1-\varepsilon_p)(\omega+\varepsilon_2-\varepsilon_q)(\omega^2-\Omega^2)^2} \\ &= -i\frac{1-\lambda}{\lambda} g^2 \sum_{pqm} \tilde{Q}^{m\mathcal{S}}_{n_1p}\, M_{pq}\, Q^{m\mathcal{S}}_{qn_2} \int_{-\infty}^{\infty} \frac{d\omega}{2\pi} \frac{\delta(\varepsilon_1,\varepsilon_2)}{(\omega^2-\Omega^2)^2} \end{aligned} \tag{4.38}$$

The remaining integral is easily evaluated using standard techniques, and yields

$$I \equiv -i\int_{-\infty}^{\infty} \frac{d\omega}{2\pi} \frac{1}{(\omega^2-\Omega^2)^2} = \int_0^{\infty} dz \sqrt{\frac{z}{4\pi}}\, e^{-z\Omega^2} = \frac{1}{4\Omega^3} \tag{4.39}$$

Hence, the gauge-dependent part of the energy shift for the vertex correction diagram is given by

$$\Delta E_{\rm a} = g^2 \frac{1-\lambda}{\lambda} \int_0^{\infty} dz \sum_{pqm} \tilde{Q}^{m\mathcal{S}}_{n_1p}\, M_{pq}\, Q^{m\mathcal{S}}_{qn_2} \sqrt{\frac{z}{4\pi}}\, e^{-z\Omega^2} \tag{4.40}$$

4.4.2 The Self-Energy Inserts

The final piece needed now to complete the discussion of the Feynman diagrams contributing to the anomalous magnetic moment is the gauge-dependent part of figure (4.1b). We shall merely quote the result, which is

$$\Delta E_{\rm b} = \frac{ig^2}{2}\frac{1-\lambda}{\lambda}\sum_{pm} M_{n_1 n_2}\,\tilde{Q}^{m\mathcal{S}}_{n_2 p}\,Q^{m\mathcal{S}}_{p n_2}\int_{-\infty}^{\infty}\frac{d\omega}{2\pi}\,\frac{\delta(\varepsilon_1,\varepsilon_2)}{(\omega^2-\Omega^2)^2} \tag{4.41}$$

$$- ig^2\frac{1-\lambda}{\lambda}\sum_{\substack{pm\\ q\neq n_2}} M_{n_1 q}\,\tilde{Q}^{m\mathcal{S}}_{qp}\,Q^{m\mathcal{S}}_{p n_2}\int_{-\infty}^{\infty}\frac{d\omega}{2\pi}\,\frac{\delta(\varepsilon_1,\varepsilon_2)(\omega+\varepsilon_q-\varepsilon_p)}{(\varepsilon_2-\varepsilon_q)(\omega^2-\Omega^2)^2}$$

After evaluating the integrals, this becomes

$$\Delta E_{\rm b} = -\frac{g^2}{2}\frac{1-\lambda}{\lambda}\int_0^{\infty} dz\sum_{pm} M_{n_1 n_2}\,\tilde{Q}^{m\mathcal{S}}_{n_2 p}\,Q^{m\mathcal{S}}_{p n_2}\sqrt{\frac{z}{4\pi}}\,e^{-z\Omega^2} \tag{4.42}$$

$$+ g^2\frac{1-\lambda}{\lambda}\int_0^{\infty} dz\sum_{\substack{pm\\ q\neq n_2}} M_{n_1 q}\,\tilde{Q}^{m\mathcal{S}}_{qp}\,Q^{m\mathcal{S}}_{p n_2}\sqrt{\frac{z}{4\pi}}\left(\frac{\varepsilon_q-\varepsilon_p}{\varepsilon_2-\varepsilon_q}\right)e^{-z\Omega^2}$$

The first term in the above expression is singular, and the second is finite. The result $\Delta E_{\rm c}$ for the other self-energy diagram, figure (4.1c), is the same as $\Delta E_{\rm b}$ above.

Although it is not obvious from the form of these gauge-dependent terms, the sum $\Delta E_{\rm a} + \Delta E_{\rm b} + \Delta E_{\rm c}$ turns out to be exactly zero, as it was in free space. This result we are unfortunately only able to demonstrate numerically. See chapter 6 for a discussion on the numerical evaluation of this expression.

Chapter 5

One-Gluon Exchange Graphs

The remaining graphs contributing to the baryon magnetic moments are the one-gluon exchange diagrams, figures (5.1a) and (5.1b). These graphs are relatively easy to calculate, compared to the loop diagrams, since they are convergent and finite.

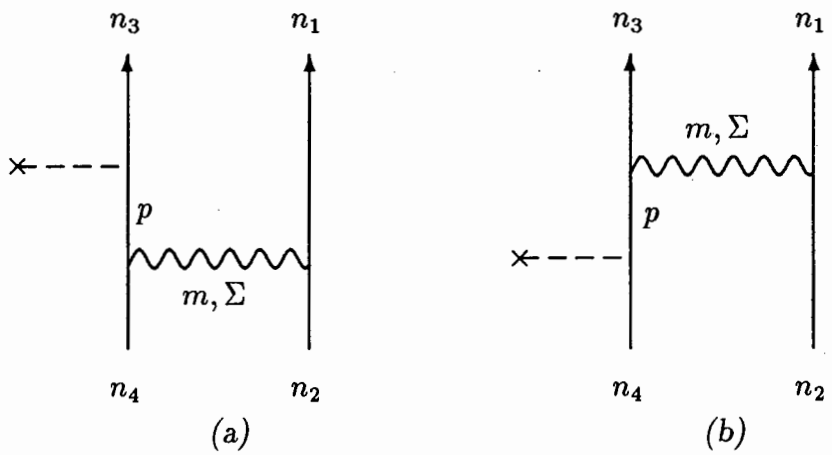

Figure 5.1: *One-gluon exchange graphs contributing to the baryon magnetic moments.*

The intrinsic, two-body nature of the one-gluon exchange graphs is of prime importance when the baryon magnetic moments are computed. If these graphs are not included in the calculation, the *ratio* of the neutron to proton magnetic moments will not change from the value of $-2/3$ obtained by using the naïve, non-relativistic quark model (the experimental value is approximately -0.685). This is because almost all such calculations use the standard $SU(6)$ flavour/spin wave functions of the model, and these yield the ratio of $-2/3$ if the magnetic moments are supposed to be due only to the constituent quarks (see, for example, Halzen and Martin [18]). Several authors have sought to improve the calculation of baryon magnetic moments by including, for example, relativistic corrections [19] (see also [20] and [21]), but

have ignored these diagrams. Of course, no improvement in the ratio has resulted. However, by including the two-body interactions, one is able to change the ratio since the origin of the baryon magnetic moments is no longer due only to the constituent quarks.

5.1 The Energy Shift

The energy shift for figure (5.1a) will be derived in detail below. The remaining diagram, figure (5.1b), gives the same contribution if the in-coming and out-going quarks are all in the same state. This may be also be seen from symmetry considerations, without performing the calculation directly. Once again, starting with the symmetric form of the Gell-Mann and Low theorem, eq. (2.31), the energy shift for diagram (a) is

$$\Delta E_{\rm a} = -\lim_{\epsilon\to 0}\frac{3i\epsilon}{2}g^2\frac{(-i)^3}{3!}\int d^4x_1\int d^4x_2\int d^4x_3\, e^{-\epsilon(|t_1|+|t_2|+|t_3|)} \qquad (5.1)$$
$$\times\left\langle N\left[\left(\bar\psi\frac{\lambda_a}{2}\not{A}_a\psi\right)_{x_1}\left(\bar\psi\frac{\lambda_b}{2}\not{A}_b\psi\right)_{x_2}\left(\bar\psi Q\not{A}_{\rm ext}\psi\right)_{x_3}\right]\right\rangle_{\rm c}$$

After substituting in the quark and gluon propagators, the gauge-independent part of this expression may be written in the usual notation as

$$\Delta E_{\rm a} = \lim_{\epsilon\to 0}\frac{3\epsilon}{2}g^2\left\langle \hat a^\dagger_{c'f'n_1}\hat a^\dagger_{d'g'n_3}\left(\frac{\lambda^a}{2}\right)_{c'c}\left(\frac{\lambda^a}{2}\right)_{d'd}Q\,\hat a_{cfn_2}\hat a_{dgn_4}\right\rangle\sum_{pm\Sigma}g^{\Sigma\Sigma}\,\tilde Q^{m\Sigma}_{n_1n_2}\,Q^{m\Sigma}_{n_3p}\,M_{pn_4}$$

$$\int_{-\infty}^{\infty}dt_1\,dt_2\,dt_3\int_{-\infty}^{\infty}\frac{d\omega}{2\pi}\,\frac{d\omega'}{2\pi}\,\frac{e^{-\epsilon(|t_1|+|t_2|+|t_3|)}\,e^{it_1(\varepsilon_1-\varepsilon_2+\omega)}\,e^{it_2(\varepsilon_3-\omega-\omega')}\,e^{it_3(\omega'-\varepsilon_4)}}{(\omega'-\varepsilon_p)(\omega^2-\Omega^2)} \qquad (5.2)$$

More of the tedious time and ω integrals have cropped up! They may be evaluated rigorously, as usual, or in the following rather sloppy way. The latter approach was inspired by the manner in which these integrals appear in free space, i.e. without the adiabatic damping factors, and is very simple. First, drop all references to the damping factor ϵ, then carry out the time integrals

$$I = \frac{1}{(2\pi)^2}\int_{-\infty}^{\infty}dt_1\,dt_2\,dt_3\int_{-\infty}^{\infty}d\omega\,d\omega'\,\frac{e^{it_1(\varepsilon_1-\varepsilon_2+\omega)}\,e^{it_2(\varepsilon_3-\omega-\omega')}\,e^{it_3(\omega'-\varepsilon_4)}}{(\omega'-\varepsilon_p)(\omega^2-\Omega^2)}$$

$$= 2\pi\int_{-\infty}^{\infty}d\omega\,d\omega'\,\frac{\delta(\varepsilon_1-\varepsilon_2+\omega)\,\delta(\varepsilon_3-\omega-\omega')\,\delta(\omega'-\varepsilon_4)}{(\omega'-\varepsilon_p)(\omega^2-\Omega^2)} \qquad (5.3)$$

Since there are no poles on the real axis, the ω integrals are trivial, yielding

$$I = 2\pi \int_{-\infty}^{\infty} d\omega' \frac{\delta(\varepsilon_1 + \varepsilon_3 - \varepsilon_2 - \omega')\,\delta(\omega' - \varepsilon_4)}{(\omega' - \varepsilon_p)\left[(\varepsilon_1 - \varepsilon_2)^2 - \Omega^2\right]}$$

$$= \frac{2\pi\delta(\varepsilon_1 + \varepsilon_3 - \varepsilon_2 - \varepsilon_4)}{(\varepsilon_4 - \varepsilon_p)\left[(\varepsilon_1 - \varepsilon_2)^2 - \Omega^2\right]} \rightarrow \frac{\delta(\varepsilon_1 + \varepsilon_3\,,\, \varepsilon_2 + \varepsilon_4)}{(\varepsilon_4 - \varepsilon_p)\left[(\varepsilon_1 - \varepsilon_2)^2 - \Omega^2\right]} \tag{5.4}$$

The last step in eq. (5.4) was to substitute 2π times the delta function, with its continuous, free-space energies, for a Kronecker delta in discrete cavity eigen-energies. This result is in perfect agreement with that obtained using the long-winded, rigorous approach. One can use this method with confidence for almost all Feynman diagrams if one first examines the free-space analogue of that diagram. If the adiabatic damping factors are not explicitly required to cure some ambiguity or pathology in the free-space graph, then this method will work in the cavity. (Clearly, this method will *not* work for graphs such as fig. (4.1b), which contain a self-energy insert on an external leg.)

Discarding the colour and flavour matrix elements for the moment, the energy shift for the one-gluon exchange graph is given by

$$\Delta E_a = g^2 \sum_{pm\Sigma} g^{\Sigma\Sigma}\, \tilde{Q}^{m\Sigma}_{n_1 n_2}\, Q^{m\Sigma}_{n_3 p}\, M_{p n_4} \frac{\delta(\varepsilon_1 + \varepsilon_3\,,\, \varepsilon_2 + \varepsilon_4)}{(\varepsilon_4 - \varepsilon_p)\left[(\varepsilon_1 - \varepsilon_2)^2 - \Omega^2\right]} \tag{5.5}$$

There is a problem with eq. (5.5); it is singular when $\varepsilon_p = \varepsilon_4$. Fortunately, this is easily remedied by letting $\varepsilon_p \rightarrow \varepsilon_4$ in (5.2), then evaluating the integrals (rigorously!). One then finds that the troublesome term vanishes if $\varepsilon_3 = \varepsilon_4$, which is the case here. Thus, the term $p = n_4$ is simply excluded from the sum.

5.2 Gauge Dependence and the One-Gluon Exchange

In figure (5.1), the virtual gluon is coupled to a conserved quark current, labelled here by n_1 and n_2. When a coupling such as this occurs in free-space QED, it is well-known that the piece depending on the gauge parameter is zero, since $q_\mu j^\mu = 0$ for a conserved current j^μ. The relation analogous to this in cavity QCD can be written in terms of the polarization vector q_Σ as $q_\Sigma j^\Sigma = 0$. A consequence of this relation is that these one-gluon exchange graphs are automatically gauge independent in the cavity.

One may also establish the gauge independence of these graphs by direct calculation. The proof is rather nice. Writing down the gauge dependent terms in the

energy shift, one has

$$\Delta E_{\rm a} = -\lim_{\epsilon\to 0}\frac{3\epsilon}{2}g^2\frac{1-\lambda}{\lambda}\sum_{pm\Sigma\Sigma'}\tilde{Q}^{m\Sigma}_{n_1n_2}\,Q^{m\Sigma'}_{n_3p}\,M_{pn_4}\,q^{\Sigma}q^{\Sigma'}\times \tag{5.6}$$

$$\frac{1}{(2\pi)^2}\int_{-\infty}^{\infty}dt_1\,dt_2\,dt_3\int_{-\infty}^{\infty}d\omega\,d\omega'\,\frac{e^{-\epsilon(|t_1|+|t_2|+|t_3|)}\,e^{it_1(\varepsilon_1-\varepsilon_2+\omega)}\,e^{it_2(\varepsilon_3-\omega-\omega')}\,e^{it_3(\omega'-\varepsilon_4)}}{(\omega'-\varepsilon_p)(\omega^2-\Omega^2)^2}$$

The polarization sums can be expressed in terms of the scalar mode only, as was done in §4.4.1, yielding

$$\sum_{\Sigma\Sigma'}\tilde{Q}^{m\Sigma}_{n_1n_2}\,Q^{m\Sigma'}_{n_3p}\,q^{\Sigma}q^{\Sigma'} \;=\; \tilde{Q}^{m\mathcal{S}}_{n_1n_2}\,Q^{m\mathcal{S}}_{n_3p}\,(\omega+\varepsilon_p-\varepsilon_3)\,(\omega+\varepsilon_1-\varepsilon_2) \tag{5.7}$$

The integrals may be done rigorously, or in the sloppy manner advocated previously. The latter is more transparent, where it suffices to evaluate only the t_1 and ω integrals.

$$I \;=\; \int_{-\infty}^{\infty}d\omega\int_{-\infty}^{\infty}\frac{dt_1}{2\pi}\,\frac{(\omega+\varepsilon_1-\varepsilon_2)\,(\omega+\varepsilon_p-\varepsilon_3)}{(\omega^2-\Omega^2)^2}\,e^{it_1(\omega+\varepsilon_1-\varepsilon_2)} \tag{5.8}$$

$$=\; \int_{-\infty}^{\infty}d\omega\,\frac{(\omega+\varepsilon_1-\varepsilon_2)\,(\omega+\varepsilon_p-\varepsilon_3)\,\delta(\omega+\varepsilon_1-\varepsilon_2)}{(\omega^2-\Omega^2)^2}$$

$$=\; \frac{(\varepsilon_2-\varepsilon_1+\varepsilon_1-\varepsilon_2)\,(\varepsilon_2-\varepsilon_1+\varepsilon_p-\varepsilon_3)}{\left[(\varepsilon_2-\varepsilon_1)^2-\Omega^2\right]^2} \;=\; 0$$

Thus, the gauge-dependent term (5.6) vanishes since the numerator of (5.8) is zero.

Chapter 6

Calculation and Results

The expressions for the energy shifts which were given in the previous two chapters are now ready for numerical calculation. As an example of the numerical methods used, the calculation of the vertex correction shift, figure (4.1a), will be discussed briefly below.

6.1 Numerical Methods

After summing over the spins of the intermediate quarks and gluon (see appendix C), the expression to be calculated is

$$\Delta E \;=\; \alpha_s \int_0^\infty dz\, \Delta E(z) \;=\; \alpha_s \int_0^\infty dz \sum_{pqm\Sigma} g^{\Sigma\Sigma}\, \Lambda_{pq}^{m\Sigma}\, I_{pq}^{m\Sigma}(z) \tag{6.1}$$

where the factor arising from the colour and flavour matrices has been omitted. The integrand $I_{pq}^{m\Sigma}(z)$ has been given in eq. (4.16), and the quantity $\Lambda_{pq}^{m\Sigma}$ is defined in terms of radial integrals (see appendix B) and Wigner $3j$- and $6j$-symbols by

$$\sum_{pqm\Sigma} g^{\Sigma\Sigma}\, \Lambda_{pq}^{m\Sigma} \;\equiv\; 4\pi \sum_{pqm\Sigma} g^{\Sigma\Sigma}\, \tilde{Q}_{n_1 p}^{m\Sigma}\, M_{pq}\, Q_{qn_2}^{m\Sigma} \tag{6.2}$$

$$= \sum_{\kappa_p \kappa_q J} \sum_{\substack{\nu_p \nu_q \\ N\Sigma}} g^{\Sigma\Sigma}\, S_{n_1 p}^{m\Sigma}\, R_{\kappa_p \kappa_q}^{\nu_p \nu_q}\, S_{q n_2}^{m\Sigma}\, (-1)^{j_1 + j_2 - J - \mu_1 + 1/2}\, \frac{(\kappa_p + \kappa_q)}{2}\, \hat{j}_1\, \hat{j}_2\, \hat{j}_p^2\, \hat{j}_q^2\, \hat{J}^2 \;\times$$

$$\left\{ \begin{matrix} j_p & J & j_1 \\ j_2 & 1 & j_q \end{matrix} \right\} \begin{pmatrix} j_1 & 1 & j_2 \\ \mu_1 & 0 & -\mu_2 \end{pmatrix} \begin{pmatrix} j_1 & J & j_p \\ \frac{1}{2} & 0 & -\frac{1}{2} \end{pmatrix} \begin{pmatrix} j_q & J & j_2 \\ \frac{1}{2} & 0 & -\frac{1}{2} \end{pmatrix} \begin{pmatrix} j_p & 1 & j_q \\ \frac{1}{2} & 0 & -\frac{1}{2} \end{pmatrix}$$

The notation $\hat{J}$ is shorthand for $\sqrt{2J+1}$. The sums over ν_p and ν_q run over all integers except zero, and the sum over N is over all positive integers, including zero. The last $3j$-symbol constrains κ_q such that $\kappa_q = \kappa_p$ or $-\kappa_q = \kappa_p + 1$, while $\kappa_p = \pm 1, \pm 2, \cdots$ and $J = 0, 1, 2 \cdots$. The infinite sum in five dimensions must be

truncated at some point, and this is done by introducing an energy cut-off $E_{\max}$ such that all terms with a mode energy below $E_{\max}$ are included in the sum. In other words, all cavity modes with ε_p, ε_q, $\Omega_m^\Sigma \leq E_{\max}$ are included. Typically, if one chooses $E_{\max} = 50$ (cf. the energy of a quark in the $1s_{\frac{1}{2}}$ state, which is 2.04 in these natural energy units), then there are approximately 1.3×10^6 terms in the series. Cut-off energies larger than this are impractical because of the rapid increase in the number of terms which are included. The computer time rises almost exponentially with the cut-off.

The spherical Bessel functions in the radial integrals are generated by either the series expansion, forward recursion or reverse recursion [22], depending on the order and argument of the Bessel function. The energy eigenvalues may be found to any desired accuracy using these Bessel functions and the eigenvalue equations (A.9) and (A.21). The integrals themselves are evaluated using Gauss-Legendre quadrature, and eq. (6.2) can be checked as a whole using the sum rule, eq. (D.18). With an energy cut-off of 50, the series and sum rule agree to 6–8 digits, depending on the quantum numbers of the incoming quark, and of the gluon.

The remaining ingredient to be calculated is the spectral function $I_{pq}^{m\Sigma}(z)$, which consists of exponential and error functions. The latter are generated from either the series expansion or a continued fraction development, with much care being taken to avoid numerical subtraction errors when the argument of the error function is large. Each term $\Lambda_{pq}^{m\Sigma}\, I_{pq}^{m\Sigma}(z)$ in the sum is calculated as a function of the parameter z, and the (infinite) sum of these z-functions yields a smooth curve $\Delta E(z)$ —the parametric representation of the energy shift.

As previously discussed, $\Delta E(z)$ is singular; it diverges as $1/z$ for small z. The functional form of this non-integrable singularity in the cavity should be exactly the same as the form derived in free space, the latter being given by eq. (3.18). In order to compare them directly, the singular, free space function Λ_S^μ must first be transformed from momentum to configuration space by restoring the external legs, which, of course, are now represented by cavity spinors, then integrated over the volume of the cavity. Finally, a factor of $-i$ is required to convert the result into an energy shift. Hence, the singular part Λ_S^μ becomes

$$\begin{aligned} \Lambda_S^\mu \;\rightarrow\; \Delta E_S \;&=\; \alpha_s \int_0^\infty dz\, \Delta E_S(z) \;=\; -\frac{\alpha_s}{4\pi}\, M_{n_1 n_2} \int_0^\infty dz\, \frac{e^{-z}}{z} \\ &=\; -2\,\frac{\alpha_s}{4\pi}\, M_{n_1 n_2} \int_0^\infty dy\, \frac{e^{-y^2}}{y} \end{aligned} \tag{6.3}$$

The last step in the above expression was to shift the variable $z \rightarrow y^2$. The reason for this shift is that the graph containing a self-energy insert has a finite component, but the 'z-form' $\Delta E(z)$ of this piece diverges as $z^{-1/2}$, i.e. it has an integrable singularity. Shifting the z variable in the above manner transforms the divergent integrand $\Delta E(z)$ into a function $\Delta E(y)$ which is regular at the origin. Of course, the non-integrable singularity in the vertex correction diagram is not affected by this transformation.

The y-form $\Delta E(y)$ for the vertex correction diagram, obtained by shifting $z \to y^2$ in eq. (6.1), can now be computed and compared directly with the singular function ΔE_S. The results of the calculation are shown in figure (6.1), where the functions $\Delta E(y)$ and ΔE_S are plotted together against y on the same axes. The initial and final quark were both in the $1s_{\frac{1}{2}}$ state with spin up for this plot, and the value of the energy cut-off used was $\Delta E_{\max} = 50$. With this cut-off, there are 1.3×10^6 of the terms $\Lambda_{pq}^{m\Sigma} I_{pq}^{m\Sigma}(y)$ in the sum, i.e. about 4 million radial integrals, and the calculation took 31 hours of CPU time on an Apollo DN3500 computer.

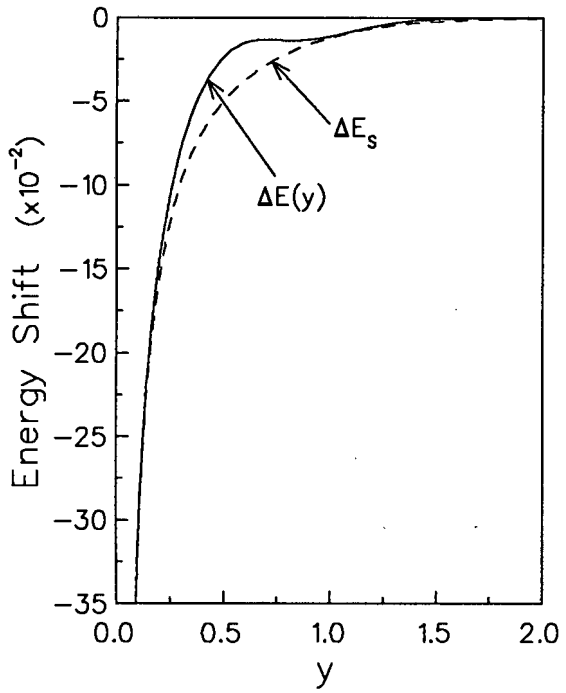

Figure 6.1: *The vertex correction energy shift (solid line) and the free space divergence ΔE_S (dashed line).*

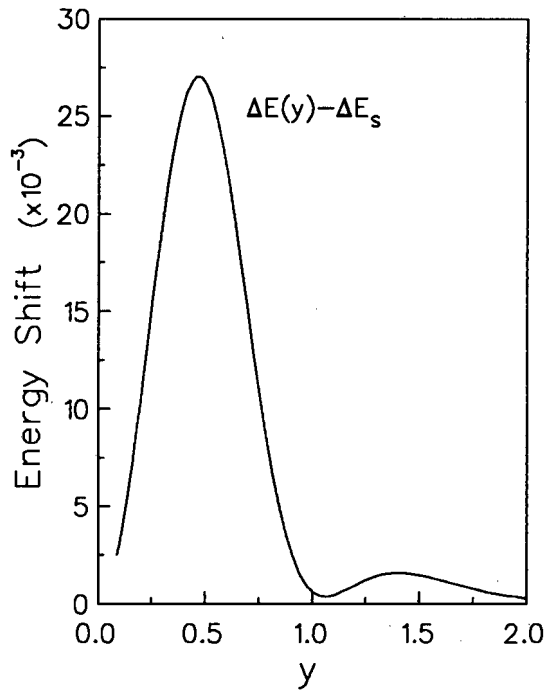

Figure 6.2: *The difference $\Delta E(y) - \Delta E_S$.*

Inspection of fig. (6.1) reveals two important points. The first is that the numerical cavity calculation produces a curve which, for small y, falls exactly on the one found by analytical means in the free space calculation. If the latter curve is subtracted from the former, as in fig. (6.2), the result is finite. In other words, the vertex correction in the cavity has been regularized by subtracting from it the divergent function ΔE_S, which contains no dependence on physical parameters such as momentum. Integrating the result over y then gives the finite contribution to the vertex correction. (However, this finite remainder is not unique. For instance, one could simply subtract an appropriately normalized curve of $1/y$ and get a finite result.)

The other point to note is that $\Delta E(y)$ does not extend all the way to zero on the y-axis. This is an effect of truncating the infinite sum over cavity modes at some energy cut-off $E_{\max}$. At some point $y_{\min}$, the error due to truncating the series cuts

in very suddenly and creates a sharp kink in the y-form. By using different values for $E_{\max}$, one can establish that this point is at

$$y_{\min} \approx \frac{\pi}{E_{\max}} \tag{6.4}$$

Apart from bringing the kink closer to the origin, increasing $E_{\max}$ does not have much of an effect on the result. The 'missing' piece of $\Delta E(y)$ in the interval $(0, y_{\min})$ may be approximated by extrapolation using Chebychev polynomials. The appearance of the error at small y is to be expected, since the spectral function goes like $\exp(-yE^2)$ and hence the largest contributions to $\Delta E(y)$ in the small y region are due to the high energy components, and these have been neglected.

6.2 Calculation of the Self-Energy Inserts and Cancellation of Divergences

Recall that the vertex graph with a self-energy insert, presented in §4.3, consisted of two separate terms; a finite one, and a term whose form resembled that of the divergent, free-space vertex function $\Lambda^{\mu}(p,p)$. After carrying out the spin sums (see appendix C) and shifting the variable $z \to y^2$, the energy shift, eq. (4.34), for this graph may be computed in the same way as the vertex correction graph. The other graph with a self-energy insert has the same contribution as this one, and is included by multiplying the result by 2. A plot of the results is presented in fig. (6.3), where the finite and singular contributions are shown separately.

Once again, the cut-off used for this calculation was $E_{\max} = 50$. The part which is regular at the origin included 7×10^5 terms in the sum and took 10 CPU hours on the Apollo DN3500, while the divergent part included 3×10^4 terms and needed a mere 33 minutes of CPU time. One may easily establish numerically that this term blows up as $1/y$ for small y.

The contribution from the self-energy inserts must now be added to that from the vertex correction. When this is done, the $1/y$ divergences from each diagram are found to cancel out exactly, as expected, leaving a piece which is regular at the origin. This can be seen in fig. (6.4). Integrating the finite remainder gives the energy shift due to the first order radiative corrections.

Finally, the gauge-dependent terms arising from the three loop diagrams can be calculated as above and added together. Again, the self-energy diagram has both a finite and a singular component, shown separately in figure (6.5), and these have been multiplied by 2 since there are two such graphs. When the two self-energy components are added to the divergent vertex correction, the result is some 8 orders of magnitude smaller than any of the contributions for all values of y, except where the usual truncation error comes in at $y_{\min}$. The area under the resultant curve, which is the gauge-dependent contribution to the anomalous magnetic moment of a quark, is found to be -4.8×10^{-8}. This number was calculated by extrapolating the

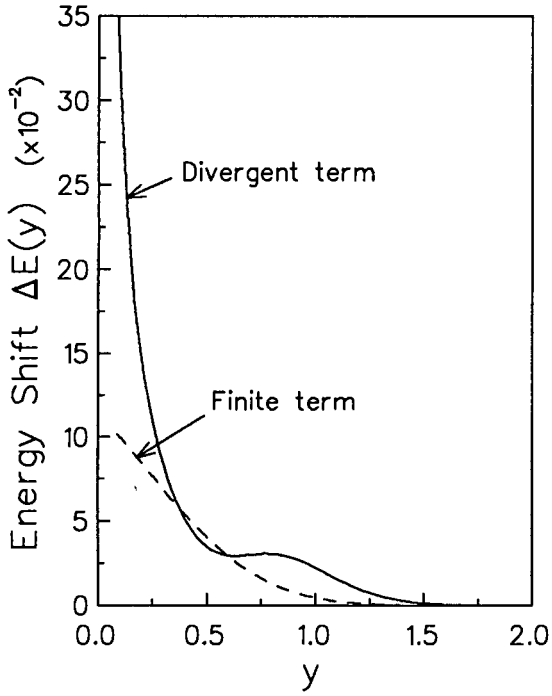

Figure 6.3: *The divergent (solid line) and finite (dashed line) parts of the self-energy inserts.*

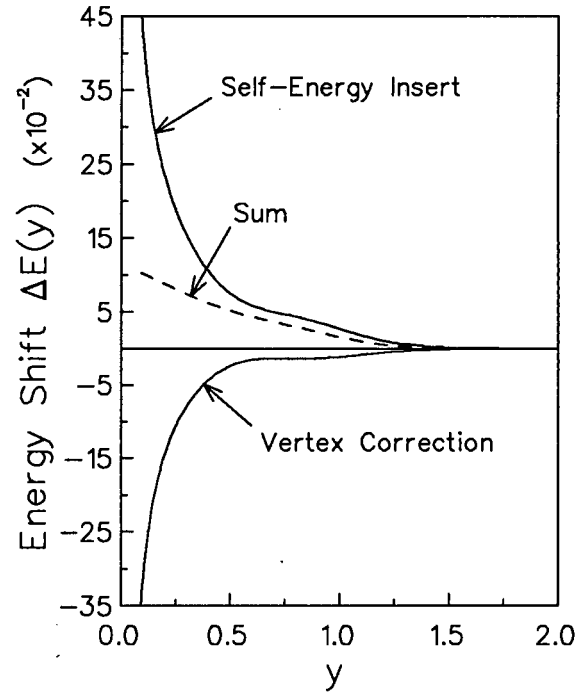

Figure 6.4: *The result after adding the energy shifts for the vertex correction and self-energy inserts.*

curve through the region where the error comes in, and is consistent with zero within the limits of accuracy of this numerical calculation.

The one-gluon exchange diagrams are much easier to compute since they are finite and absolutely convergent. Conservation of angular momentum constrains the sum over j and J of the intermediate quark and gluon to a few values, leaving only two infinite sums over the radial modes ν and N, which are simply truncated at the 60^{th} radial mode. The vertex integrals agree with the sum rule, eq. (D.34), to 8 digits, and the energy shift, eq. (5.5), converges to 10 digits with this method of truncation.

6.3 Results

As mentioned above, the energy shift due to the vertex graphs is obtained by integrating the area under the curve which results when the y-forms for these graphs are added together. This has been done in table 6.1 below, where the energy shifts for the first few quark states are presented. The colour factor of 4/3 is not included.

Similarly, the energy shifts due to the one-gluon exchange graphs for a few quark states are given in table 6.2. In this case, the energy shift involves a two-particle operator acting on the quarks between which the gluon is exchanged. Once again, the colour factor has not been included.

Using the values for the energy shifts given in tables 6.1 and 6.2, and the colour-

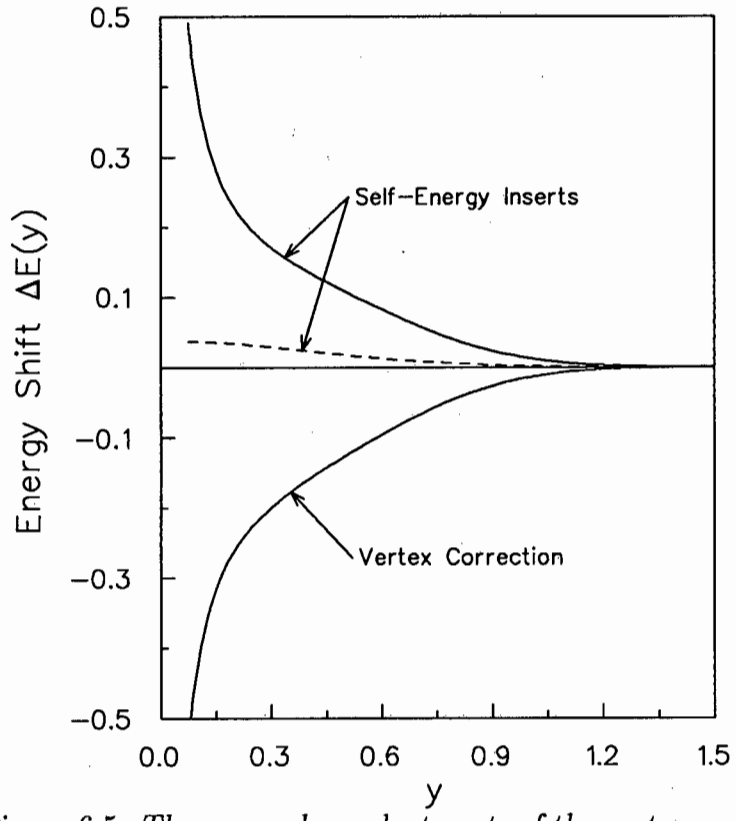

Figure 6.5: *The gauge-dependent parts of the vertex correction and self-energy diagrams.*

flavour matrix elements given in appendix E, the first order radiative corrections to the proton and neutron magnetic moments may immediately be found. The zero'th order values may be calculated using the quark-quark-photon vertex integrals derived in appendix B. Restoring all factors of $\hbar$ and c, setting the cavity radius $R = 1$ fm, $\alpha_s = 2.2$ and writing the magnetic moments in the form

$$\mu_{\rm p} \;=\; \mu_{\rm p}^{(0)} + \alpha_s \delta\mu_{\rm p}^{(1)} + \alpha_s \delta\mu_{\rm p}^{(2)}$$

for the zero'th order, and first order one- and two-body corrections, the results are

	Zero'th Order	First Order Corrections			Theory	Experiment
		1-body	2-body	Total		
$\mu_{\rm p}$	1.924	−1.683	0.0267	−1.656	0.2680	2.793
$\mu_{\rm n}$	−1.282	1.122	0.1238	1.245	−0.0365	−1.913

The magnetic moments are in units of the nuclear magnetons, $\mu_{\rm N} = e\hbar/2m_{\rm p}$.

Cavity mode	Eigen-energy	Energy Shift
$1s_{\frac{1}{2}}\uparrow$	2.043	0.06032
$1s_{\frac{1}{2}}\downarrow$	2.043	−0.06032
$2s_{\frac{1}{2}}\uparrow$	5.396	0.01226
$1p_{\frac{1}{2}}\uparrow$	3.812	0.04035
$1p_{\frac{3}{2}}\uparrow$	3.204	0.01618
$1d_{\frac{3}{2}}\uparrow$	5.123	0.01545

Table 6.1: *Energy shifts due to the radiative corrections to the quark-quark-photon vertex in units of* $\alpha_s R$. $\mu = \frac{1}{2}$, *and the arrow indicates the spin projection.*

6.4 Conclusion

The proton and neutron magnetic moments, with the $O(\alpha_s)$ corrections due to the 5 Feynman diagrams shown in fig. (4.1), are found to be

$$\mu_{\rm p} = 0.2680\ \mu_{\rm N}$$

$$\mu_{\rm n} = -0.0365\ \mu_{\rm N}$$

The poor agreement between theory and experiment obtained here is immediately seen to be due to the contributions from the one-body corrections, which are large and apparently have the 'wrong' sign. In view of this discrepancy, some comparison should be made between these results and other calculations available in the literature.

The calculation of the two-body corrections has been presented in several papers, the most recent of which are due to Tsushima *et al.* [5], and to Høgaasen and Myhrer [23]. The latter is, in fact, a re-calculation and confirmation of earlier results by Ushio [24] and Krivoruchenko [25]. These authors calculate the contribution to $\delta\mu^{(2)}$ due to the transverse magnetic gluon, and get $\delta\mu_{\rm p}^{(2)} = 0$ for the proton, and $\alpha_s\delta\mu_{\rm n}^{(2)} = 0.133\,\mu_{\rm N}$ for the neutron. These numbers are confirmed in the present calculation when the scalar gluon is omitted from the calculation. (The transverse electric and longitudinal gluons do not contribute anyway.)

The calculation by Maxwell and Vento (M&V) of these corrections [17] uses a similar formalism to that employed here, and it includes a rigorous treatment of the divergent vertex correction diagram. However, the authors have not calculated the vertex diagrams containing self-energy inserts, so their results for the one-body corrections are gauge-dependent and thus no comparison can be made between the current results and their ones for these terms. On the other hand, the one-gluon exchange corrections are automatically gauge independent, so their results can be compared with this calculation.

Cavity mode ; $\mu_1\,\mu_2\,\mu_3\,\mu_4$	Energy Shift $\times 10^{-3}$
$1s_{\frac{1}{2}}$; $\uparrow\uparrow\uparrow\uparrow$	-8.0878
$1s_{\frac{1}{2}}$; $\uparrow\uparrow\downarrow\downarrow$	-7.1328
$1s_{\frac{1}{2}}$; $\downarrow\downarrow\uparrow\uparrow$	7.1328
$1s_{\frac{1}{2}}$; $\uparrow\downarrow\downarrow\uparrow$	0.5020
$1s_{\frac{1}{2}}$; $\downarrow\uparrow\uparrow\downarrow$	-0.5020
$2s_{\frac{1}{2}}$; $\uparrow\uparrow\uparrow\uparrow$	-1.7751
$2s_{\frac{1}{2}}$; $\uparrow\uparrow\downarrow\downarrow$	-2.4039
$1p_{\frac{1}{2}}$; $\uparrow\uparrow\uparrow\uparrow$	-2.8374
$1p_{\frac{1}{2}}$; $\uparrow\uparrow\downarrow\downarrow$	-5.6727
$1p_{\frac{3}{2}}$; $\uparrow\uparrow\uparrow\uparrow$	-4.9517
$1p_{\frac{3}{2}}$; $\uparrow\uparrow\downarrow\downarrow$	-2.6862

Table 6.2: *Energy shifts due to the one-gluon exchange, with all quarks in the same cavity mode. The spins of the incoming and outgoing quarks are indicated by the arrows.*

	M&V	O'C
$\delta\mu_{\rm p}$	-0.11	0.0267
$\delta\mu_{\rm n}$	0.22	0.1238

Correction due to the one-gluon exchange

Maxwell and Vento's result for the proton has the opposite sign to ours, and is larger by a factor of 4, while the neutron correction has the same sign but is twice as large. Further investigation has not revealed the source of the discrepancy.

The formalism developed here can be extended very easily to the calculation of other properties of the baryons, such as g_A, $\langle r^2\rangle$, etc. In fact, one should be able to calculate *all* one-loop diagrams in cavity QCD using this formalism, provided that the renormalization scheme employed is meaningful. In the case of the proton magnetic moment, the divergences arising from the contributing diagrams cancel. Another example is the gluon self-energy, where the divergences from the ghost- and gluon loops, and the gluon tadpole all cancel out. The quark loop contributing to the gluon self-energy may be separated into two components, and the divergences in each piece are also found to cancel each other [26]. Alternatively, it has been shown here that the cavity diagrams can be renormalized by subtracting from them the free-space divergences, but this process is less attractive because the renormalization scheme

is not well defined. (There may be some unknown constants factors, e.g. Euler's γ, arising from the cavity calculation which are not present in the free-space diagram.) It has also been shown that this formalism enables one to work in an arbitrary gauge without increasing the difficulty of the calculations, a feature which has proved to be useful for divergent loop diagrams.

Another method of renormalizing the divergent loop diagrams in the cavity is the multiple reflection expansion (MRE) of Hansson and Jaffe [27], where the divergent, boundary independent contribution to the diagram is isolated analytically. For a discussion of the relative merits of the MRE and the method presented in this work, see Stoddart and Viollier [7] [8], who have performed a calculation of the quark self-energy in a cavity and compared it to a MRE calculation of the same quantity by Goldhaber *et al.* [28].

6.5 Acknowledgments

I am grateful to the Foundation for Research and Development and the University of Cape Town for their financial support, in the form of FRD bursaries and Research Associateships, during the preparation of this thesis.

My sincere thanks go to my supervisor, Professor R. D. Viollier, for his patience and encouragement when progress on this project was slow, and for providing the excellent computer systems required for these calculations.

The staff and students of the Institute of Theoretical Physics deserve mention for all the helpful discussions had with them, especially Dr. Andrew Stoddart, who provided valuable guidance through the many difficulties encountered at the start of a new project, and Dr. Gary Tupper for his help with free-space QCD. Most of all, I would like to thank my fellow student Gunhild Schreiber for taking an active interest in this work, a compliment which has been much appreciated. In addition, she deserves special thanks for producing all the diagrams used here in LaTeX, and for proof-reading this manuscript.

Appendix A

The Cavity Modes

The quark and gluon cavity modes will be presented in this appendix for easy reference. The source of much of this material is ref. [6].

A.1 Quark Cavity Modes

The quark wave functions are solutions of the Dirac equation, (2.10), subject to the boundary condition eq. (2.13) of the M.I.T. bag model. The time-independent Dirac equation for a quark with flavour f and mass m_f is

$$\left(-i\vec{\gamma}\cdot\vec{\nabla}+m_f\right)u_n(\vec{r})=\varepsilon_n\gamma^0 u_n(\vec{r}) \tag{A.1}$$

where ε_n is the energy of the quark. The solutions of this equation, subject to the M.I.T. boundary condition, are given by the spinors

$$u_n(\vec{r})=\begin{pmatrix} g_n(r)\chi^\mu_\kappa(\hat{\boldsymbol{r}}) \\ if_n(r)\chi^\mu_{-\kappa}(\hat{\boldsymbol{r}}) \end{pmatrix} \tag{A.2}$$

and the adjoint spinor by

$$\bar{u}_n(\vec{r})=u_n^\dagger(\vec{r})\gamma^0 \tag{A.3}$$

Here, $n=\{\nu,\kappa,\mu\}$ labels respectively the radial, Dirac and magnetic quantum numbers of the cavity mode, and $\chi^\mu_\kappa(\hat{\boldsymbol{r}})$ is the usual two-component spherical spinor. The radial functions $g_n(r)$ and $f_n(r)$ are given by

$$g_n(r) = \frac{\mathcal{N}_n}{R^{3/2}}\,j_\ell(p_n r) \tag{A.4}$$

$$f_n(r) = \frac{\mathcal{N}_n}{R^{3/2}}\,\mathrm{sgn}(\kappa)\,\frac{p_n}{\varepsilon_n+m_f}\,j_{\bar{\ell}}(p_n r) \tag{A.5}$$

where $j_\ell(x)$ is the spherical Bessel function and R is the radius of the cavity. The total and orbital angular momentum j and ℓ are defined in terms of the Dirac quantum

number κ by

$$j(\kappa) = |\kappa| - \tfrac{1}{2} \tag{A.6}$$

$$\ell(\kappa) = j(\kappa) + \tfrac{1}{2}\,\mathrm{sgn}(\kappa) \tag{A.7}$$

$$\bar{\ell}(\kappa) = j(\kappa) - \tfrac{1}{2}\,\mathrm{sgn}(\kappa) \tag{A.8}$$

The momentum p_n is determined by the boundary conditions imposed on the quark fields at the surface of the cavity. For a static and spherical bag, p_n is a solution of the transcendental equation

$$j_\ell(x_n) + \frac{x_n}{\omega_n + \zeta_f}\,\mathrm{sgn}(\kappa) j_{\bar{\ell}}(x_n) = 0 \tag{A.9}$$

where, for convenience, the energy, momentum and mass have been written in terms of the dimensionless quantities ω_n, x_n and ζ_f respectively. These are defined by

$$x_n = p_n R \tag{A.10}$$

$$\zeta_f = m_f R \tag{A.11}$$

$$\omega_n = \varepsilon_n R = \mathrm{sgn}(\nu)\sqrt[+]{x_n^2 + \zeta_f^2} \tag{A.12}$$

The positive and negative energy solutions are characterized by $\nu > 0$ and $\nu < 0$ respectively, and by symmetry, $\varepsilon_{-\nu,\kappa} = -\varepsilon_{\nu,-\kappa}$. Finally, the normalization constant $\mathcal{N}_n$ is given by

$$\mathcal{N}_n^2 = \frac{1}{2\omega_n(\omega_n + \kappa) + \zeta_f}\left(\frac{x_n}{j_\ell(x_n)}\right)^2 \tag{A.13}$$

The spinors (A.2) form a complete and orthonormal set of states defined within the cavity. Explicitly, the completeness relation is given by

$$\sum_n u_n(\vec{r}) u_n^\dagger(\vec{r}') = \delta^{(3)}(\vec{r}, \vec{r}')\, I \tag{A.14}$$

where I is the unit 4×4 matrix, and the orthonormality by

$$\int d^3r\, u_n^\dagger(\vec{r}) u_{n'}(\vec{r}) = \delta_{nn'} \tag{A.15}$$

A.2 The Gluon Cavity Modes

The gluon modes $a^\mu_{m\Sigma}(\vec{r})$ are solutions of the wave equation for massless vector fields subject to the M.I.T. boundary conditions (2.14)

$$\left(\nabla^2 + \Omega_m^2\right) a_m^\mu(\vec{r}) = 0 \tag{A.16}$$

The solutions of these equations are labelled by $\Sigma = \mathcal{S}, \mathcal{L}, \mathcal{M}, \mathcal{E}$ for the scalar, longitudinal, transverse magnetic and transverse electric polarizations respectively, and

$m = \{N, J, M\}$ denotes the radial, total angular momentum and magnetic quantum numbers respectively. In terms of spherical Bessel functions and vector spherical harmonics, the cavity modes are

$$a^0_{m\mathcal{S}}(\vec{r}) = \frac{\mathcal{N}_{m\mathcal{S}}}{R^{3/2}}\, i j_J(\Omega^{\mathcal{S}}_m r)\, Y_{JM}(\hat{\boldsymbol{r}}) \tag{A.17}$$

$$\vec{a}_{m\mathcal{L}}(\vec{r}) = \frac{\mathcal{N}_{m\mathcal{L}}}{\sqrt{R^3(2J+1)}}\left[\sqrt{J}\, j_{J-1}(\Omega^{\mathcal{L}}_m r)\, \vec{Y}^{J-1}_{JM}(\hat{\boldsymbol{r}}) + \sqrt{J+1}\, j_{J+1}(\Omega^{\mathcal{L}}_m r)\, \vec{Y}^{J+1}_{JM}(\hat{\boldsymbol{r}})\right] \tag{A.18}$$

$$\vec{a}_{m\mathcal{M}}(\vec{r}) = \frac{\mathcal{N}_{m\mathcal{M}}}{R^{3/2}}\, j_J(\Omega^{\mathcal{M}}_m r)\, \vec{Y}^{J}_{JM}(\hat{\boldsymbol{r}}) \tag{A.19}$$

$$\vec{a}_{m\mathcal{E}}(\vec{r}) = \frac{\mathcal{N}_{m\mathcal{E}}}{\sqrt{R^3(2J+1)}}\left[\sqrt{J+1}\, j_{J-1}(\Omega^{\mathcal{E}}_m r)\, \vec{Y}^{J-1}_{JM}(\hat{\boldsymbol{r}}) - \sqrt{J}\, j_{J+1}(\Omega^{\mathcal{E}}_m r)\, \vec{Y}^{J+1}_{JM}(\hat{\boldsymbol{r}})\right] \tag{A.20}$$

The total angular momentum J is defined such that $J \geq 0$ for $\Sigma = \mathcal{S}, \mathcal{L}$ and $J \geq 1$ for $\Sigma = \mathcal{M}, \mathcal{E}$. The boundary conditions for a spherical cavity reduce to the following eigenvalue conditions for the gluon energy

$$\begin{aligned} J j_J(\Omega^{\mathcal{S}}_m R) - \Omega^{\mathcal{S}}_m R\, j_{J+1}(\Omega^{\mathcal{S}}_m R) = 0 \qquad & \Sigma = \mathcal{S},\ \mathcal{L} \\ (J+1)\, j_J(\Omega^{\mathcal{M}}_m R) - \Omega^{\mathcal{M}}_m R\, j_{J+1}(\Omega^{\mathcal{M}}_m R) = 0 \qquad & \Sigma = \mathcal{M} \\ j_J(\Omega^{\mathcal{E}}_m R) = 0 \qquad & \Sigma = \mathcal{E} \end{aligned} \tag{A.21}$$

It turns out that the energies of the scalar and longitudinal modes are equal, $\Omega^{\mathcal{L}}_m = \Omega^{\mathcal{S}}_m$. The normalization constants are given by

$$\mathcal{N}^{-2}_{m\mathcal{S}} = \mathcal{N}^{-2}_{m\mathcal{L}} = \tfrac{1}{2} j^2_J(\Omega^{\mathcal{S}}_m R)\left[1 - \frac{J(J+1)}{(\Omega^{\mathcal{S}}_m R)^2}\right] \tag{A.22}$$

$$\mathcal{N}^{-2}_{m\mathcal{M}} = \tfrac{1}{2} j^2_J(\Omega^{\mathcal{M}}_m R)\left[1 - \frac{J(J+1)}{(\Omega^{\mathcal{M}}_m R)^2}\right] \tag{A.23}$$

$$\mathcal{N}^{-2}_{m\mathcal{E}} = \tfrac{1}{2} j^2_{J+1}(\Omega^{\mathcal{E}}_m R) \tag{A.24}$$

The set of gluon modes satisfying eq. (A.16) is complete and orthonormal. These properties are most conveniently expressed by introducing the metric tensor in polarization space, $g^{\Sigma\Sigma}$. With its help, the completeness relation may be written as

$$\sum_{m\Sigma} g^{\Sigma\Sigma}\, a^{\mu}_{m\Sigma}(\vec{r})\, a^{\nu *}_{m\Sigma}(\vec{r}') = g^{\mu\nu}\, \delta^{(3)}(\vec{r},\vec{r}') \tag{A.25}$$

and orthonormality is then given by

$$\int d^3r\, g_{\mu\nu}\, a^{\mu}_{m\Sigma}(\vec{r})\, a^{\nu *}_{m'\Sigma'}(\vec{r}) = g^{\Sigma\Sigma'}\delta_{mm'} \tag{A.26}$$

The diagonal metric $g^{\Sigma\Sigma}$ is represented as

$$g^{\mathcal{SS}} = -g^{\mathcal{LL}} = -g^{\mathcal{MM}} = -g^{\mathcal{EE}} = 1 \quad ; \qquad g^{\Sigma\Sigma'} = 0 \quad \text{if } \Sigma \neq \Sigma' \tag{A.27}$$

Finally, a few useful identities concerning the cavity modes are noted. Using the properties of the vector spherical harmonics, the complex conjugate of $a^{\mu}_{m\Sigma}(\vec{r})$ is

$$a^{\mu *}_{m\Sigma}(\vec{r}) = (-1)^M \eta^{\Sigma} a^{\mu}_{m^*\Sigma}(\vec{r}) \tag{A.28}$$

with the definition $m^* = \{N, J, -M\}$. The phase η^{Σ} is shorthand for

$$\eta^{\Sigma} = \begin{cases} -1 & \text{if } \Sigma = \mathcal{S}, \mathcal{M} \\ +1 & \text{if } \Sigma = \mathcal{L}, \mathcal{E} \end{cases} \tag{A.29}$$

The scalar and longitudinal modes are related by current conservation in the following way:

$$a^0_{m\mathcal{S}}(\vec{r}) \;=\; -\frac{i}{\Omega^{\mathcal{S}}_m}\vec{\nabla}\cdot\vec{a}_{m\mathcal{L}}(\vec{r}) \tag{A.30}$$

$$\vec{a}_{m\mathcal{L}}(\vec{r}) \;=\; -\frac{i}{\Omega^{\mathcal{S}}_m}\vec{\nabla} a^0_{m\mathcal{S}}(\vec{r}) \tag{A.31}$$

Appendix B

Vertex Integrals

The integrals associated with the quark-quark-gluon vertex, and the coupling of quarks to the external operator will evaluated in this appendix.

B.1 The Quark-Gluon Vertex Integral

The interaction between quarks and gluons is described by the integral which is defined as

$$Q^{m\Sigma}_{nn'} = i \int d^3r\, \bar{u}_n(\vec{r})\gamma_\mu u_{n'}(\vec{r})\, a^\mu_{m\Sigma}(\vec{r}) \tag{B.1}$$

Closely associated with this integral is one in which the gluon field is replaced with its complex conjugate, which will be written as

$$\tilde{Q}^{m\Sigma}_{nn'} = i \int d^3r\, \bar{u}_n(\vec{r})\gamma_\mu u_{n'}(\vec{r})\, a^{\mu *}_{m\Sigma}(\vec{r}) \tag{B.2}$$

Using (A.28), this may be reduced to (B.1) as follows:

$$\tilde{Q}^{m\Sigma}_{nn'} = (-1)^M \eta^\Sigma i \int d^3r\, \bar{u}_n(\vec{r})\gamma_\mu u_{n'}(\vec{r})\, a^\mu_{m^*\Sigma}(\vec{r}) = (-1)^M \eta^\Sigma Q^{m^*\Sigma}_{nn'} = -Q^{m\Sigma}_{n'n} \tag{B.3}$$

Following Viollier *et al.* in ref. [29], but using a slightly different notation, the radial and angular dependence of (B.1) can be separated as

$$\begin{aligned} Q^{m\Sigma}_{nn'} &= R^{-3/2} R^{m\Sigma}_{nn'} \int d\Omega\, \chi^{\mu\dagger}_\kappa(\hat{\boldsymbol{r}}) Y_{JM}(\hat{\boldsymbol{r}}) \chi^{\mu'}_{\kappa'}(\hat{\boldsymbol{r}}) && \Sigma = \mathcal{S}, \mathcal{L}, \mathcal{E} \\ Q^{m\mathcal{M}}_{nn'} &= R^{-3/2} R^{m\mathcal{M}}_{nn'} \int d\Omega\, \chi^{\mu\dagger}_\kappa(\hat{\boldsymbol{r}}) Y_{JM}(\hat{\boldsymbol{r}}) \chi^{\mu'}_{-\kappa'}(\hat{\boldsymbol{r}}) && \Sigma = \mathcal{M} \end{aligned} \tag{B.4}$$

The integral over the angular variables is readily done by expanding the spinors and spherical harmonics in a Clebsch-Gordan series. In terms of the Wigner $3j$-symbols,

the result is

$$\int d\Omega\, \chi^{\mu\dagger}_{\kappa}(\hat{\boldsymbol{r}}) Y_{JM}(\hat{\boldsymbol{r}}) \chi^{\mu'}_{\kappa'}(\hat{\boldsymbol{r}}) = \frac{(-1)^{\mu+1/2}}{\sqrt{4\pi}} \frac{1+(-1)^{\ell+J+\ell'}}{2} \hat{j}\hat{J}\hat{j}' \times \begin{pmatrix} j & J & j' \\ -\mu & M & \mu' \end{pmatrix} \begin{pmatrix} j & J & j' \\ \frac{1}{2} & 0 & -\frac{1}{2} \end{pmatrix} \tag{B.5}$$

where the abbreviation $\hat{J} = \sqrt{2J+1}$ has been introduced. The notation for the $3j$-symbols is that of the encyclopedic Varshalovich *et al.* [30], and is consistent with the standard notation of Edmonds [31]. The radial integrals are given by

$$R^{m\mathcal{S}}_{nn'} = -\mathcal{N}_{m\mathcal{S}} \int_0^R dr\, r^2\, j_J(\Omega^{\mathcal{S}}_m r) S_{nn'}(r) \tag{B.6}$$

$$R^{m\mathcal{L}}_{nn'} = -\frac{\mathcal{N}_{m\mathcal{S}}}{\Omega^{\mathcal{S}}_m} \int_0^R dr\, r \Big\{ \Big[\Omega^{\mathcal{S}}_m r\, j_{J+1}(\Omega^{\mathcal{S}}_m r) - J\, j_J(\Omega^{\mathcal{S}}_m r) \Big] U_{nn'}(r) + (\kappa - \kappa')\, j_J(\Omega^{\mathcal{S}}_m r) T_{nn'}(r) \Big\} \tag{B.7}$$

$$R^{m\mathcal{M}}_{nn'} = \frac{\kappa + \kappa'}{\sqrt{J(J+1)}} \mathcal{N}_{m\mathcal{M}} \int_0^R dr\, r^2\, j_J(\Omega^{\mathcal{M}}_m r) T_{nn'}(r) \tag{B.8}$$

$$R^{m\mathcal{E}}_{nn'} = \frac{\mathcal{N}_{m\mathcal{E}}}{\Omega^{\mathcal{E}}_m \sqrt{J(J+1)}} \int_0^R dr\, r \Big\{ (\kappa - \kappa') \Big[J\, j_J(\Omega^{\mathcal{E}}_m r) - \Omega^{\mathcal{E}}_m r\, j_{J-1}(\Omega^{\mathcal{E}}_m r) \Big] T_{nn'}(r) + J(J+1)\, j_J(\Omega^{\mathcal{E}}_m r) U_{nn'}(r) \Big\} \tag{B.9}$$

Three further abbreviations have been introduced here for the radial parts of the quark wave functions. They are

$$\begin{aligned} S_{nn'} &= g_n g_{n'} + f_n f_{n'} \\ T_{nn'} &= g_n f_{n'} + f_n g_{n'} \\ U_{nn'} &= g_n f_{n'} - f_n g_{n'} \end{aligned} \tag{B.10}$$

It is convenient to include the phase factor from the angular integration (B.5), which contains the parity selection rule, into the radial functions by defining a new quantity:

$$S^{m\Sigma}_{nn'} = \frac{1 - g^{\Sigma\Sigma}\eta_\Sigma\,(-1)^{\ell+J+\ell'}}{2} R^{m\Sigma}_{nn'} \tag{B.11}$$

The vertex integrals involving the scalar and longitudinal modes are related by current conservation, (B.12).

$$Q^{m\mathcal{L}}_{nn'} = \frac{\varepsilon_{n'} - \varepsilon_n}{\Omega^{\mathcal{S}}_m} Q^{m\mathcal{S}}_{nn'} \tag{B.12}$$

The angular integrals for the quark-quark-gluon vertex are fairly easy to compute, either analytically or numerically. This is unfortunately not so for the radial integrals, which present a formidable numerical task. The main problem here is in achieving a satisfactory balance between computational speed and accuracy. The integrands in which the sum of the radial quantum numbers $\nu + \nu' + N$ is large are highly oscillatory, having approximately $(\nu + \nu' + N)$ oscillations in the range $0 \leq r \leq R$. Although the contributions from these terms are individually small, there are a great many of them, so they must be calculated reasonably accurately. On the other hand, the computer time increases prohibitively if one tries to integrate the oscillatory matrix elements with the same accuracy as the smooth ones.

Ideally then, the radial integrals should be done analytically. The basic problem is to evaluate the following integral of three Bessel functions

$$I = \int dr\, r^2\, j_m(ar) j_n(br) j_p(cr) \tag{B.13}$$

for arbitrary real numbers a, b and c and integers m, n and p. A full frontal assault on (B.13) using Bessel's differential equation and the recurrence relations for spherical Bessel functions [32] proved to be of no avail, although the definite integral, with limits $0 \rightarrow \infty$, has been done recently by Gervois and Navelet [33]. This just recovers the free space limit. A series solution for the finite integral was tried, but the Appell functions which resulted were not useful for numerical calculation. The remaining hope for an analytical solution is that the problem simplifies if the special properties of the energy eigenvalues are exploited instead of using the general variables a, b and c. This has not yet been attempted.

B.2 The Quark-Quark-External Photon Vertex

The integral which describes the interaction between a quark and the external field is defined here as

$$M_{nn'} = \int d^3r\, \bar{u}_n(\vec{r}) \gamma_\mu u_{n'}(\vec{r})\, A^\mu_{\rm ext}(\vec{r}) \tag{B.14}$$

The external operator used in the calculation of magnetic moments is the potential due to a static magnetic field oriented along the z-axis. However, the entire formalism developed so far is quite general: if one wished to calculate other observables in the cavity, the only change to be made would be to substitute the appropriate operator into the above expression.

The external field is given by

$$\vec{A}_{\rm ext}(\vec{r}) \;=\; -\tfrac{1}{2}\,(y, -x, 0) \;=\; -\tfrac{1}{2}\,\vec{r} \times \vec{B} \tag{B.15}$$

Henceforth, the strength of the magnetic field B will be set to unity, since its value cancels out in any case when the magnetic moment is taken.

An approach to separating the radial and angular dependence in (B.14) which is both rather elegant and quite fun is to first re-write $\vec{A}_{\rm ext}(\vec{r})$ in terms of the angular

momentum operator

$$\vec{A}_{\rm ext}(\vec{r}) = -i\sqrt{\frac{\pi}{3}}\,\vec{L}rY_{10}(\hat{r}) \tag{B.16}$$

from which the vertex integral becomes

$$M_{nn'} = \sqrt{\frac{\pi}{3}}\int d^3r\left[g_n f_{n'}\,\chi^{\mu\dagger}_{\kappa}\left(\vec{\sigma}\cdot\vec{L}rY_{10}\right)\chi^{\mu'}_{-\kappa'} - f_n g_{n'}\,\chi^{\mu\dagger}_{-\kappa}\left(\vec{\sigma}\cdot\vec{L}rY_{10}\right)\chi^{\mu'}_{\kappa'}\right] \tag{B.17}$$

where the $\vec{\sigma}$'s are the Pauli matrices. Using the shorthand $\hat{r}\cdot\vec{\sigma} = \sigma_r$ where $\sigma_r^2 = 1$, and noting that

$$\sigma_r\left(\vec{\sigma}\cdot\vec{L}\right)\sigma_r = -\vec{\sigma}\cdot\vec{L} \tag{B.18}$$

the second term in eq. (B.17) can be re-written in the following form

$$\chi^{\mu\dagger}_{-\kappa}\left(\vec{\sigma}\cdot\vec{L}rY_{10}\right)\chi^{\mu'}_{\kappa'} \;=\; \chi^{\mu\dagger}_{\kappa}\sigma_r\left(\vec{\sigma}\cdot\vec{L}rY_{10}\right)\sigma_r\,\chi^{\mu'}_{-\kappa'} \;=\; -\chi^{\mu\dagger}_{\kappa}\left(\vec{\sigma}\cdot\vec{L}rY_{10}\right)\chi^{\mu'}_{-\kappa'} \tag{B.19}$$

since $\sigma_r\,\chi^{\mu}_{-\kappa} = \chi^{\mu}_{\kappa}$. Hence, (B.17) becomes

$$M_{nn'} = \sqrt{\frac{\pi}{3}}\int_0^R dr\,r^3\left(g_n f_{n'} + f_n g_{n'}\right)\int d\Omega\,\chi^{\mu\dagger}_{\kappa}(\hat{r})\left(\vec{\sigma}\cdot\vec{L}\,Y_{10}(\hat{r})\right)\chi^{\mu'}_{-\kappa'}(\hat{r}) \tag{B.20}$$

The Hermitean operator $\vec{\sigma}\cdot\vec{L}$ acts only on Y_{10}, but it is convenient to change its action according to

$$\chi^{\mu\dagger}_{\kappa}\left(\vec{\sigma}\cdot\vec{L}\,Y_{10}\right)\chi^{\mu'}_{-\kappa'} = \chi^{\mu\dagger}_{\kappa}\left(\vec{\sigma}\cdot\vec{L}\,Y_{10}\chi^{\mu'}_{-\kappa'}\right) - \chi^{\mu\dagger}_{\kappa}Y_{10}\left(\vec{\sigma}\cdot\vec{L}\,\chi^{\mu'}_{-\kappa'}\right) \tag{B.21}$$

Recalling that the action of $\vec{\sigma}\cdot\vec{L}$ on a spinor is simply

$$\vec{\sigma}\cdot\vec{L}\,\chi^{\mu}_{\kappa}(\hat{r}) = -(\kappa+1)\,\chi^{\mu}_{\kappa}(\hat{r}) \tag{B.22}$$

and exploiting the Hermitean nature of the operator, eq. (B.21) becomes

$$\begin{aligned}\chi^{\mu\dagger}_{\kappa}\left(\vec{\sigma}\cdot\vec{L}\,Y_{10}\right)\chi^{\mu'}_{-\kappa'} \;&=\; \left(\vec{\sigma}\cdot\vec{L}\,\chi^{\mu}_{\kappa}\right)^{\dagger}Y_{10}\chi^{\mu'}_{-\kappa'} - \chi^{\mu\dagger}_{\kappa}Y_{10}\left(\vec{\sigma}\cdot\vec{L}\,\chi^{\mu'}_{-\kappa'}\right)\\ &=\; -(\kappa+\kappa')\,\chi^{\mu\dagger}_{\kappa}Y_{10}\chi^{\mu'}_{-\kappa'}\end{aligned} \tag{B.23}$$

Eq. (B.20) now becomes

$$M_{nn'} = -\sqrt{\frac{\pi}{3}}\int_0^R dr\,r^3\left(g_n f_{n'} + f_n g_{n'}\right)\int d\Omega\,(\kappa+\kappa')\,\chi^{\mu\dagger}_{\kappa}(\hat{r})Y_{10}(\hat{r})\chi^{\mu'}_{-\kappa'}(\hat{r}) \tag{B.24}$$

The total angular momentum of the external field is $J = 1$, which means that the angular momentum which can be transferred to the quark field is either 0 or 1. Because of this, the radial and angular integrals may be evaluated analytically, since κ is restricted to either $\kappa = \kappa'$ or $\kappa = -\kappa' - 1$. Defining the angular integral as

$$A_{\kappa\kappa'} \;\equiv\; -\sqrt{\frac{\pi}{3}}\,(\kappa+\kappa')\int d\Omega\,\chi^{\mu\dagger}_{\kappa}(\hat{r})Y_{10}(\hat{r})\chi^{\mu'}_{-\kappa'}(\hat{r}) \tag{B.25}$$

the explicit results are

$$\begin{aligned} A_{\kappa\kappa} &= \frac{2\kappa\mu}{4\kappa^2-1} && \text{if } \kappa' = \kappa \\ A_{\kappa,-\kappa-1} &= \frac{\mathrm{sgn}(\kappa)}{4\,|\kappa|+2}\sqrt{\left(|\kappa|+\tfrac{1}{2}\right)^2-\mu^2} && \text{if } \kappa' = -\kappa-1 \end{aligned} \tag{B.26}$$

where the quantity $A_{\kappa,-\kappa-1} = A_{-\kappa-1,\kappa}$ is symmetric. All other possibilities are zero.

For the radial matrix elements, the following two integrals involving Bessel functions are needed. They may be derived using only the recursion relations of the spherical Bessel functions.

$$\int dr\, r^3\, j_n(ar) j_{n+1}(ar) = \tag{B.27}$$

$$\frac{r^3}{4a}\left[(2n+3)\, j_{n+1}^2(ar) + (2n+1)\, j_n^2(ar) - \frac{(2n+1)(2n+3)}{ar}\, j_n(ar)\, j_{n+1}(ar)\right]$$

$$\int dr\, r^3\, j_n(ar) j_{n+1}(br) = -\frac{2br^2}{(a^2-b^2)\,(a+b)}\left[j_{n+1}(ar)\, j_n(br) - j_n(ar)\, j_{n+1}(br)\right]$$

$$\frac{r^2}{(a^2-b^2)}\left[ar\, j_{n+1}(ar)\, j_{n+1}(br) + br\, j_n(ar)\, j_n(br) - (2n+1)\, j_n(ar)\, j_{n+1}(br)\right] \tag{B.28}$$

With the help of these two relations, and after much algebra, the radial part of (B.24) reduces to

$$\begin{aligned} R^{\nu\nu'}_{\kappa\kappa'} &\equiv \int_0^R dr\, r^3 \left(g_n f_{n'} + f_n g_{n'}\right) \\ R^{\nu\nu}_{\kappa\kappa} &= \frac{R}{2}\,\frac{4\omega\kappa - 2\zeta_f + 4\kappa^2 - 1}{2\omega(\omega+\kappa)+\zeta_f} \qquad \text{if } \kappa = \kappa' \text{ and } \nu = \nu'. \end{aligned} \tag{B.29}$$

Here, the dimensionless energy, momentum and mass variables, introduced in equation (A.10) of appendix A, are being used, and the notation is such that $\omega' \equiv \omega_{n'}$, etc. The remaining two possibilities for the radial integral are $\kappa = \kappa'$, $\nu \neq \nu'$ and $\kappa = -\kappa' - 1$. These are

$$R^{\nu\nu'}_{\kappa\kappa} = \frac{-2xx'R}{(\omega+\omega')^2\sqrt{\left[2\omega(\omega+\kappa)+\zeta_f\right]\left[2\omega'(\omega'+\kappa)+\zeta_f\right]}} \times \phi \tag{B.30}$$

$$R^{\nu\nu'}_{-\kappa,\kappa+1} = \frac{-2xx'R\left[\omega-\omega'+\mathrm{sgn}(\kappa)\,(2\,|\kappa|+1)\right]}{(\omega+\omega')\,(x^2-x'^2)\sqrt{\left[2\omega(\omega+\kappa)+\zeta_f\right]\left[2\omega'(\omega'+\kappa)+\zeta_f\right]}} \times \phi \tag{B.31}$$

Once again, the radial integral is symmetric, i.e. $R^{\nu\nu'}_{-\kappa,\kappa+1} = R^{\nu'\nu}_{\kappa,-\kappa-1}$. These are the only non-zero matrix elements, which is simply a re-statement of the parity selection rule: $\kappa = \kappa'$ or $\kappa = -\kappa' - 1$. The factor ϕ is a phase which is given by

$$\phi \;=\; (-1)^{\rho+\rho'} \quad , \qquad \rho \;=\; \begin{cases} |\mu|+1 & \kappa < 0, \;\; \nu < 0 \\ |\mu| & \text{otherwise} \end{cases} \tag{B.32}$$

Finally, the radial and angular parts of the integral describing the quark-external operator vertex can be put together into

$$M_{nn'} \;=\; R^{\nu\nu'}_{\kappa\kappa'}\, A_{\kappa\kappa'} \tag{B.33}$$

Appendix C

Spin Sums

The sums over the spins of the intermediate particles in the vertex- and one-gluon exchange diagrams are presented in this appendix.

C.1 Vertex Correction Spin Sum

The sum over spins in the expression for the energy shift due to the vertex correction diagram, eq. (4.19), is readily evaluated. In terms of the Wigner $3j$- and $6j$-symbols, the result is

$$4\pi \sum_{\mu_p \mu_q M} \tilde{Q}^{m\Sigma}_{n_1 p} M_{pq} Q^{m\Sigma}_{q n_2} = S^{m\Sigma}_{n_1 p} R^{\nu_p \nu_q}_{\kappa_p \kappa_q} S^{m\Sigma}_{q n_2} (-1)^{j_1+j_2-J-\mu_1+1/2} \frac{(\kappa_p + \kappa_q)}{2} \hat{j}_1 \hat{j}_2 \hat{j}_p^2 \hat{j}_q^2 \hat{J}^2$$

$$\times \begin{Bmatrix} j_p & J & j_1 \\ j_2 & 1 & j_q \end{Bmatrix} \begin{pmatrix} j_1 & 1 & j_2 \\ \mu_1 & 0 & -\mu_2 \end{pmatrix} \begin{pmatrix} j_1 & J & j_p \\ \frac{1}{2} & 0 & -\frac{1}{2} \end{pmatrix} \begin{pmatrix} j_q & J & j_2 \\ \frac{1}{2} & 0 & -\frac{1}{2} \end{pmatrix} \begin{pmatrix} j_p & 1 & j_q \\ \frac{1}{2} & 0 & -\frac{1}{2} \end{pmatrix} \tag{C.1}$$

where the labels p, q and m should now be understood to include only the radial and angular momentum quantum numbers. The definitions of $S^{m\Sigma}_{nn'}$ and $R^{\nu\nu'}_{\kappa\kappa'}$ may be found in appendix B.

C.2 The Self-Energy Insert Spin Sum

Similarly, the sum over spins in eq. (4.34) for the self-energy diagrams yields

$$4\pi \sum_{\mu_p \mu_q M} M_{n_1 q} \tilde{Q}^{m\Sigma}_{qp} Q^{m\Sigma}_{p n_2} = \frac{(\kappa_1 + \kappa_q)}{2} R^{\nu_1 \nu_q}_{\kappa_1 \kappa_q} S^{m\Sigma}_{qp} S^{m\Sigma}_{p n_2} \times \tag{C.2}$$

$$(-1)^{\mu_1 - 1/2} \hat{j}_1 \hat{j}_2 \hat{j}_p^2 \hat{J}^2 \delta_{j_q j_2} \begin{pmatrix} j_1 & 1 & j_2 \\ -\mu_1 & 0 & \mu_2 \end{pmatrix} \begin{pmatrix} j_1 & 1 & j_2 \\ \frac{1}{2} & 0 & -\frac{1}{2} \end{pmatrix} \begin{pmatrix} j_p & J & j_2 \\ \frac{1}{2} & 0 & -\frac{1}{2} \end{pmatrix}^2$$

C.3 One-Gluon Exchange Spin Sum

In the case of the energy shift for one-gluon exchange, eq. (5.5), the spin sum does not simplify, and has to be carried out numerically. The expression to be evaluated is

$$4\pi \sum_{\mu_p M} \tilde{Q}^{m\Sigma}_{n_1 n_2} Q^{m\Sigma}_{n_3 p} M_{p n_4} = (-1)^{\mu_1+\mu_3+\mu_4+3/2} \frac{(\kappa_p + \kappa_4)}{2} S^{m\Sigma}_{n_1 n_2} S^{m\Sigma}_{n_3 p} R^{\nu_4 \nu_4}_{\kappa_p \kappa_4} \times$$

$$\hat{j}_1 \hat{j}_2 \hat{j}_3 \hat{j}_4 \hat{j}_p^2 \hat{J}^2 \begin{pmatrix} j_1 & J & j_2 \\ \frac{1}{2} & 0 & -\frac{1}{2} \end{pmatrix} \begin{pmatrix} j_3 & J & j_p \\ \frac{1}{2} & 0 & -\frac{1}{2} \end{pmatrix} \begin{pmatrix} j_p & 1 & j_4 \\ \frac{1}{2} & 0 & -\frac{1}{2} \end{pmatrix} \begin{pmatrix} j_p & 1 & j_4 \\ -\mu_4 & 0 & \mu_4 \end{pmatrix} \times$$

$$\sum_M (-1)^M \begin{pmatrix} j_1 & J & j_2 \\ -\mu_1 & -M & \mu_2 \end{pmatrix} \begin{pmatrix} j_3 & J & j_p \\ -\mu_3 & M & \mu_4 \end{pmatrix} \tag{C.3}$$

Appendix D

Sum Rules

The heart of all the cavity QCD calculations performed here lies in the sum of of vertex integrals, where the sum is over the *complete* set of quark or gluon cavity modes. This sum has to be performed numerically, and since an infinite sum cannot be done on a computer, some assumption has to be made on when the sum should be truncated. This is a fairly large computational task, and there is a good chance that errors will occur.

A simple and elegant way of checking both the computer code performing the sum and the method of truncating it is to use a sum rule derived from the original expression involving vertex integrals. A 'sum rule' is obtained by analytically summing over the intermediate quarks or gluons, using their completeness relations, before doing the integrals. To illustrate this procedure, we shall derive a sum rule in detail for the vertex correction diagram.

D.1 Vertex Correction Sum Rule

The expression for the vertex correction energy shift was given in eq. (4.19) as

$$\Delta E_{\rm a} = g^2 \int_0^\infty dz \sum_{pqm\Sigma} g^{\Sigma\Sigma}\, \tilde{Q}^{m\Sigma}_{n_1 p}\, M_{pq}\, Q^{m\Sigma}_{qn_2}\, I^{m\Sigma}_{pq}(z) \tag{D.1}$$

For the purposes of the sum rule, only the terms containing vertex integrals in the expression above will be retained. These terms will be defined as

$$V^{m\Sigma}_{nn'} = 4\pi g^{\Sigma\Sigma} \sum_{pqM} \tilde{Q}^{m\Sigma}_{np}\, M_{pq}\, Q^{m\Sigma}_{qn'} \tag{D.2}$$

where the sum $\sum_M$ runs over the gluon spin projections. Writing (D.2) out in full, one arrives at

$$V^{m\Sigma}_{nn'} = -4\pi g^{\Sigma\Sigma} \sum_{pqM} \int d^3x\, \bar{u}_n(\vec{x})\gamma_\mu u_p(\vec{x}) a^{\mu *}_{m\Sigma}(\vec{x}) \int d^3y\, \bar{u}_p(\vec{y})\gamma_\nu u_q(\vec{y}) A^\nu_{\rm ext}(\vec{y})$$
$$\times \int d^3z\, \bar{u}_q(\vec{z})\gamma_\rho u_{n'}(\vec{z}) a^\rho_{m\Sigma}(\vec{z}) \tag{D.3}$$

Using the completeness relation for the quark cavity modes (A.14), the sum over p and q may be performed immediately to give

$$V_{nn'}^{m\Sigma} = -4\pi g^{\Sigma\Sigma} \sum_M \int d^3r\, \bar{u}_n(\vec{r})\gamma_\mu\gamma_0\gamma_\nu\gamma_0\gamma_\rho u_{n'}(\vec{r}) a_{m\Sigma}^{\mu *}(\vec{r}) A_{\rm ext}^{\nu}(\vec{r}) a_{m\Sigma}^{\rho}(\vec{r}) \qquad \text{(D.4)}$$

Instead of summing over q, say, the sum over m, Σ could have been done using the gluon completeness relations. However, only two of the three intermediate particles in (D.4) may be summed over if $V_{nn'}^{m\Sigma}$ is to remain finite. The third sum would produce an inconvenient delta function in co-ordinate space. Hence, one must choose which two sets of quantum numbers to sum over (p and q in this case), then fix the remaining one.

Returning to (D.4), the Dirac algebra yields

$$\begin{aligned} \gamma_0\gamma_\mu\gamma_0\gamma_\nu\gamma_0\gamma_\rho\, a^{\mu *} A^\nu a^\rho &= a\cdot a^* \left(\gamma_0 \not{A} - 2A_0\right) + 2\left(a_0 A_0 + \vec{a}\cdot\vec{A}\right)\gamma_0 \not{a}^* \\ &= \gamma_0 a\cdot a^* \not{A} + 2\gamma_0 \vec{a}\cdot\vec{A}\not{a}^* \end{aligned} \qquad \text{(D.5)}$$

where $A_{\rm ext}^0 = 0$ since $A_{\rm ext}^\mu$ describes the potential due to a static magnetic field. The sum becomes

$$V_{nn'}^{m\Sigma} = -4\pi g^{\Sigma\Sigma} \sum_M \int d^3r\, \bar{u}_n(\vec{r}) \left(\not{A}_{\rm ext}(\vec{r}) \left| a_{m\Sigma}(\vec{r}) \right|^2 + 2\vec{a}_{m\Sigma}(\vec{r})\cdot\vec{A}_{\rm ext}(\vec{r})\, \not{a}_{m\Sigma}^*(\vec{r}) \right) u_{n'}(\vec{r}) \qquad \text{(D.6)}$$

If the potentials of the gluon fields are now expanded in terms of vector spherical harmonics and Bessel functions, the sum over spins in the first term of (D.6) can easily be done. Using

$$\sum_{M=-J}^{J} \vec{Y}_{JM}^{L\,*}(\hat{\boldsymbol{r}})\cdot\vec{Y}_{JM}^{L'}(\hat{\boldsymbol{r}}) = \frac{2J+1}{4\pi}\delta_{LL'} \qquad \text{(D.7)}$$

the first term is

$$4\pi g^{\Sigma\Sigma} \sum_M \left| a_{m\Sigma}(\vec{r}) \right|^2 = (2J+1)\,\Phi_{m\Sigma}(r) \qquad \text{(D.8)}$$

where $\Phi_{m\Sigma}(r)$ is given by

$$\Phi_{m\mathcal{S}}(r) = N_{m\mathcal{S}}^2\, j_J^2(\Omega r) \qquad \text{(D.9)}$$

$$\Phi_{m\mathcal{L}}(r) = N_{m\mathcal{L}}^2 \left(\frac{J+1}{2J+1} j_{J+1}^2(\Omega r) + \frac{J}{2J+1} j_{J-1}^2(\Omega r) \right) \qquad \text{(D.10)}$$

$$\Phi_{m\mathcal{M}}(r) = N_{m\mathcal{M}}^2\, j_J^2(\Omega r) \qquad \text{(D.11)}$$

$$\Phi_{m\mathcal{E}}(r) = N_{m\mathcal{E}}^2 \left(\frac{J}{2J+1} j_{J+1}^2(\Omega r) + \frac{J+1}{2J+1} j_{J-1}^2(\Omega r) \right) \qquad \text{(D.12)}$$

The spin sum in the second term of (D.6) requires a bit more work than the first one. Consider, for example, the term involving the longitudinal polarization $2g^{\mathcal{LL}}\vec{a}_{m\mathcal{L}}(\vec{r})\cdot\vec{A}_{\rm ext}(\vec{r})\,\not{a}^{*}_{m\mathcal{L}}(\vec{r})$. Writing the external field in a spherical basis,

$$\vec{A}_{\rm ext}(\vec{r}) \;=\; \frac{1}{2}(-y,\,x,\,0) \;=\; -ir\sqrt{\frac{\pi}{3}}\left(-\,Y_{1\,-1}(\hat{\boldsymbol{r}})\,\hat{e}_{+1}+Y_{1\,1}(\hat{\boldsymbol{r}})\,\hat{e}_{-1}\right) \qquad \text{(D.13)}$$

and using the expansion of the gluon potential, the first vector dot product in this term becomes

$$\vec{a}_{m\mathcal{L}}(\vec{r})\cdot\vec{A}_{\rm ext}(\vec{r}) = \frac{irN_{m\mathcal{L}}}{2J+1}\Big[j_{J+1}(\Omega r)+j_{J-1}(\Omega r)\Big]\,M\,Y_{JM}(\hat{\boldsymbol{r}}) \qquad \text{(D.14)}$$

Including the second dot product, it follows that

$$2g^{\mathcal{LL}}\vec{a}_{m\mathcal{L}}(\vec{r})\cdot\vec{A}_{\rm ext}(\vec{r})\,\vec{\gamma}\cdot\vec{a}^{*}_{m\mathcal{L}}(\vec{r}) \;=\; \frac{irN^{2}_{m\mathcal{L}}}{2J+1}\Big[j_{J+1}(\Omega r)+j_{J-1}(\Omega r)\Big]\,M\,Y_{JM}(\hat{\boldsymbol{r}})$$

$$\times\,\vec{\gamma}\cdot\left[\sqrt{\frac{J+1}{2J+1}}\,j^{2}_{J+1}(\Omega r)\vec{Y}^{J+1\,*}_{JM}(\hat{\boldsymbol{r}})+\sqrt{\frac{J}{2J+1}}\,j^{2}_{J-1}(\Omega r)\vec{Y}^{J-1\,*}_{JM}(\hat{\boldsymbol{r}})\right] \qquad \text{(D.15)}$$

One can now write the vector harmonics in a spherical basis, expand the spherical harmonics in a Clebsch-Gordan series and establish, after 'sum' algebra, that

$$r\sum_{M}M\,Y_{JM}(\hat{\boldsymbol{r}})\vec{Y}^{J+1\,*}_{JM}(\hat{\boldsymbol{r}}) \;=\; r\frac{J}{4}\sqrt{\frac{(2J+1)(J+1)}{3\pi}}\left(-\,Y_{1\,-1}(\hat{\boldsymbol{r}})\,\hat{e}_{+1}+Y_{1\,1}(\hat{\boldsymbol{r}})\,\hat{e}_{-1}\right)$$

$$= \;\frac{i}{4\pi}J\sqrt{(2J+1)(J+1)}\;\vec{A}_{\rm ext}(\vec{r}) \qquad \text{(D.16)}$$

A similar expression results for the sum $\sum_{M}M\,Y_{JM}(\hat{\boldsymbol{r}})\vec{Y}^{J-1\,*}_{JM}(\hat{\boldsymbol{r}})$. Hence, the longitudinal polarization term becomes

$$2g^{\mathcal{LL}}\sum_{M}\vec{a}_{m\mathcal{L}}(\vec{r})\cdot\vec{A}_{\rm ext}(\vec{r})\vec{\gamma}\cdot\vec{a}^{*}_{m\mathcal{L}}(\vec{r}) = -\frac{N^{2}_{m\mathcal{L}}}{4\pi}\frac{J(J+1)}{2J+1}\Big[j_{J+1}(\Omega r)+j_{J-1}(\Omega r)\Big]^{2}\,\vec{\gamma}\cdot\vec{A}_{\rm ext}(\vec{r}) \qquad \text{(D.17)}$$

In a similar fashion, the spin sums of the remaining polarizations may be evaluated. Combining all of these terms together and adding them to the first term in (D.6), one arrives at

$$V^{m\Sigma}_{nn'} \;=\; -\int d^{3}r\,\bar{u}_{n}(\vec{r})\,\not{A}_{\rm ext}(\vec{r})\,u_{n'}(\vec{r})\Phi'_{m\Sigma}(r) \qquad \text{(D.18)}$$

$$= \int dr\,r^{3}\Big(f_{n}(r)g_{n'}(r)+g_{n}(r)f_{n'}(r)\Big)\,\Phi'_{m\Sigma}(r)\int d\Omega\,\chi^{\mu\dagger}_{\kappa}(\hat{\boldsymbol{r}})Y_{10}(\hat{\boldsymbol{r}})\chi^{\mu'}_{\kappa'}(\hat{\boldsymbol{r}})$$

where

$$\Phi'_{m\mathcal{S}}(r) = N^2_{m\mathcal{S}}\, j^2_J(\Omega r) \tag{D.19}$$

$$\Phi'_{m\mathcal{L}}(r) = \frac{N^2_{m\mathcal{L}}}{2J+1}\Big[(J+1)\, j_{J+1}(\Omega r) - J\, j_{J-1}(\Omega r)\Big]^2 \tag{D.20}$$

$$\Phi'_{m\mathcal{M}}(r) = 0 \tag{D.21}$$

$$\Phi'_{m\mathcal{E}}(r) = N^2_{m\mathcal{E}}\, \frac{J(J+1)}{2J+1}\Big[j_{J+1}(\Omega r) + j_{J-1}(\Omega r)\Big]^2 \tag{D.22}$$

and the angular integral may be found in appendix B. Equation (D.18) can readily be evaluated numerically after choosing the quantum numbers of the intermediate gluon m, Σ and the initial and final quarks n and n'.

D.2 Sum Rule for the Self-Energy Inserts

The energy shift for the diagram containing a self-energy insert on an external leg, figure (4.1), was given by

$$\Delta E_{\rm b} = g^2 \int_0^\infty dz \sum_{\substack{pm\Sigma \\ q\neq n_2}} g^{\Sigma\Sigma}\, M_{n_1 q}\, \tilde{Q}^{m\Sigma}_{qp}\, Q^{m\Sigma}_{pn_2}\, K^{m\Sigma}_{pq}(z) \tag{D.23}$$

Defining the vertex integral part of this expression as $U^{m\Sigma}_{nn'}$, one has

$$U^{m\Sigma}_{nn'} = 4\pi g^{\Sigma\Sigma} \sum_{pqM} \tilde{Q}^{m\Sigma}_{np}\, Q^{m\Sigma}_{pq}\, M_{qn'} \tag{D.24}$$

Writing this out in full, and summing over p and q, this becomes

$$U^{m\Sigma}_{nn'} = -4\pi g^{\Sigma\Sigma} \sum_M \int d^3r\, \bar{u}_n(\vec{r})\gamma_\mu\gamma_0\gamma_\nu\gamma_0\gamma_\rho u_{n'}(\vec{r}) a^{\mu\,*}_{m\Sigma}(\vec{r}) a^\nu_{m\Sigma}(\vec{r}) A^\rho_{\rm ext}(\vec{r}) \tag{D.25}$$

which is very similar to (D.4), with the only difference being in the position of the external potential $A^\rho_{\rm ext}(\vec{r})$. This immediately leads to

$$U^{m\Sigma}_{nn'} = -(2J+1)\int dr\, r^3 \Big(f_n(r)g_{n'}(r) + g_n(r)f_{n'}(r)\Big)\, \Phi_{m\Sigma}(r) \int d\Omega\, \chi^{\mu\dagger}_\kappa(\hat{r}) Y_{10}(\hat{r}) \chi^{\mu'}_{\kappa'}(\hat{r}) \tag{D.26}$$

where $\Phi_{m\Sigma}(r)$ was defined in equation (D.9).

D.3 A One-Gluon Exchange Sum Rule

In principle, one of the sum rules above could be modified and used to check the computer code summing up the one-gluon exchange vertex integrals. However, it is

much more convenient to check the code with a sum rule which works in exactly the same way as the code, so a sum rule will be derived from the energy shift

$$\Delta E = g^2 \sum_{pm\Sigma} g^{\Sigma\Sigma}\, \tilde{Q}^{m\Sigma}_{n_1 n_2}\, Q^{m\Sigma}_{n_3 p}\, M_{p n_4}\, \frac{1}{(\varepsilon_4 - \varepsilon_p)\left[(\varepsilon_1 - \varepsilon_2)^2 - \Omega^2\right]} \tag{D.27}$$

The vertex integral part is defined as

$$W^{n_1 n_2}_{n_3 n_4} = 4\pi g^{\Sigma\Sigma} \sum_{pm\Sigma} \tilde{Q}^{m\Sigma}_{n_1 n_2}\, Q^{m\Sigma}_{n_3 p}\, M_{p n_4} \tag{D.28}$$

In this case, both of the intermediate particles may be summed over using the quark (A.14) and gluon (A.25) completeness relations. This gives

$$W^{n_1 n_2}_{n_3 n_4} = -4\pi \int d^3 r\, \bar{u}_{n_1}(\vec{r}) \gamma_\mu u_{n_2}(\vec{r})\, \bar{u}_{n_3}(\vec{r}) \gamma^\mu \gamma_0 \gamma_\nu u_{n_4}(\vec{r}) A^\nu_{\rm ext}(\vec{r}) \tag{D.29}$$

At this point, it is convenient to note some of the properties of the external field $A^\mu_{\rm ext}(\vec{r})$. It was defined as $\vec{A}_{\rm ext}(\vec{r}) = -\frac{1}{2}\vec{r} \times \vec{B}$ in (B.15), where $\vec{B}$ is a static magnetic field of unit strength along the z-axis. Using the properties of the Pauli matrices, one can derive the following useful identities that the external field satisfies:

$$\sigma_r\, \vec{\sigma} + \vec{\sigma}\, \sigma_r = 2\hat{\boldsymbol{r}} \tag{D.30}$$

$$\sigma_r \left(\vec{\sigma} \cdot \vec{A}_{\rm ext}\right) = -\left(\vec{\sigma} \cdot \vec{A}_{\rm ext}\right) \sigma_r \tag{D.31}$$

$$\sigma_r\, \vec{\sigma} \left(\vec{\sigma} \cdot \vec{A}_{\rm ext}\right) = 2\hat{\boldsymbol{r}} \left(\vec{\sigma} \cdot \vec{A}_{\rm ext}\right) + \vec{\sigma} \left(\vec{\sigma} \cdot \vec{A}_{\rm ext}\right) \sigma_r \tag{D.32}$$

$$\vec{\sigma} \left(\vec{\sigma} \cdot \vec{A}_{\rm ext}\right) = \vec{A}_{\rm ext} + \frac{i}{2}\sigma_z \vec{r} - \frac{i}{2}\sigma_r \hat{\boldsymbol{e}}_z \tag{D.33}$$

The spinors and γ-matrices in (D.29) can now be multiplied out and written, with the help of the preceding identities, in terms of σ-matrices as

$$W^{n_1 n_2}_{n_3 n_4} = 4\pi \int dr\, r^2 \left(g_{n_1} f_{n_2} + f_{n_1} g_{n_2}\right)\left(g_{n_3} g_{n_4} + f_{n_3} f_{n_4}\right) \left[\frac{r}{2} \int d\Omega\, \chi^{\mu_1 \dagger}_{\kappa_1} \chi^{\mu_2}_{\kappa_2}\, \chi^{\mu_3 \dagger}_{\kappa_3}\, \sigma_z\, \chi^{\mu_4}_{\kappa_4} - \right.$$

$$\left. \frac{r}{2} \int d\Omega\, \chi^{\mu_1 \dagger}_{\kappa_1}\, \sigma_z\, \chi^{\mu_2}_{-\kappa_2}\, \chi^{\mu_3 \dagger}_{\kappa_3} \chi^{\mu_4}_{-\kappa_4} + i \int d\Omega\, \chi^{\mu_1 \dagger}_{\kappa_1} \left(\vec{\sigma} \cdot \vec{A}_{\rm ext}\right) \chi^{\mu_2}_{-\kappa_2}\, \chi^{\mu_3 \dagger}_{\kappa_3} \chi^{\mu_4}_{\kappa_4} \right] +$$

$$i \int dr\, r^2 \left[2 f_{n_1} g_{n_2} g_{n_3} g_{n_4} + 2 g_{n_1} f_{n_2} f_3 f_{n_4} - \left(g_{n_1} g_{n_2} + f_{n_1} f_{n_2}\right)\left(g_{n_3} f_{n_4} + g_{n_4} f_{n_3}\right)\right] \times$$

$$\int d\Omega\, \chi^{\mu_1 \dagger}_{\kappa_1} \chi^{\mu_2}_{\kappa_2}\, \chi^{\mu_3 \dagger}_{\kappa_3} \left(\vec{\sigma} \cdot \vec{A}_{\rm ext}\right) \chi^{\mu_4}_{-\kappa_4} \tag{D.34}$$

The angular integrals in the expression above are evaluated here by brute force, i.e. expanding all the spinors and spherical harmonics as Clebsch-Gordan series until only two are left, when the integral is elementary. The results are

$$4\pi \int d\Omega\, \chi^{\mu_1\dagger}_{\kappa_1}(\hat{\boldsymbol{r}})\, \sigma_z\, \chi^{\mu_2}_{\kappa_2}(\hat{\boldsymbol{r}})\, \chi^{\mu_3\dagger}_{\kappa_3}(\hat{\boldsymbol{r}}) \chi^{\mu_4}_{\kappa_4}(\hat{\boldsymbol{r}}) = (-1)^{\mu_1+\mu_3} \sum_{mL} (-1)^L\, \hat{j}_1\, \hat{j}_2\, \hat{j}_3\, \hat{j}_4\, \hat{\ell}_1\, \hat{\ell}_2\, \hat{L}^2 \times$$

$$\begin{pmatrix} \ell_1 & \frac{1}{2} & j_1 \\ \mu_1 - m & m & -\mu_1 \end{pmatrix} \begin{pmatrix} \ell_2 & \frac{1}{2} & j_2 \\ \mu_2 - m & m & -\mu_2 \end{pmatrix} \begin{pmatrix} \ell_1 & L & \ell_2 \\ m - \mu_1 & \mu_1 - \mu_2 & \mu_2 - m \end{pmatrix} \times$$

$$\begin{pmatrix} j_3 & L & j_4 \\ -\mu_3 & \mu_2 - \mu_1 & \mu_4 \end{pmatrix} \begin{pmatrix} j_3 & L & j_4 \\ \frac{1}{2} & 0 & -\frac{1}{2} \end{pmatrix} \begin{pmatrix} \ell_1 & \ell_2 & L \\ 0 & 0 & 0 \end{pmatrix} \frac{1 + (-1)^{\ell_3 + L + \ell_4}}{2} \qquad \text{(D.35)}$$

where the abbreviation $\hat{\ell} = \sqrt{2\ell + 1}$ has been used. The other integral needed here is given by

$$4\pi \int d\Omega\, \chi^{\mu_1\dagger}_{\kappa_1}(\hat{\boldsymbol{r}}) \chi^{\mu_2}_{\kappa_2}(\hat{\boldsymbol{r}})\, \chi^{\mu_3\dagger}_{\kappa_3}(\hat{\boldsymbol{r}}) \left(\vec{\sigma} \cdot \vec{A}_{\rm ext}(\vec{r})\right) \chi^{\mu_4}_{\kappa_4}(\hat{\boldsymbol{r}}) = -\frac{ir}{\sqrt{2}} (-1)^{\mu_2+\mu_4}\, \hat{j}_1\, \hat{j}_2\, \hat{j}_3\, \hat{j}_4$$

$$\sum_{mm'LL'} (-1)^{L+L'-m-m'}\, \hat{L}^2 \hat{L}'^2 \begin{pmatrix} \ell_1 & \frac{1}{2} & j_1 \\ \mu_1 - m & m & -\mu_1 \end{pmatrix} \begin{pmatrix} \ell_2 & \frac{1}{2} & j_2 \\ \mu_2 - m & m & -\mu_2 \end{pmatrix} \times$$

$$\begin{pmatrix} \ell_3 & \frac{1}{2} & j_3 \\ \mu_3 + m' & -m' & -\mu_3 \end{pmatrix} \begin{pmatrix} \ell_4 & \frac{1}{2} & j_4 \\ \mu_4 - m' & m' & -\mu_4 \end{pmatrix} \begin{pmatrix} \ell_1 & \ell_2 & L \\ 0 & 0 & 0 \end{pmatrix} \begin{pmatrix} \ell_3 & \ell_4 & L' \\ 0 & 0 & 0 \end{pmatrix} \times$$

$$\begin{pmatrix} \ell_1 & L & \ell_2 \\ m - \mu_1 & \mu_4 - \mu_3 & \mu_2 - m \end{pmatrix} \begin{pmatrix} \ell_3 & L' & \ell_4 \\ -\mu_3 - m' & \mu_3 - \mu_4 + 2m' & \mu_4 - m' \end{pmatrix} \times$$

$$\begin{pmatrix} L' & 1 & L \\ 0 & 0 & 0 \end{pmatrix} \begin{pmatrix} L' & 1 & L \\ \mu_4 - \mu_3 - 2m' & 2m' & \mu_3 - \mu_4 \end{pmatrix} \hat{\ell}_1\, \hat{\ell}_2\, \hat{\ell}_3\, \hat{\ell}_4 \qquad \text{(D.36)}$$

One point to note is that the gluon completeness relation used in deriving this sum rule includes one cavity mode which is not normally used when a numerical sum is performed. This mode is a scalar with zero energy, and has the quantum numbers $m_0 = \{0, 0, 0\}$. The origin of this term has been discussed by Stoddart [8]. It is given by

$$a^0_{m_0 \mathcal{S}}(\vec{r}) = \sqrt{3}\, Y_{00}(\hat{\boldsymbol{r}}) \qquad \text{(D.37)}$$

The contribution to the sum rule from this term is easily found to be

$$4\pi g^{\mathcal{SS}} \sum_p \tilde{Q}^{m_0 \mathcal{S}}_{n_1 n_2}\, Q^{m_0 \mathcal{S}}_{n_3 p}\, M_{p n_4} = -3 \delta_{n_1 n_2} M_{n_3 n_4} \qquad \text{(D.38)}$$

Hence, this term may be subtracted from the sum rule if the numerical sum does not include this zero-energy scalar mode.

Appendix E

Colour and Flavour Matrix Elements

The matrix elements of the external operator and quark creation/annihilation operators between proton and neutron states will be derived in this appendix. There are two distinct types of these matrix elements, corresponding to the one- and two-body interactions. The former are fairly well known from the non-relativistic quark model, whereas the latter are rather more complicated since they depend on four variables, and need to be derived with some care.

E.1 One-Body Colour and Flavour Matrix Elements

The colour and flavour matrix elements for the one-body interaction are given in the main text as

$$\left\langle p \left| a^\dagger_{c'f'n_1} \left(\frac{\lambda^a}{2}\right)_{c'd} \left(\frac{\lambda^a}{2}\right)_{dc} Q\, a_{cfn_2} \right| p \right\rangle \tag{E.1}$$

where Q is the quark charge matrix, the λ^a's are the Gell-Mann matrices and $|p\rangle$ is the wave function for spin-up protons, given in second quantization by

$$|p\rangle = \frac{\varepsilon^{abc}}{\sqrt{18}} \left[a^\dagger_{a,u,1s\uparrow}\, a^\dagger_{b,d,1s\downarrow} - a^\dagger_{a,u,1s\downarrow}\, a^\dagger_{b,d,1s\uparrow} \right] a^\dagger_{c,u,1s\uparrow} \left|0\right\rangle \tag{E.2}$$

The operator $a^\dagger_{a,u,1s\uparrow}$ creates a spin-up quark with colour a and flavour u in the $1s$ state, and ε^{abc} is the completely anti-symmetric tensor of rank 3. The charge matrix Q for u and d quarks may be written in terms of the unit and isospin matrices as

$$Q = \tfrac{1}{6}(I + 3\tau_3) \tag{E.3}$$

The action of the diagonal matrices I and τ_3 can be represented by δ-functions which restrict the flavour f of the quark to either u or d.

$$I \;=\; \delta_{f,u} + \delta_{f,d}$$

$$\tau_3 \;=\; \delta_{f,u} - \delta_{f,d} \tag{E.4}$$

The external operator Q attached to the quark line $n'n$ does not change the colour or flavour of the quarks on either side of its vertex since it interacts only through the colourless electromagnetic field. Furthermore, conservation of angular momentum and energy at the external vertex, coupled with the fact that the energy eigenvalues are discrete in the cavity, means that the radial and angular quantum numbers of the quarks must also be the same on either side of the operator insert. Thus, after noting the standard relation

$$\sum_d \left(\frac{\lambda^a}{2}\right)_{c'd} \left(\frac{\lambda^a}{2}\right)_{dc} \;=\; \frac{4}{3}\,\delta_{c'c} \tag{E.5}$$

the expression for the colour and flavour matrix elements becomes

$$\left\langle p \left| a^\dagger_{c'f'n_1} \left(\frac{\lambda^a}{2}\right)_{c'd} \left(\frac{\lambda^a}{2}\right)_{dc} Q\, a_{cfn_2} \right| p \right\rangle \;=\; \frac{4}{3} \left\langle p \left| a^\dagger_{cfn_1} Q\, a_{cfn_1} \right| p \right\rangle \tag{E.6}$$

There is an implicit sum over the colour, flavour, radial and angular quantum numbers c, f and n in eq. (E.6), which arises from the expansion of the field operator ψ in terms of cavity modes and creation operators. This sum may be carried out using the anti-commutation relations for the creation and annihilation operators

$$\left\{ a_{cfn}\,,\; a^\dagger_{c'f'n'} \right\} = \delta_{cc'}\,\delta_{ff'}\,\delta_{nn'} \tag{E.7}$$

With the help of this relation, the annihilation operators are anti-commuted to the right, through the wave function, and the creation operators to the left until the vacuum state is reached, where $a_{cn}\,|0\rangle = 0$ and $\langle 0|\, a^\dagger_{cn} = 0$. It is rather amusing to carry out these sums and ordering operations on a computer using REDUCE 3.3, which is a package that performs calculations symbolically rather than numerically. Some of these calculations take a surprisingly long time on the computer, although the matrix elements of I and τ_3 turn out to be quite simple. Using REDUCE, they are found to be

$$\sum_{cfn} \left\langle p \left| a^\dagger_{cfn}\, I\, a_{cfn} \right| p \right\rangle \;=\; \left(2\delta_{\mu,\uparrow} + \delta_{\mu,\downarrow}\right) \delta_{n,1s} \tag{E.8}$$

$$\sum_{cfn} \left\langle p \left| a^\dagger_{cfn}\, \tau_3\, a_{cfn} \right| p \right\rangle \;=\; \frac{1}{3}\left(4\delta_{\mu,\uparrow} - \delta_{\mu,\downarrow}\right) \delta_{n,1s} \tag{E.9}$$

The matrix elements of Q can immediately be found by using these expressions and the definition (E.3). The final expression is

$$\sum_{c'cfn} \left\langle p \left| a^\dagger_{c'fn} \left(\frac{\lambda^a}{2}\right)_{c'd} \left(\frac{\lambda^a}{2}\right)_{dc} Q\, a_{cfn} \right| p \right\rangle \;=\; \frac{4}{3}\,\delta_{\mu,\uparrow}\,\delta_{n,1s} \tag{E.10}$$

The corresponding colour and flavour matrix elements taken between neutron states are

$$\sum_{c'cfr} \left\langle n \left| a^\dagger_{c'fr} \left(\frac{\lambda^a}{2}\right)_{c'd} \left(\frac{\lambda^a}{2}\right)_{dc} Q\, a_{cfr} \right| n \right\rangle = -\frac{4}{9} \left(\delta_{\mu,\uparrow} - \delta_{\mu,\downarrow}\right) \delta_{r,1s} \tag{E.11}$$

E.2 The Two-Body Matrix Elements

The two-body matrix elements arising from the one-gluon exchange diagrams were given in chapter 5 as

$$\left\langle p \left| \hat{a}^\dagger_{c'f'n_1} \hat{a}^\dagger_{d'g'n_3} \left(\frac{\lambda^a}{2}\right)_{c'c} \left(\frac{\lambda^a}{2}\right)_{d'd} Q\, \hat{a}_{cfn_2} \hat{a}_{dgn_4} \right| p \right\rangle \tag{E.12}$$

The gluon which is exchanged between the two quark lines $n_2 n_1$ and $n_4 n_3$ carries no flavour, and neither does the external operator attached to the line $n_4 n_3$, so the flavour cannot change along either of these lines. In other words, $f' = f$ and $g' = g$. The λ^a matrices yield the colour factor

$$\left(\frac{\lambda^a}{2}\right)_{c'c} \left(\frac{\lambda^a}{2}\right)_{d'd} = \frac{1}{2}\left(\delta_{c'd}\,\delta_{cd'} - \frac{1}{3}\,\delta_{c'c}\,\delta_{d'd}\right) \tag{E.13}$$

which restricts the colour changes along these quark lines. With the help of this relation and REDUCE, the sum over all allowed colours, flavours and radial states yields the following matrix element for I:

$$\sum_{\substack{\text{colours}\\ \text{flavours}}} \left\langle p \left| \hat{a}^\dagger_{c'fn_1} \hat{a}^\dagger_{d'gn_3} \left(\frac{\lambda^a}{2}\right)_{c'c} \left(\frac{\lambda^a}{2}\right)_{d'd} I\, \hat{a}_{cfn_2} \hat{a}_{dgn_4} \right| p \right\rangle$$

$$= \frac{2}{3}\Big[\left(\delta_{\mu_1\mu_3,\uparrow} + 2\delta_{\mu_1,\uparrow}\,\delta_{\mu_3,\downarrow} + 2\delta_{\mu_1,\downarrow}\,\delta_{\mu_3,\uparrow}\right) \delta_{\mu_1,\mu_2}\,\delta_{\mu_3,\mu_4}$$

$$+ \left(\delta_{\mu_1\mu_3,\uparrow} - \delta_{\mu_1,\uparrow}\,\delta_{\mu_3,\downarrow} - \delta_{\mu_1,\downarrow}\,\delta_{\mu_3,\uparrow}\right) \delta_{\mu_2,\mu_3}\,\delta_{\mu_1,\mu_4} \Big] \delta_{n_1 n_2 n_3 n_4, 1s} \tag{E.14}$$

where a shorthand notation for repeated δ-functions having one argument in common has been introduced.

$$\delta_{ab\cdots c,z} \equiv \delta_{a,z}\,\delta_{b,z}\cdots\delta_{c,z} \tag{E.15}$$

Similarly, the matrix element containing the operator τ_3 is found to be

$$\sum_{\substack{\text{colours}\\ \text{flavours}}} \left\langle p \left| \hat{a}^\dagger_{c'fn_1} \hat{a}^\dagger_{d'gn_3} \left(\frac{\lambda^a}{2}\right)_{c'c} \left(\frac{\lambda^a}{2}\right)_{d'd} \tau_3 \, \hat{a}_{cfn_2} \hat{a}_{dgn_4} \right| p \right\rangle$$

$$= \frac{2}{9} \Big[2 \left(\delta_{\mu_1\mu_3,\uparrow} + 2\delta_{\mu_1,\downarrow}\,\delta_{\mu_3,\uparrow} - \delta_{\mu_1,\uparrow}\,\delta_{\mu_3,\downarrow} \right) \delta_{\mu_1,\mu_2}\,\delta_{\mu_3,\mu_4}$$

$$+ \left(2\delta_{\mu_1\mu_3,\uparrow} + \delta_{\mu_1,\downarrow}\,\delta_{\mu_3,\uparrow} + \delta_{\mu_1,\uparrow}\,\delta_{\mu_3,\downarrow} \right) \delta_{\mu_2,\mu_3}\,\delta_{\mu_1,\mu_4} \Big] \delta_{n_1n_2n_3n_4,1s} \qquad \text{(E.16)}$$

A considerable simplification results when these two matrix elements, in conjunction with the definition of Q in eq. (E.3), are added together. The final result for the matrix element of Q is

$$\sum_{\substack{\text{colours}\\ \text{flavours}}} \left\langle p \left| \hat{a}^\dagger_{c'fn_1} \hat{a}^\dagger_{d'gn_3} \left(\frac{\lambda^a}{2}\right)_{c'c} \left(\frac{\lambda^a}{2}\right)_{d'd} Q \, \hat{a}_{cfn_2} \hat{a}_{dgn_4} \right| p \right\rangle$$

$$= \frac{2}{3} \left(\delta_{\mu_1\mu_2,\uparrow} + \delta_{\mu_1\mu_2,\downarrow} \right) \delta_{\mu_3\mu_4,\uparrow}\,\delta_{n_1n_2n_3n_4,1s} \qquad \text{(E.17)}$$

In a similar manner, the matrix elements of the colour, flavour and charge operators of a two-body state taken between neutron wave functions yield

$$\sum_{\substack{\text{colours}\\ \text{flavours}}} \left\langle n \left| \hat{a}^\dagger_{c'fn_1} \hat{a}^\dagger_{d'gn_3} \left(\frac{\lambda^a}{2}\right)_{c'c} \left(\frac{\lambda^a}{2}\right)_{d'd} Q \, \hat{a}_{cfn_2} \hat{a}_{dgn_4} \right| n \right\rangle$$

$$= \frac{1}{9} \Big[\left(4\delta_{\mu_1,\uparrow}\,\delta_{\mu_3,\downarrow} - 2\delta_{\mu_1,\downarrow}\,\delta_{\mu_3,\uparrow} - \delta_{\mu_1\mu_3,\uparrow} \right) \delta_{\mu_1,\mu_2}\,\delta_{\mu_3,\mu_4}$$

$$- \left(2\delta_{\mu_1,\uparrow}\,\delta_{\mu_3,\downarrow} + 2\delta_{\mu_1,\downarrow}\,\delta_{\mu_3,\uparrow} + \delta_{\mu_1\mu_3,\uparrow} \right) \delta_{\mu_2,\mu_3}\,\delta_{\mu_1,\mu_4} \Big] \delta_{n_1n_2n_3n_4,1s} \qquad \text{(E.18)}$$

Appendix F

Conventions and Units

Natural units i.e. $\hbar = 1 = c$ are employed throughout this work. These factors may be restored at the end of a calculation by examining the dimensions of the quantities in the formulae. The numerical values of $\hbar c$ and the proton mass used here are

$$\begin{aligned} \hbar c &= 197.327\,053 \text{ MeV fm} \\ m_{\rm p} &= 938.272 \text{ MeV}/c^2 \end{aligned}$$

The natural unit of length in the cavity is the radius R, and this unit should also be restored if c.g.s. units are required. For example, the dimensionless mass parameter becomes

$$\zeta_f = m_f R c/\hbar$$

The usual metric in Minkowski space has been used

$$g^{\mu\nu} = g_{\mu\nu} = \text{diag}\{-1,+1,+1,+1\} \quad , \quad g^{\mu}_{\nu} = \delta^{\mu}_{\nu}$$

and the 4×4 Dirac γ matrices satisfy

$$\{\gamma^{\mu},\gamma^{\nu}\} = 2g^{\mu\nu}$$

The γ matrices may be represented as

$$\gamma^0 = \begin{pmatrix} I & 0 \\ 0 & -I \end{pmatrix}, \quad \gamma^k = \begin{pmatrix} 0 & \sigma^k \\ -\sigma^k & 0 \end{pmatrix}$$

where the σ^k are the 2×2 Pauli matrices:

$$\sigma^1 = \begin{pmatrix} 0 & 1 \\ 1 & 0 \end{pmatrix}, \quad \sigma^2 = \begin{pmatrix} 0 & -i \\ i & 0 \end{pmatrix}, \quad \sigma^3 = \begin{pmatrix} 1 & 0 \\ 0 & -1 \end{pmatrix}$$

Bibliography

[1] H. Fritsch, M. Gell-Mann and H. Leutwyler, Phys. Lett. **B47** (1973) 365.

[2] A. Chodos, R. L. Jaffe, K. Johnson, C.B. Thorn and V. F. Weisskopf, Phys. Rev. **D9** (1974) 3471.

A. Chodos, R. L. Jaffe, K. Johnson and C.B. Thorn Phys. Rev. **D10** (1974) 2599.

T. DeGrand, R. L. Jaffe, K. Johnson and J. Kiskis Phys. Rev. **D12** (1975) 2060.

[3] G. E. Brown and M. Rho, Phys. Lett. **B82** (1979) 177.

G. E. Brown, M. Rho and V. Vento, Phys. Lett. **B84** (1979) 383.

[4] A. W. Thomas, Advances in Nuclear Physics, **13** (1983) 1.

[5] K. Tsushima, T. Yamaguchi, Y. Kohyama and K. Kubodera, Nucl. Phys. **A489** (1988) 557.

[6] R. F. Buser, R. D. Viollier and P. Zimak, International Journal of Theoretical Physics, **27** (1988) 925.

[7] A. J. Stoddart and R. D. Viollier, Phys. Lett. **B236** (1990) 387, and Nucl. Phys. **A** (to be published).

[8] A. J. Stoddart, *Renormalization of Cavity Field Theories*, PhD thesis, unpublished, University of Cape Town preprint UCT-TP 139/90 (1990).

[9] F. E. Close and R. R. Horgan, Nucl. Phy. **B164** (1980) 413 and Nucl. Phy. **B185** (1981) 333.

[10] M. Gell-Mann and F. Low, Phys. Rev. **84** (1951) 350.

[11] A. L. Fetter and J. D. Walecka, *Quantum Theory Of Many Particle Systems* (McGraw-Hill, New York, 1971).

[12] J. Sucher, Phys. Rev. **107** (1957) 1448.

[13] P. J. Mohr, Phys. Rev. **A32** (1985) 1949.

[14] S. S. Schweber, *An Introduction to Relativistic Quantum Field Theory* (Harper & Row, New York, 1961).

[15] L. H. Ryder, *Quantum Field Theory* (Cambridge University Press, Cambridge, 1985).

[16] R. P. Feynman, Phys. Rev. **76** (1949) 769.

[17] O. V. Maxwell and V. Vento, Nucl. Phys. **A407** (1983) 366.

[18] F. Halzen and A. D. Martin, *Quarks and Leptons: An Introductory Course in Modern Particle Physics* (John Wiley & Sons, New York, 1984).

[19] N. Barik and M. Das, Phys. Rev. **D28** (1983) 2823.

[20] H. Georgi and A. Manohar, Phys. Lett. **132B** (1983) 183.

[21] J. P. Singh, Phys. Rev. **D31** (1985) 1097.

[22] E. Gillman and H. R. Fiebig, Computers in Physics, Vol. **2** no. 1, (1988) 62.

[23] H. Høgaasen and F. Myhrer, Phys. Rev. **D37** (1988) 1950.

[24] K. Ushio, Phys. Lett. **158B** (1985) 71.

[25] M. I. Krivoruchenko, Sov. J. Nucl. Phys. **40** (1984) 514.
I. Yu. Kobzarev, L. A. Kondratyuck, M. I. Krivoruchenko, B. V. Martem'yanov and M. G. Shchepkin, Sov. J. Nucl. Phys. **43** (1986) 803.

[26] G. U. Schreiber, *The Gluon Self-Energy in Cavity QCD*, PhD thesis, University of Cape Town, May 1991, unpublished.

[27] T. H. Hansson and R. L. Jaffe, Phys. Rev. **D28** (1983) 882.
T. H. Hansson, Annals of Physics, **151** (1983) 204.

[28] S. Goldhaber, T. H. Hansson and R. L. Jaffe, Phys. Lett. **131B** (1983) 445, and Nucl. Phys. **B277** (1986) 674.

[29] R. D. Viollier, S. A. Chin and A. K. Kerman, Nucl. Phys. **A407** (1983) 269.

[30] D. A. Varshalovich, A. N. Moskalev and V. K. Khersonskii, *Quantum Theory of Angular Momentum* (World Scientific, Singapore, 1988).

[31] A. R. Edmonds, *Angular Momentum in Quantum Mechanics* (Princeton University Press, New Jersey, 1957).

[32] M. Abramowitz and I. A. Stegun, *Handbook of Mathematical Functions* (Dover, New York, 1965).

[33] A. Gervois and H. Navelet, SIAM J. Math. Anal. **20** (1989) 1006.